



HAL
open science

Water as a driver of evolution: the example of aquatic snakes

Marion Segall

► **To cite this version:**

Marion Segall. Water as a driver of evolution: the example of aquatic snakes. Animal biology. Université Sorbonne Paris Cité, 2017. English. NNT : 2017USPCB058 . tel-02127227

HAL Id: tel-02127227

<https://theses.hal.science/tel-02127227v1>

Submitted on 13 May 2019

HAL is a multi-disciplinary open access archive for the deposit and dissemination of scientific research documents, whether they are published or not. The documents may come from teaching and research institutions in France or abroad, or from public or private research centers.

L'archive ouverte pluridisciplinaire **HAL**, est destinée au dépôt et à la diffusion de documents scientifiques de niveau recherche, publiés ou non, émanant des établissements d'enseignement et de recherche français ou étrangers, des laboratoires publics ou privés.



Thèse de doctorat de l'Université Paris Descartes

Spécialité Biologie Interdisciplinaire

Ecole Doctorale Interdisciplinaire Européenne Frontière du Vivant (ED 474)

*Water as a driver of evolution:
the example of aquatic snakes*

Par Marion Segall

Réalisée dans les laboratoires :

Mécanismes Adaptatifs & Evolution, Equipe FUNEVOL, UMR 7179, CNRS/MNHN

Physique et Mécanique des Milieux Hétérogènes, UMR 7636, ESPCI/CNRS/Paris Diderot/UPMC

Encadrée par Anthony Herrel et Ramiro Godoy-Diana

Présentée et soutenue publiquement le 10 novembre 2017

Devant un jury composé de :

Harvey Lillywhite	Professor, University of Florida, USA	Rapporteur
Patricia Ern	Directeur de Recherche, CNRS	Rapporteuse
Raphaël Cornette	Docteur, MNHN	Examineur
Catherine Quilliet	Maître de Conférences, UGA	Examinatrice
Sam Van Wassenbergh	Docteur, University of Antwerp, BE	Examineur
Anthony Herrel	Directeur de Recherche, CNRS	Directeur
Ramiro Godoy-Diana	Chargé de Recherche, CNRS	Directeur

Table of Content

Résumé	1
General Introduction	3
Chapter 1: Does aquatic foraging impact head shape evolution in snakes?	19
<i>Introduction</i>	21
<i>Material & Methods</i>	23
<i>Specimens</i>	23
<i>Geometric morphometrics</i>	24
<i>Analyses</i>	25
<i>Results</i>	26
<i>Discussion</i>	29
Chapter 2: Hydrodynamics of the frontal strike in aquatic snakes: drag, added mass and the possible consequences for prey capture success	35
<i>Introduction</i>	37
<i>Material & Methods</i>	39
<i>3D models</i>	39
<i>Experimental setup</i>	41
<i>Drag coefficient and added mass</i>	41
<i>Detection distance</i>	43
<i>Particle Image Velocimetry</i>	43
<i>Statistical analyses</i>	45
<i>Results</i>	45
<i>Drag and added mass</i>	45
<i>Detection distance</i>	46
<i>Flow characterization</i>	46
<i>Discussion</i>	48

Chapter 3: The complexity of convergence: from one-to-one mapping of form to function to many-to-one mapping of function to ecology 53

Introduction	55
Material & Methods	57
<i>Specimens</i>	57
<i>Geometric morphometrics</i>	59
<i>3D models</i>	59
<i>Experimental setup</i>	60
<i>Drag coefficient</i>	60
<i>Statistical analyses</i>	61
Results	61
<i>Morphometry</i>	61
<i>Drag coefficients</i>	64
Discussion	65

Chapter 4: Behavioral adaptation 69

Introduction	71
Material & Methods	73
<i>Experimental setups and tracking</i>	73
<i>Hydrophis platura</i> experiments	73
<i>Enhydris bocourti</i> experiments	74
<i>Cerberus schneiderii</i> experiments	74
<i>Video analysis</i>	74
<i>Data from literature</i>	75
<i>Statistical analyses</i>	76
Results	77
<i>Description of the behavior and kinematics of H. platura</i>	77
<i>Description of the behavior and kinematics of E. bocourti</i>	78
<i>Description of the behavior and kinematics of C. schneiderii</i>	79
<i>Strike performance</i>	80
<i>Meta-analysis</i>	80

Discussion	82
<i>Comparison of the prey capture behavior of H. platura, E. bocourti and C. schneiderii</i>	82
<i>Relationships between form, function and behavior</i>	84
General Conclusion	87
References	97
Appendices	111

Résumé

L'environnement dans lequel les espèces animales vivent joue un rôle important dans leur évolution. Les contraintes physiques sont particulièrement intéressantes car elles induisent souvent une pression évolutive qui pousse les espèces, même éloignées, à développer des réponses adaptatives similaires. Les contraintes physiques liées à la vie en milieu aquatique ont un impact important sur les trajectoires évolutives des espèces et notamment sur leur comportement et leur morphologie. De nombreux cas de convergences ont été démontrés, comme l'évolution d'une forme profilée chez les poissons, les mammifères marins et certains oiseaux aquatiques. Ces contraintes, appelées contraintes hydrodynamiques, sont particulièrement présentes lors de la réalisation d'un mouvement. On peut caractériser deux contraintes principales : la traînée et la masse ajoutée. La traînée est la résistance que le fluide oppose au mouvement de l'animal. La masse ajoutée elle, est la masse d'eau déplacée lorsque le corps se met en mouvement donc lors d'une accélération. Ces contraintes sont particulièrement présentes lors de la capture d'une proie dans l'eau. Ainsi, beaucoup d'animaux aquatiques ont développé un système de succion qui leur permet d'aspirer leur proie afin de limiter ces contraintes. Cependant, certains animaux, comme les serpents, ne peuvent pas développer ce type d'adaptation. Pourtant, plus de 200 espèces de serpents attrapent des proies dans l'eau.

A travers ce manuscrit, nous nous intéressons aux stratégies adaptatives développées par les serpents aquatiques afin de devenir de performants prédateurs. Deux hypothèses sont explorées : l'adaptation morphologique de la tête des serpents ainsi qu'une adaptation comportementale qui permettraient de réduire les contraintes hydrodynamiques. Des analyses morphologique et comportementale sont réalisées sur plusieurs espèces de serpents aquatiques afin de tester ces hypothèses. Les contraintes associées aux différentes formes de tête et comportements mis en évidence sont caractérisées à l'aide d'expériences d'hydrodynamique. L'interdisciplinarité qui est le cœur de ce manuscrit permet d'apporter un regard nouveau sur ces questions qui intriguent tant les biologistes que les physiciens.

General introduction

General introduction

Water as a driver of evolution: the example of aquatic snakes

Water plays a central role in the evolution of species. The first living organisms originated in water more than 3 billion years ago under the form of prokaryote cells. The chemistry and biology of the first cells were consequently driven by the properties of water and all organisms, both extinct and extant, are composed of cells that are mostly made of water. When multicellular forms emerged in water, they evolved in a way to be adapted to the properties of the fluid. The first amphibious organisms developed ways to be less dependent on this environment and conquered the terrestrial environment but remained highly dependent on water. Later, organisms managed to limit this dependency to drinking water and became completely terrestrial. Yet, several groups of terrestrial organisms have returned to the aquatic medium (e.g. aquatic mammals such as whales, dolphins, pinnipeds...). These organisms were initially adapted to terrestrial conditions, and needed to re-adapt to life under water. This return to an aquatic lifestyle required a drastic re-arrangement of organisms, from the organization of the skeleton to physiological processes (e.g. osmoregulation) (for an overview of recent examples see Houssaye & Fish 2016). But they also needed to cope with the physical properties of this fluid.

Water is a medium that is physically constraining in comparison with air, mainly because of its density, its viscosity, and its incompressibility (see Table 1). These properties induce a drastic change in the forces an aquatic animal has to deal with. For example, the propagation of signals such as chemicals, sound or vision will be highly impacted by the properties of the fluid. Thus, organisms that have returned to a life under water but that were initially adapted to hearing and smelling in air have had to adapt their sensory systems or to develop new senses such as pressure change detection (i.e. mechanosensory organs) (Crowe-Riddell et al. 2016). Locomotor abilities are also highly affected by the physics of water. On land, organisms have to deal principally with gravity whereas in water, gravity is largely compensated by buoyancy, since the density of the

water which is close to the density of the animal. However, as the density is the same, aquatic organisms have to develop a system to control their buoyancy to counterbalance their tendency to float at the surface. Moreover, the incompressibility principle implies that any movement of an organism will induce the surrounding fluid to move and/or will induce a motion of its own body (Sfakiotakis et al. 1999). Thus, a secondary return to an aquatic lifestyle has constrained animals to adapt their locomotion.

<i>Media</i> (at 20°C)	<i>Dynamic viscosity μ</i> (Pa.s ⁻¹)	<i>Density ρ</i> (kg.m ⁻³)	<i>Kinematic viscosity ν</i> (m ² .s ⁻¹)
Air	18.08x10 ⁻⁶	1.205	15.00x10 ⁻⁶
Freshwater	1.002x10 ⁻³	0.998x10 ³	1.004x10 ⁻⁶
Sea water	1.072x10 ⁻³	1.024x10 ³	1.047x10 ⁻⁶

Table 1: Comparison of the physical properties of air, freshwater and seawater, from (Vogel 1994).

Locomotion is one of the most important characteristics of animals as it is involved in many behaviors that are directly related to the fitness of an individual, such as to find a mate, to defend a territory, to escape a predator, or to find food. The latter two are particularly interesting behaviors as they push the animal to the limit of its performance, as it has to outperform the predator that is chasing it or the prey that is being chased. This Red Queen scenario or evolutionary arms race (van Valen 1973) impacts the locomotor abilities of these animals, pushing them to be highly performant. However, added to this co-evolution race are the physical constraints associated with locomotion under water. There are two main forces that act in opposition to the movement of an animal during locomotion in open water (Daniel & Webb 1987): hydrodynamic drag and acceleration reaction. The hydrodynamic drag is usually described separating two components: viscous drag (or skin friction) and pressure drag. The role of each of these in the force balance during locomotion depends on the properties of the flow, which are governed by the Reynolds number (Re).

The Reynolds number allows to characterize the fluid flow, either as laminar (i.e. all the particles of the fluid move in an orderly and unidirectional way) or turbulent (i.e. chaotic movement of the particles). This number is defined as the ratio of the inertial forces over the viscous forces, and its numerical definition is:

$$Re = \frac{lU}{\nu} = \frac{\rho lU}{\mu}, \quad (1)$$

where U is the velocity of the flow (or the object), ν is the kinematic viscosity of the fluid (cf. Table 1) and l is a “characteristic length”, which corresponds to any measure that reflects the dimensions of the flow (or the object). The latter feature is adaptable depending on the case. For example, for a flow in a circular tube, either the radius or the diameter of the pipe can be considered as the characteristic length. For an immersed object, by convention, the greatest length that is facing the flow is considered as the characteristic length (Vogel 1994). A small Reynolds number is associated with laminar flow, where the viscous forces are dominant, and a large Reynolds number characterizes a turbulent flow. According to the equation (1), a small object moving at low speed has a small Reynolds number, meaning that the main forces involved will be viscous forces. For large object at high velocity (i.e. large Re) the inertial forces will play a major role.

The critical value of Re depends on the geometry of the object. In the case of aquatic locomotion, some studies consider that turbulence occurs when $Re > 10^3 - 10^4$ (Gazzola et al. 2014; Landau & Lifshitz 1959). Thus, low Reynolds numbers, below this transition value, usually only apply for organisms at the microscopic or millimetric scale (e.g. bacteria swimming at $0.01\text{mm}\cdot\text{s}^{-1}$, $Re = 10^{-5}$; sea urchin sperm at $0.2\text{mm}\cdot\text{s}^{-1}$, $Re = 3\cdot 10^{-2}$; copepod at $0.2\text{m}\cdot\text{s}^{-1}$, $Re = 300$) (Vogel 1994). In other cases, Reynolds numbers are almost always in the turbulent regime (Fig. 1). The Reynolds number is very useful to simulate or build an experiment that mimics any behavior at a convenient scale. As an example, the fluid flow around a blue whale can be reproduced at a smaller scale by adapting the speed and/or the viscosity of the fluid, the same can be done for a bacteria swimming. Moreover, the respective contribution of the two components of the hydrodynamic drag and the acceleration reaction during locomotion in animals are highly dependent of the Reynolds number and so is the drag coefficient (Fig. 1).

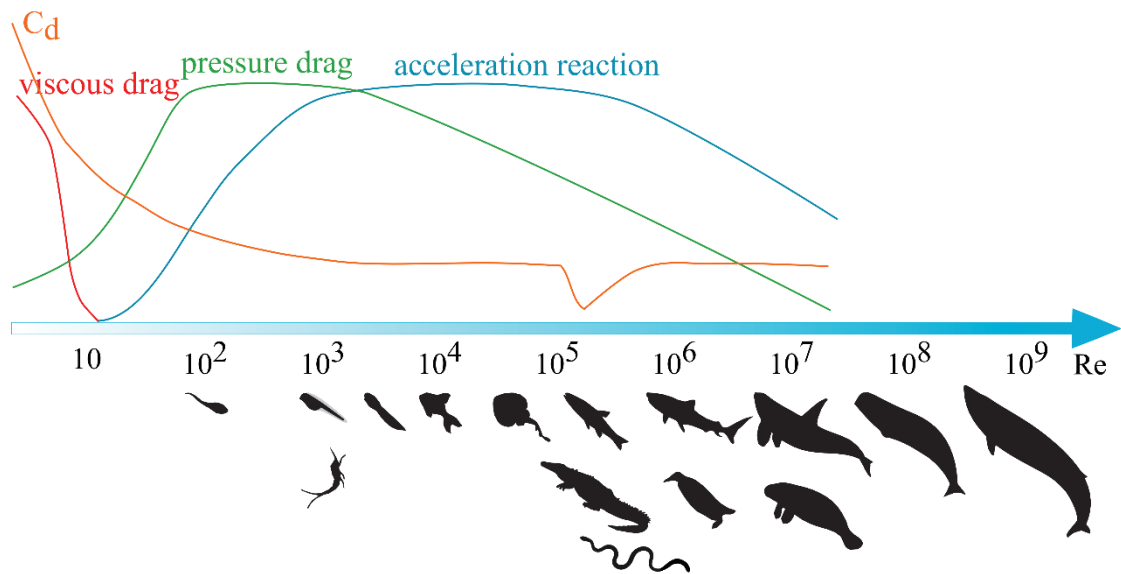


Figure 1: Scale of Reynolds number for swimming animals of different sizes, from larvae to large mammals. An approximate representation of the relative importance of force components during aquatic locomotion depending on the Reynolds number is given (based on Webb 1988; Gazzola et al. 2014; Vogel 1994). Note that the values are fictional as they depend not only on the Reynolds number, but also on the shape of the object and the kinematics of the motion, but the curves generally behave the same way.

The two components of drag have distinct characteristics. The viscous drag (or friction drag or skin friction) is related to the viscosity of the fluid and is always part of the forces applied to an animal during locomotion (Webb 1988). In simple terms, the viscous fluid will stick to the surface of the animal, and when the animal initiates a movement, the fluid will exert a force that will be opposed to this movement (Vogel 1994) (Fig. 2). At a microscopic scale, viscous drag is the main force that resists the movement. At a macroscopic scale, this force is reduced to a layer at the surface of an animal, which is called the “boundary layer”.

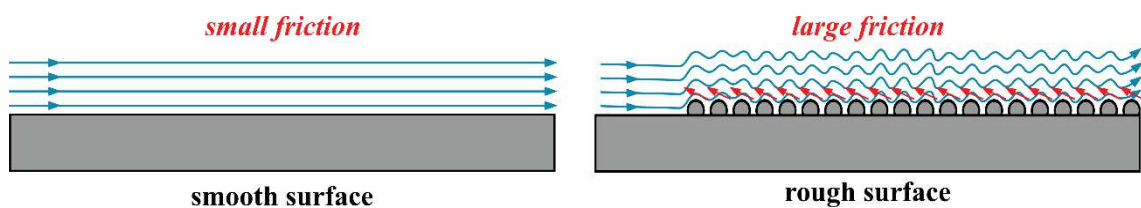


Figure 2: Illustration of viscous drag on a smooth and rough surface. Streamlines (blue) and arrows indicate the direction of the flow. Red arrows represent friction forces.

During locomotion in a fluid at high Reynolds number, a high pressure zone is generated at the front of the animal, and the flow tends to separate from the animal at the rear producing a recirculation zone that generates a low-pressure zone resulting in a pressure gradient between the front and the rear of the body (Fig. 3). This asymmetry in the pressure field results in a force that is opposed to the movement, this force is called the pressure drag and it is the second component of the drag. The pressure drag is also named form drag as mostly depends on the area that is facing the flow and thus, on the shape of the object. The pressure drag also depends on the Reynolds number and the respective importance of viscous and pressure drag can be approximated using the Reynolds number. The usual expression for the drag force is:

$$F_d = \frac{1}{2} C_d \rho S U^2; \text{ where } C_d = \left(\frac{\rho l U}{\mu} \right)^\alpha = f(Re), \quad (2)$$

where C_d is the drag coefficient that depends on the shape of the object and on the Reynolds number, ρ is the density of the fluid, S is the surface area that faces the flow and U is the velocity of the flow (or the object).

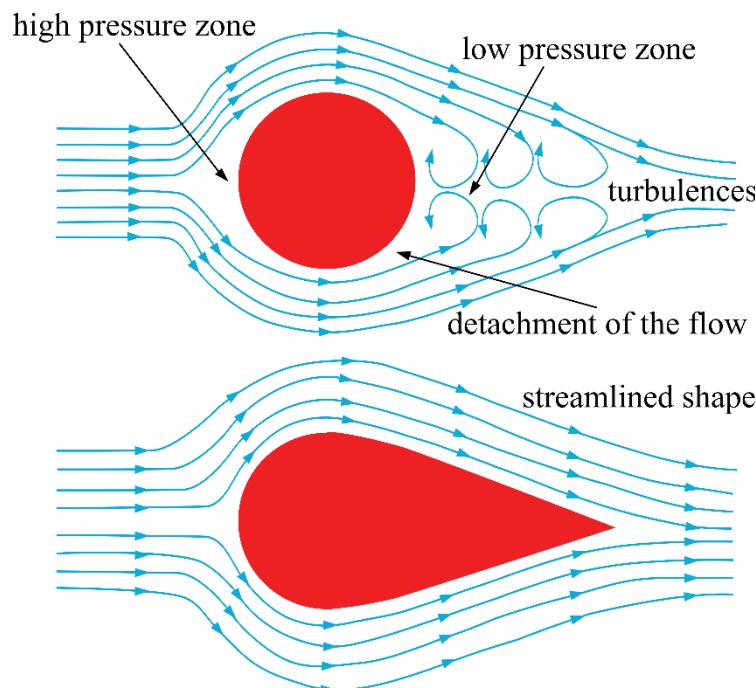


Figure 3: Pressure drag behind a sphere and comparison with a streamlined shape. For a streamlined body, the pressure drag is reduced because the flow can re-attach at the rear.

If the movement involves an acceleration then another force opposes motion, the acceleration reaction. When an object is accelerating, it accelerates a certain volume of the surrounding fluid. This volume has a certain mass, which is added to the own mass of the object during the acceleration; this mass is called the **added mass**. This mass of fluid that is accelerated depends on the properties of the fluid, the volume occupied by the object, the form of the object, and the acceleration (Vogel 1994; Webb 1988). The definition of the acceleration reaction is:

$$F = (m + M)a; \text{ where } M = C_a \rho V a, \quad (3)$$

where m is the mass of the object, M is the mass of the fluid that is accelerated, a is the acceleration, C_a is the added mass coefficient and V is the volume of the object.

The Reynolds number, the drag and the acceleration reaction, all are dependent of some aspect of the size and shape of the object. Thus, by changing the shape of the object, it should be possible to reduce the energy lost due to hydrodynamic constraints (Webb 1988) which are mainly caused by the separation of the flow at the rear of the object.

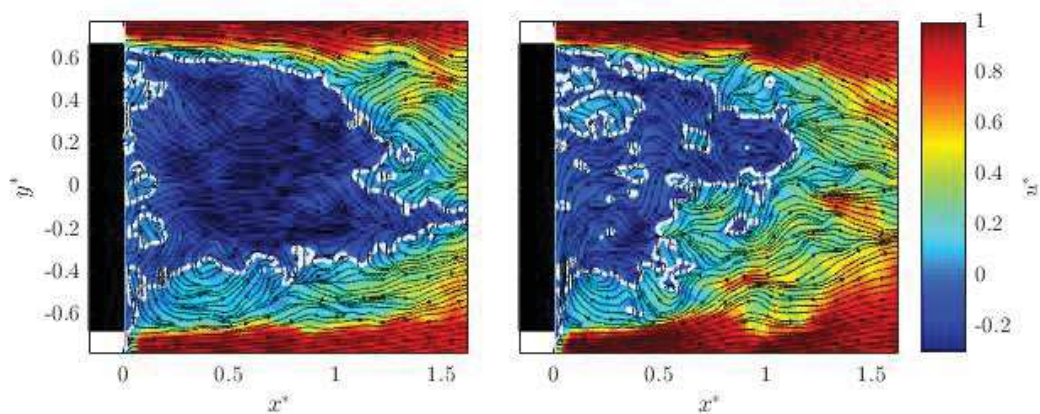


Figure 4: Visualization of the turbulent wake in 2D at the rear of a simplified model of a car visualized using particle image velocimetry. The flow is going from the left to the right. The colormap represents the velocity of the flow in $m \cdot s^{-1}$. The plane is located at the middle height of the car. The image on the left is the wake of a non-modified car and on the right propulsive jets have been added to reduce the drag (Varon 2017).

Adapting the shape to reduce the separation effect is called “streamlining”, it consists of a modification of the rear part of the object to allow the flow to re-attached at and thus to avoid the pressure differential that causes pressure drag (Fig. 3). This is a huge challenge for fluid mechanicians working on airplane, car and boat design (Fig. 4) but it is also a challenge in an evolutionary context.

Aquatic animals also have to deal with these hydrodynamic constraints during locomotion. Locomotion is involved in almost all the fitness-relevant activities of a fully aquatic animal, meaning that their survival depends on their locomotor abilities. These animals have to move to find food, to find a mate, to escape predators, and this, at a minimal energetic cost. Foraging (i.e. from searching for food to the ingestion of the prey) is particularly interesting for several reasons. The first is the involvement of feeding in fitness; feeding is the behavioral sequence leading to the energy intake of an animal which will basically fuel any behavior and activity of the animal (Bennett 1980; Vitt & Congdon 1978; Huey & Pianka 1981). Second, there are two main foraging strategies in animals: “sit-and-wait” and “active searching” (Huey & Pianka 1981; Eckhardt 1979) that involve different types of locomotion. The active searching involves swimming at constant speed over a long period of time whereas sit-and-wait involves a burst of acceleration toward the prey. Regarding the hydrodynamic constraints, both induce drag but the sit-and-wait strategy also implies acceleration reaction forces. As foraging has a central role for survival and as it requires specific adaptations to deal with the hydrodynamic constraints, it is a perfect model to study how the physical constraints related to the environment can impact the evolution of the phenotype of a species.

Adaptations to the aquatic media are numerous; the most famous example being the streamlined body of aquatic animals (Howell 1971) (Fig. 5). These animals are very distant in terms of their phylogenetic relationships, yet they have evolved similar shapes. This illustrates that evolution of body shape is constrained by the physical characteristics of the medium and that optimal solutions are limited for animals such as vertebrates. This phenomenon is called evolutionary convergence or convergence. As Lewontin wrote in his book: *“It is no accident that fish have fins, aquatic mammals have altered their appendages to form finlike flippers, ... and even seasnakes, lacking fins, are flattened in cross-section. It is obvious that these traits are adaptations for aquatic locomotion”*.

(Lewontin et al. 1984). This streamlined phenotype allows these animals to reduce the pressure drag (Webb 1988). It can be noted that, despite their shared body shape, these animals use different swimming behaviors: most fish, most reptiles, and most aquatic mammals use undulatory swimming, where the propulsor is the tail which is called lift-based propulsion, whereas birds use their limbs as paddles using what is called drag-based propulsion (Webb 1988). Semi-aquatic animals such as penguins, turtles, pinnipeds, have to deal with both land and water-related constraints including gravity and hydrodynamic constraints. Consequently most of them use drag based swimming (Fish 1993).

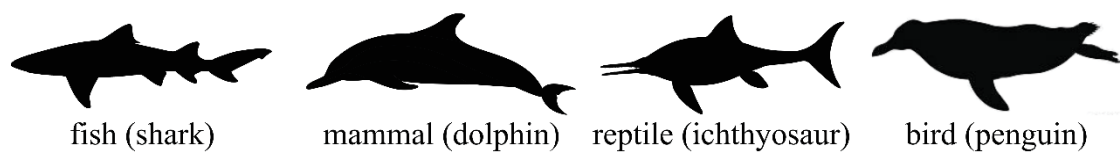


Figure 5: Morphological convergence of the streamlined body of phylogenetically distant groups, inspired from Howell (1971).

Adaptations for swimming efficiency and so for drag reduction and thrust maximization have been extensively studied in animals, both experimentally and computationally (Gazzola et al. 2014; Sfakiotakis et al. 1999; Webb 1971a; Webb 1971b; Tytell 2004; Fish 1993). Similarly, adaptations for feeding have also been studied as the kinematics are different in different predators and especially for those feeding on elusive prey. As the prey evolves in a way to detect the predator before being captured, the predator needs to be faster than the prey. Thus, the prey capture behavior requires an acceleration phase that involves acceleration reaction forces and consequently the animal is pushing a certain amount of water. This plus the increased pressure at the front could potentially push the prey away from the mouth of the predator (Vincent et al. 2004; Vincent et al. 2005; Van Wassenbergh et al. 2010; Young 1991; Herrel et al. 2008; Taylor 1987). To circumvent this, aquatic animals have developed either a “pincer jaw” which consists in a pair of long and slender jaws and use sideways motion to capture the prey (e.g. gharials, ichthyosaurs, some dolphins, garpikes). The long and slender shape allows avoiding displacing too much water with the mouth during the closure. However, this long apparatus has some disadvantages during locomotion as it will increase the pressure

drag if not aligned in the direction of the movement (Taylor 1987). Another strategy has evolved and is used by most of the aquatic predators: suction feeding (Deban & Wake 2000; Wainwright et al. 1989; Muller & Osse 1984; Lauder & Prendergast 1992; Van Damme & Aerts 1997; Werth 2006). Suction feeding consists in generating a negative intra-oral pressure by an expansion of the bucco-pharyngeal cavity which is typically generated by a rapid depression of the hyoid apparatus. Thus, the prey is drawn into the mouth of the predator with the engulfed water (Fig. 6).

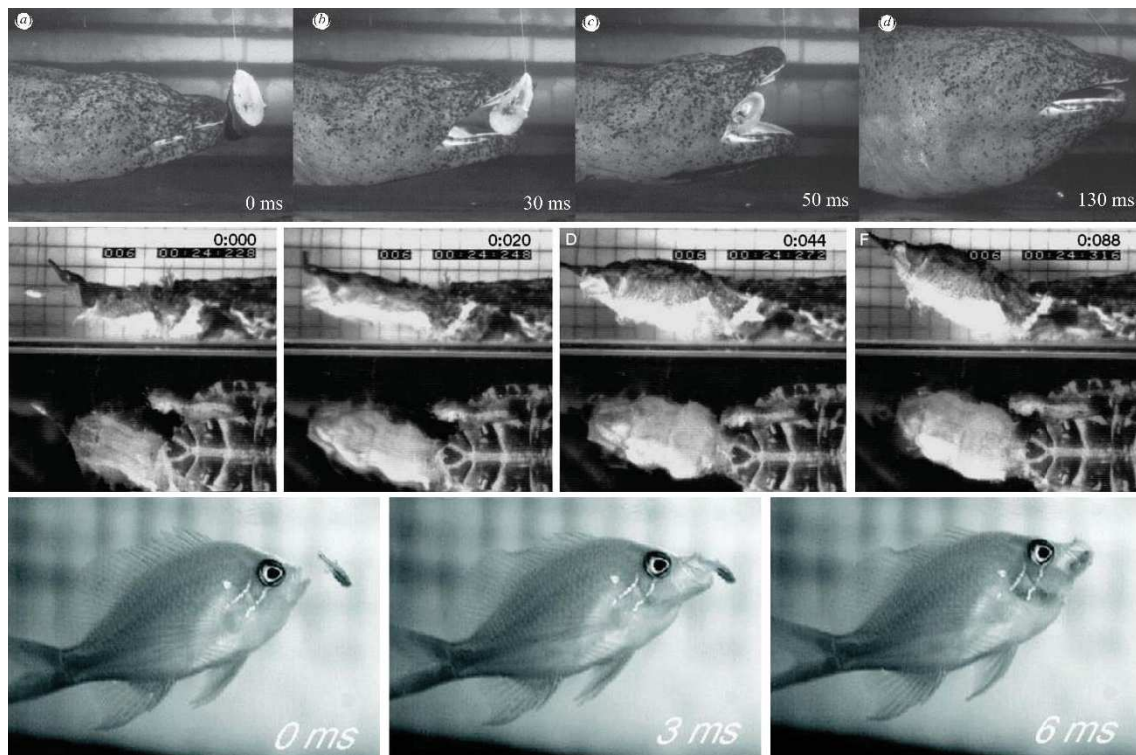


Figure 6: Sequence of suction feeding in salamander (*Andrias davidianus*) (Heiss et al. 2013), a turtle (*Chelonia fimbriatus*) (Lemell et al. 2002) and a fish (*Serranocirrhinus latus*) (Oufiero et al. 2012). Time is indicated in ms on each picture.

These two strategies occur in distantly related species and as such they are examples of convergent phenotypes in response to the physical constraints of capturing prey under water. It may then seem like underwater feeding is closed case requiring no further study. Yet, there is a third case that has not been explored in great detail. Some animals have

not developed any of these strategies but they are nevertheless successful aquatic predators: aquatic snakes.

Snakes are among the most ecologically and evolutionary successful groups of vertebrates (Gans 1961). Despite their uniform appearance (i.e. their limbless body) they have invaded all possible habitats; some are terrestrial ranging from the desert to high elevation in the mountains; arboreal, aquatic, ranging from freshwater to marine; and some have fossorial habits (Fig. 7).



Figure 7: Ecological and morphological diversity of snakes. Top line from left to right: Asian vine snake (*Ahaetulla prasina*); Gaboon viper (*Bitis gabonica*) © Tyron Ping; sidewinder (*Crotalus cerastes*), bottom line: Blyth's earth snake (*Rhinophis blythii*) and leucistic elegant sea snake (*Hydrophis elegans*) © Giuseppe Mazza.

Among the approximately 3364 extant species of snakes, more than 10% use the aquatic medium either for occasional foraging or on a regular basis (e.g. sea snakes or some homalopsids (Murphy 2012). The return to an aquatic life has occurred several times independently during the evolutionary history of snakes (Fig. 8).

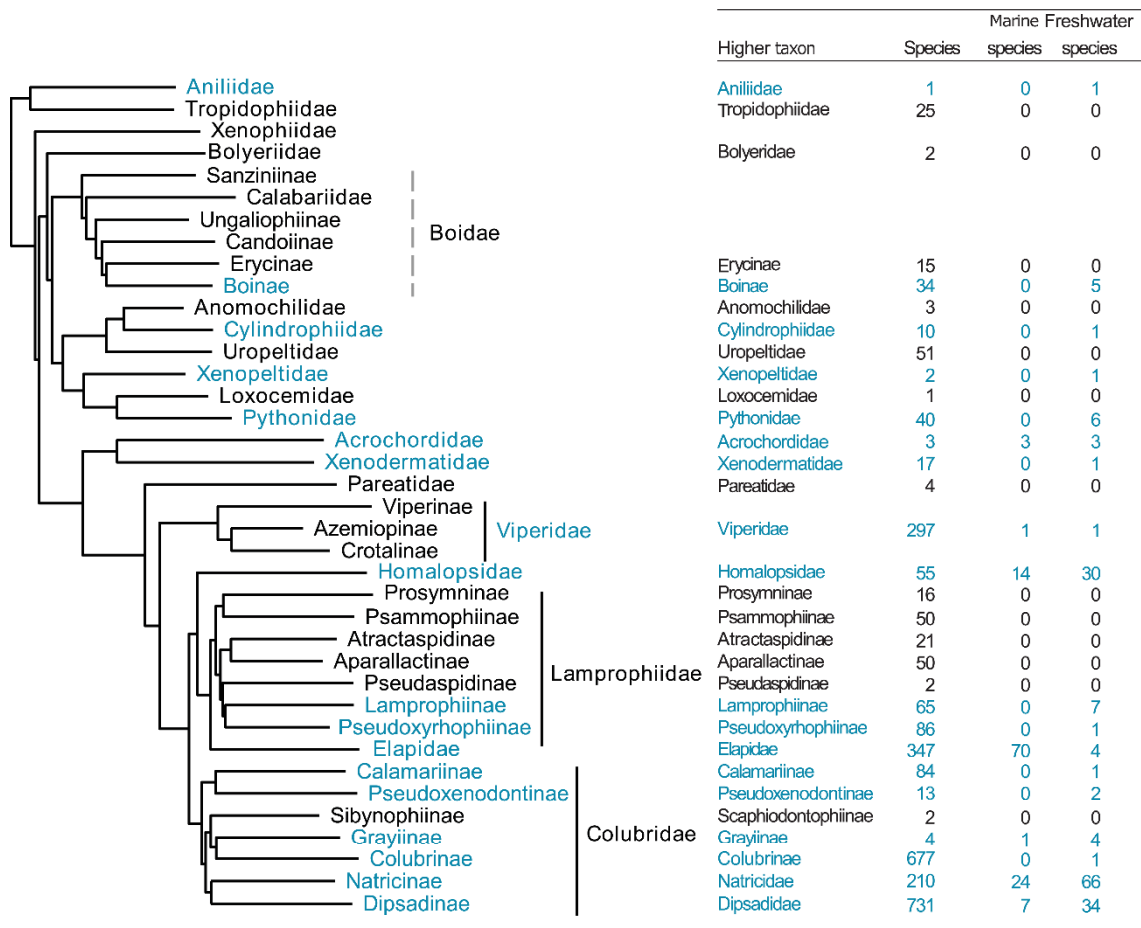


Figure 8: Phylogeny of families and subfamilies of snakes from Pyron et al. 2013 and a table with the number of species that have invaded the aquatic medium in each clade adapted from Murphy 2012. (Note that Sibynophiinae and Scaphiodontophiinae are synonymous).

Among these species, some are fully aquatic such as sea snakes (Hydrophiinae) and sea kraits (Laticaudinae) that are part of the Elapidae and represent 70 species. Other groups are highly aquatic and spend most of their time under water such as some Homalopsidae or Acrochordidae. These species present specific adaptations related to their aquatic lifestyle such as salt glands (Dunson & Dunson 1973), mechanoreceptors (Crowe-Riddell et al. 2016; Povel & Van Der Kooij 1997), or a lateral compression of

the body and a paddle-like tail (Lillywhite 2014). However, these snakes do not present any of the two typical strategies to reduce the hydrodynamic constraints associated with prey capture. They do not have a typical “pincer-jaw” and they cannot perform suction because of their highly reduced hyoid apparatus, due to the specialization of their tongue for chemoreception (Schwenk 1994; Langebartel 1968). This prevents them from expanding their bucco-pharyngeal cavity to generate suction. Nevertheless, there is a large number of snake species that manage to capture elusive prey under water, implying that they have potentially evolved another strategy to circumvent the hydrodynamic constraints related with prey capture under water. One might think that the slender profile of snakes makes them streamlined enough to reduce the drag associated with prey capture but aquatic snakes tend to chase their prey with the mouth opened (Vincent et al. 2009; Fabre et al. 2016; van Netten 2006; McHenry et al. 2009). This behavior should have a dramatic impact on the pressure drag as the frontal area that faces the flow largely increases when the snake opens its mouth.

The central question of this thesis is then: how do snakes cope with the hydrodynamic constraints to successfully capture a prey underwater? Two hypotheses have been explored; the first is a convergence in head shape towards a more streamlined phenotype that confers a hydrodynamic advantage to the aquatically foraging snakes. Snakes are limbless animals that use their head to capture prey. Thus, their head is under a strong selective pressure. The cost of prey capture underwater is related to the pressure drag and the added mass; thus a modification of the head shape is expected. Furthermore, the hypothetical solutions to reduce drag and added mass are limited, and so convergence is expected (Taylor 1987; Young 1991; Webb 1984). This hypothesis is tested in Chapter 1 by using 3D geometric morphometrics on a broad sample of species, comparing 62 aquatically foraging species with 21 phylogenetically close species that do not forage under water.

In Chapter 2, the potential hydrodynamic advantage of a convergent head shape is explored using a fluid mechanics experiment in which the shapes associated with the aquatic and the non-aquatic species are 3D printed. Next, a setup was built to mimic a frontal underwater attack. Force measurements and particle image velocimetry are used to assess the hydrodynamic forces and fluid flow in relation to each head model.

In Chapter 3, the variability of head shape among aquatically foraging species was analyzed in greater detail to assess whether the different phenotypes are related with other ecological or anatomical features. I also explored whether this variability is an example of many-to-one mapping of form to function. A many-to-one mapping occurs when several phenotypes give rise to the same functional response (Wainwright et al. 2005). Here, the hydrodynamic characteristics is the function so different head shapes were 3D printed and tested to assess the hydrodynamic forces associated with each phenotype.

The second hypothesis about how snakes deal with the hydrodynamic constraints is by an adaptation of their prey capture behavior. Indeed, two strategies of attack have been described in aquatically foraging snakes: the lateral and the frontal strikes (Herrel et al. 2008). The aim of this part is to link morphology and function by focusing on the link between head shape and the prey capture strategy; in other words, is a specific shape related with a specific behavioral strategy? This question is tackled in Chapter 4.

The ultimate goal of this work is to draw the link between morphology, behavior and hydrodynamics in aquatically foraging snakes in light of the morphology-performance-fitness paradigm (Arnold 1983) (Fig. 9).

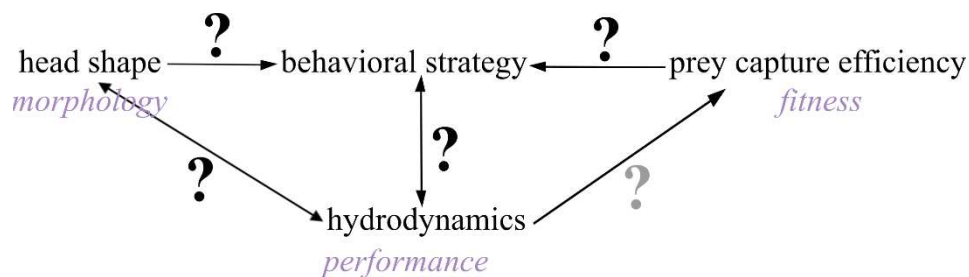


Figure 9: Scheme of the hypothetical relationships between the hydrodynamic constraints, the morphology of the head shape and the behavior of aquatically foraging snakes. In purple are represented the components of Arnold's paradigm.

Chapter 1

**Does aquatic foraging impact head
shape evolution in snakes?**

Does aquatic foraging impact head shape evolution in snakes?

2016, Proceeding of the Royal Society London, B Biological Sciences 283(1645)

Abstract

Evolutionary trajectories are often biased by developmental and historical factors. However, environmental factors can also impose constraints on the evolutionary trajectories of organisms leading to convergence of morphology in similar ecological contexts. The physical properties of water impose strong constraints on aquatic feeding animals by generating pressure waves that can alert prey and potentially push them away from the mouth. These hydrodynamic constraints have resulted in the independent evolution of suction feeding in most groups of secondarily aquatic tetrapods. Despite the fact that snakes cannot use suction they have invaded the aquatic milieu many times independently. Here we test whether the aquatic environment has constrained head shape evolution in snakes and whether shape converges on that predicted by biomechanical models. To do so, we used 3D geometric morphometrics and comparative, phylogenetically informed analyses on a large sample of aquatic snake species. Our results show that aquatic snakes partially conform to our predictions and have a narrower anterior part of the head and dorsally positioned eyes and nostrils. This morphology is observed irrespective of the phylogenetic relationships among species suggesting that the aquatic environment does indeed drive the evolution of head shape in snakes, thus biasing the evolutionary trajectory of this group of animals.

Key words: aquatic snakes, head morphology, hydrodynamics, constraints, convergence, geometric morphometrics

Introduction

Physical constraints imposed by the environment play an important role in the evolution of species. Evolution can be predictable when the constraints caused by the physical environment are strong (Herrel et al. 2008). When different species are faced with similar constraints, convergence in morphology or behavior is predicted (Winemiller et al. 1995; Schluter 2000). The study of convergence can help understand whether and how the constraints imposed by the physical environment drive phenotypic diversification. The physical properties of water induce strong constraints on physiology, anatomy and behavior resulting in a suite of adaptations in animals that have secondarily invaded the aquatic environment (Taylor 1987; Gans 1969; Vogel 1994). In spite of these hydrodynamic constraints, numerous species with diverse phylogenetic backgrounds have invaded aquatic habitats. The range of phenotypic responses in vertebrates is, however, limited by functional and structural constraints, leading to convergence as is observed for underwater locomotion (Videler et al. 1999; Howell 1971; Fish 1993) or feeding (Taylor 1987).

Underwater prey capture is extremely challenging. Indeed, any movement through water is resisted by the drag and inertial forces acting on the body of the animal. These forces are greater than in air because of the greater density and viscosity of the fluid. When animals attempt to catch prey underwater, the forward motion of the strike will involve the generation of a pressure wave that has two main adverse effects: it tends to push the prey away from the predator (Van Wassenbergh et al. 2010), and may trigger the escape response of the prey. Indeed, very fast escape responses, called C-starts or S-starts in fish, can be triggered by chemical cues emitted by prey or predators (Chivers & Jan 1998; Feminella & Hawkins 1994) or by physical cues such as water displacement (Faber et al. 1989; Zottoli 1977; Zeddies & Fay 2005). Both the diffusion of chemical compounds and physical cues highly depend on water displacement and consequently, predators have to limit the amount of water that they displace when chasing or attacking a prey.

To circumvent these constraints, aquatic predators have developed strategies such as suction feeding that help compensate for the displacement of water by the predator.

This behavior involves an expansion of the bucco-pharyngeal cavity owing to the displacement of the hyobranchial apparatus (i.e. the apparatus that supports the tongue in terrestrial tetrapods). Thus, a low pressure zone is created inside the mouth of the predator that drags the surrounding water and prey into the mouth. This is one of the most widespread aquatic prey capture strategies in vertebrates (Deban & Wake 2000; Wainwright et al. 1989; Muller & Osse 1984; Lauder & Prendergast 1992; Van Damme & Aerts 1997). Snakes, however, have a reduced hyoid apparatus because of the specialization of their tongue for chemoreception (Langebartel 1968; Schwenk 1994) and consequently are not able to expand their bucco-pharyngeal cavity. Despite this limitation, a secondary return to an aquatic lifestyle has occurred independently in many snake genera (Murphy 2012). Moreover, numerous species of snakes are proficient in the capture of elusive aquatic prey and some species have become entirely piscivorous (Alfaro 2002; Lillywhite 1996; Murphy 2007; Glodek & Voris 1982; Heatwole 1987). As drag is highly dependent on the shape of the head, and impairs the swimming or targeting efficiency of the predator (Taylor 1987; Van Wassenbergh et al. 2010) the 'ideal' aquatic snake should have a slender, streamlined, narrow and long head (Young 1991; Taylor 1987; Savitzky 1983). However, prey capture is not the only selective pressure acting on head morphology in snakes. Indeed, snakes use their head not only to capture prey but also to handle and swallow them. Prey handling and swallowing prey are performed by means of a 'pterygoid walk' (Cundall & Gans 1979; Boltz & Ewer 1964) which is more efficient in snakes with wider heads and longer quadrates (Young 1991). Thus, the 'ideal' morphology for an aquatic snake is likely determined by the trade-off between a streamlined head that is still able to swallow large or bulky prey efficiently.

Previous studies that have compared head shape in snakes have mainly focused on skull bones or scalation and/or used linear measurements to quantify morphology (Vincent et al. 2004; Marx & Rabb 1972; Savitzky 1983; Camilleri & Shine 1990; Vincent et al. 2006; Murphy 2012; Hibbitts & Fitzgerald 2005). In the present study we test the hypothesis that the physical constraints related to underwater prey capture constrain head shape evolution in aquatic snakes. We hypothesize that the head shape of snakes that are able to capture elusive prey underwater has converged to an 'optimal' shape. We predict that these snakes will present narrower and longer heads compared to

snakes that do not capture prey under water. Our predictions follow previous work on aquatic snakes (Hibbitts & Fitzgerald 2005; Young 1991) but here we provide a large and diverse sample of aquatic snakes in order to test the generality of these predictions in snakes that capture elusive aquatic prey. We use 3D geometric morphometric approaches (Gunz & Mitteroecker 2013; Adams 2014) to quantify the shape of the entire head as the hydrodynamics of movement under water will likely impact the overall shape of the head. We include species representing all families of snakes in which aquatic prey capture has evolved. These species are compared with closely related species of snakes that do not eat aquatic prey, within an explicit phylogenetic framework. Finally, we describe the head shape associated with species that capture elusive prey under water and compare it to a priori predictions based on previous studies (Young 1991; Taylor 1987; Hibbitts & Fitzgerald 2005; Savitzky 1983) and biomechanical models (Herrel et al. 2008).

Materials & Methods

Specimens

3D scans of the heads of 419 snakes were obtained using a high resolution surface scanner: a Stereoscan^{3D} Breuckmann white light fringe StereoSCAN3D with a camera resolution of 1.4 megapixels, available at the Museum National d'Histoire Naturelle, Paris (Fig. 10). The specimens came from different collections; the collections of the Museum National d'Histoire Naturelle, the Field Museum of Natural History, the American Museum of Natural History, the California Academy of Sciences, the personal collection of Anthony Herrel, and the personal collection of Antoine Fouquet. Only specimens with a well-preserved head and closed mouth were scanned. At least five specimens per species were used in this study where possible (Appendix 1).

We included 83 species of snakes in total. We considered as 'aquatic' species of snakes that consume elusive aquatic prey (e.g. fish, amphibians, crustaceans...) and as 'non-aquatic' those that do not eat aquatic prey (See Appendix 1 for references on the diet). We tried to choose at least one aquatic species among each family of snakes in which a return to an aquatic lifestyle has occurred. Non-aquatic species were chosen to

be phylogenetically close to the aquatic species in our analysis (Pyron et al. 2013). In total, we compared 62 aquatic species with 21 species that do not feed on elusive aquatic prey (Appendix 1). The phylogenetic tree of Pyron (Pyron et al. 2013) was pruned in Mesquite 3.03 (Maddison & Maddison 2015) to only keep the species included in our data set (Appendix 2).



Agkistrodon contortrix *Laticauda colubrina* *Tachymenis peruviana*

Figure 10 : Example of 3D scans of the head of some specimens of snakes analyzed in this study from three different species with three different views.

Geometric morphometrics

To quantify shape variation between species, we recorded the 3D coordinates of 10 landmarks and 6 curves (Fig. 11) using the 'Landmark' software package (Wiley et al. 2005). These landmarks include both anatomical landmarks and maxima of curvature (Appendix 3). To assess the repeatability of the landmark positioning, we placed the set of landmarks ten times on three specimens of the same species and checked if the variability between specimens was higher than the variability related to the landmark positioning (Appendix 4). To obtain an accurate description of the head shape, we created a template consisting of 921 landmarks including 10 anatomical landmarks, 74 sliding-landmarks on curves and 837 sliding-landmarks on the surface of the head (Fig. 11) (Gunz & Mitteroecker 2013). This template was positioned based on the anatomical landmarks and curves for each specimen. Next, semi-landmarks were projected onto the surface of the specimen and allowed to slide while minimizing the bending energy between the template and the specimen (Botton-Divet et al. 2015; Gunz & Mitteroecker 2013). The sliding procedure was performed using the Morpho package (Schlager 2013) in R (R

Development Core Team 2014). After sliding, all landmarks were rendered symmetrical, a Procrustes superimposition was run (Rohlf & Slice 1990) and an average head shape per species was calculated in MorphoJ (Klingenberg 2011). A principal component analysis (PCA) was then run using the Rmorph library (Baylac 2012) to evaluate the overall shape variation in the dataset. The first 11 principal components (PC) accounting for more than 95% of the shape variability were extracted and used for further analyses (Table 2).

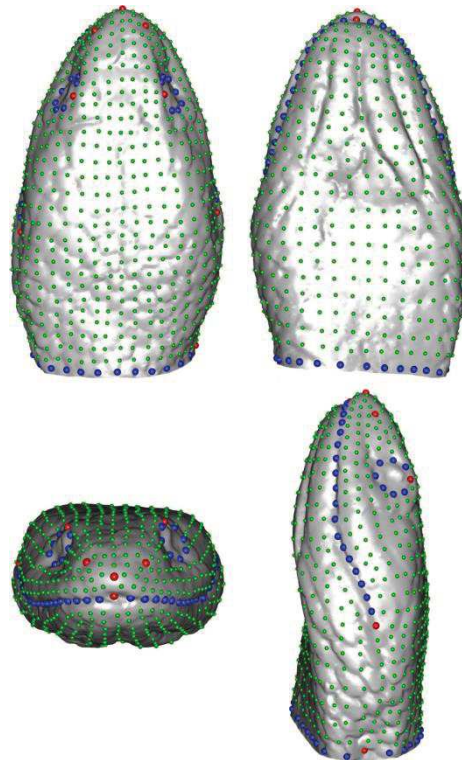


Figure 11: Template used for the geometric morphometric analyses. Anatomical landmarks are indicated in red, semi-landmarks on curves in blue and surface semi-landmarks in green.

Analyses

We first assessed whether a phylogenetic signal was present in the data set using the multivariate version of the K-statistic (Blomberg et al. 2003; Adams 2014). This test was performed using the ‘geomorph’ library (Adams & Otárola-Castillo 2013) in R. Next, the univariate K-statistic was calculated to test for phylogenetic signal in the first eleven PC axes using the ‘picante’ library in R (Kembel et al. 2010). Given that a significant

phylogenetic signal was detected, a phylogenetic MANOVA was performed on the first eleven PC axes to test for differences in shape between species that capture elusive aquatic prey and those that do not. Subsequently we ran phylogenetic ANOVAs to evaluate which axes contributed to the observed differences in head shape. To evaluate whether size impacted the results we ran a MANCOVA with the Log10-transformed centroid size as a covariate. Finally, a linear discriminant analysis (LDA) was performed. We extracted the shapes associated with species that capture elusive aquatic prey and those that do not (Fig. 12). Reclassification rates using a leave-one-out cross validation were then calculated. To relate the observed shape differences to differences in hydrodynamics we opened the jaws of the shapes extracted from the LDA in silico (Blender 2.75). The gape angle was set at 70° for both models based on *in vivo* video recordings of snakes striking (Herrel et al. 2008; Bilcke et al. 2006; Vincent et al. 2005). Next, we measured the size of the jaws as well as the projected frontal surface area (area of the mouth facing the current) to assess the drag associated with both shapes during prey capture (Table 3). Finally, we also measured the projected frontal surface area for identical gape distance (Table 3). All statistical analyses were performed using R (R Development Core Team 2014). The significance level of all statistical tests was set at 5%.

Results

The first and the second axes of the PCA respectively accounted for 49.3% and 13.7% of the overall variability (Table 2). We detected a phylogenetic signal in our morphological dataset ($P = 0.001$) with a multivariate K that was less than one ($K_{\text{mult}} = 0.34$). The univariate K-statistics are significant for the majority of the PC axes with K-values around 0.3 (Table 2).

The phylogenetic MANOVA reveals significant differences between the head shapes of snakes that capture elusive aquatic prey and those that do not (Wilk's lambda = 0.47, $F_{1,81} = 7.25$, $P_{\text{phy}} = 0.0009$). Phylogenetic ANOVAs run on each of the PC axes highlight a significant difference between the two groups on the axes 2 and 9 (Table 2, Appendix 5). Both ecology and size impact the head shape of snakes (MANCOVA:

ecology: $F_{1,79} = 7.83$, $P < 0.001$; size: $F_{1,79} = 3.25$, $P = 0.001$) but the interaction between both was not significant (MANCOVA: $F_{1,79} = 0.68$, $P = 0.7$).

	Proportion of variance (%)		Univariate K statistics		Phylogenetic ANOVA	
	Proportion	Cumulative proportion	K	P-value	$F_{1,81}$	P-value
PC1	49.3	49.3	0.37	0.0009	3.23	0.1
PC2	13.7	63.0	0.34	0.0009	30.62	0.0009
PC3	7.3	70.3	0.41	0.0009	0.64	0.5
PC4	6.6	76.9	0.28	0.001	0.46	0.5
PC5	5.6	82.6	0.24	0.1	4.82	0.06
PC6	4.0	86.6	0.25	0.04	0.001	0.9
PC7	3.0	89.7	0.30	0.3	0.15	0.7
PC8	1.8	91.5	0.26	0.02	0.43	0.5
PC9	1.5	93.0	1.45	0.0009	8.25	0.02
PC10	1.1	94.2	0.37	0.004	1.03	0.4
PC11	0.8	95.0	0.30	0.0009	2.88	0.1

Table 2: Results of the statistical analyses performed on the first eleven principal components. Statistical significance highlighted in bold.

The following shape description is based on the linear discriminant analysis that allowed us to extract mean head shapes for species that capture elusive prey under water and those that do not (Fig. 12). The linear discriminant analysis shows a difference between the aquatic group and the non-aquatic one ($F_{1,81} = 9.54$, $P = 0.002$). The LDA reclassification rates are high (LDA: aquatic group = 89%; non-aquatic = 71%) meaning that the linear discriminant function accurately describes the differences between groups.

As the ‘non-aquatic’ group is non-homogeneous (i.e. species were selected to because they are closely related to an aquatic species or group of species only) we here focus only on differences between aquatic and non-aquatic species and the shape observed in the aquatic group. The shape associated with the ‘non-aquatic’ group is globally oblong with the head-neck transition that is clearly marked. The shape associated with snakes that capture elusive prey under water is strikingly different (Fig. 12). The anterior part of the head is proportionally narrower in the aquatic species whereas the posterior part is larger in comparison with the non-aquatic foragers. The height, width and length of the anterior part are lower in the aquatic snakes. The posterior part of the

head is longer and the jaw is proportionally shorter in the aquatic species. Additionally, the shape of the mouth profile is more curved in the aquatic species. The eyes are proportionally smaller and more dorsally positioned in the aquatic species whereas they are positioned on the lateral side of the head in the 'non-aquatic' species. Likewise, the nostrils are in a more dorsal position and closer to each other in the 'aquatic' species whereas they are positioned more laterally in the 'non-aquatic' ones. In absolute terms and both when controlling for gape angle and gape distance, the size of the parts of the head that face the fluid flow are smaller in the aquatic group, both in terms of projected frontal surface area and linear measurements. The only feature that is greater in the aquatic group is the maximal width of the mouth which is the distance between the commissures of the mouth (Fig. 12, Table 3).

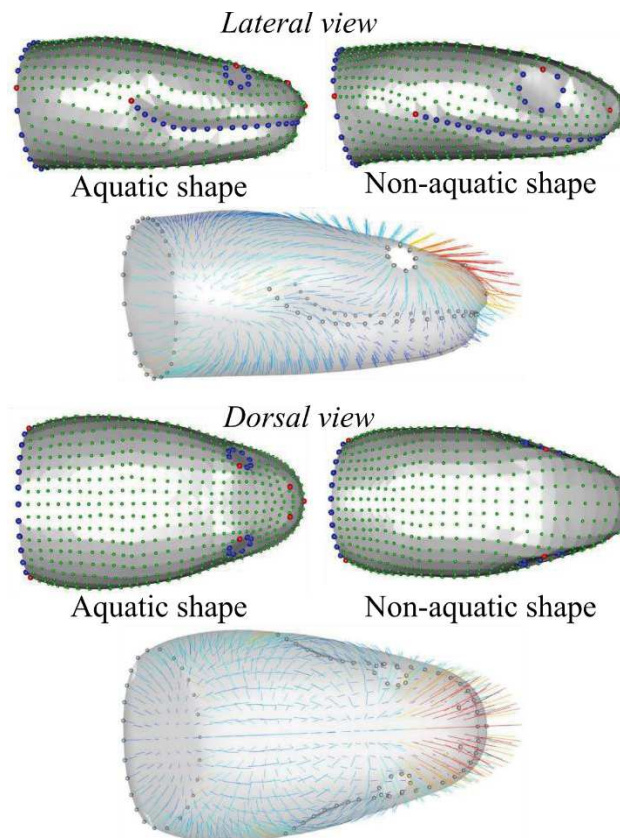
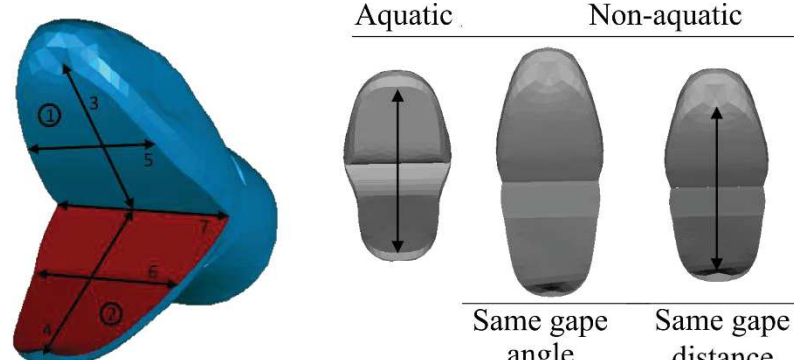


Figure 12: Results of the linear discriminant analysis illustrating the head shapes associated with species capturing elusive aquatic prey on the left and the non-aquatic ones on the right. Anatomical landmarks are indicated in red, semi-landmarks on curves in blue and surface semi-landmarks in green. Vectors are colored by deformation intensity from dark blue to red and from the aquatic to the non-aquatic shape.



	Aquatic	Non-aquatic	
		Same gape angle	Same gape distance
Projected surface area		33.9%	19.7%
1. area of the upper jaw			17.6%
2. area of the lower jaw			17.5%
3. length of the upper jaw			17.6%
4. length of the lower jaw			17.7%
5. width at the middle of the upper jaw			7.5%
6. width at the middle of the lower jaw			8.7%
7. maximal width of the mouth	9%		

Table 3: Quantitative comparison between the aquatic head shape and the non-aquatic one. Measurements are indicated by number on the first scheme. The shapes associated with both ecologies are at the same scale. The non-aquatic gape was adjusted to be equal to the aquatic shape gape distance or gape angle. Values in the table indicate the percentage of extra surface or length.

Discussion

We detected a significant phylogenetic signal in our dataset meaning that the head shape of the snakes in our data set is at least partly constrained by shared ancestry. As the multivariate K was lower than one, species resemble each other less than expected under Brownian motion evolution. One possible explanation of such a result is convergent evolution to specific environmental constraints (Blomberg et al. 2003). The analyses of the overall shape variation in the dataset highlighted differences in head shape between the species that capture elusive prey under water versus those that do not. We found two PC axes (PC2 and PC9) that statistically differentiate between aquatic and non-aquatic snakes irrespective of phylogeny. This demonstrates that the selective pressure associated with the underwater capture of elusive prey is strong enough to drive convergence in head shape across snakes despite a significant phylogenetic signal. Although snakes that

capture elusive prey under water have evolved independently many times in the evolutionary history of snakes, most studies to date have focused on a single family, the natricines (Drummond 1985; Hibbitts & Fitzgerald 2005; Bilcke et al. 2006; Vincent et al. 2009; Herrel et al. 2008). Our results show that convergence in head shape is independent of phylogeny and suggest that the aquatic medium has indeed constrained the evolutionary trajectory of these animals.

Snakes that capture elusive prey under water tend to have narrower heads as predicted *a priori*, but only for the anterior part of the head. The head is also dorsoventrally flattened in comparison with species that do not capture elusive aquatic prey. This dorso-ventral compression of the head is a feature that has been suggested to be associated with an aquatic life-style and the need to be more streamlined in aquatic reptiles in general (Taylor 1987). Proportionally, aquatic snakes have an enlarged posterior part of the head. This could reflect a solution to the trade-off between the need for a more streamlined head to circumvent the physical constraints of underwater prey capture, and the need to be able to swallow large or bulky prey. The jaw is shorter in species that capture elusive aquatic prey in contrast to results of previous studies (Hibbitts & Fitzgerald 2005). Moreover, the mouth is more curved, which, once the mouth is opened (Table 3) allows a large opening while limiting the surface area facing the flow. The reduction of both length and width of the front part of the head were predicted by Taylor (Taylor 1987). Indeed, these parts of the head play a major role in prey capture in snakes. The opening of the mouth during underwater prey capture produces considerable drag that can decrease capture success (Taylor 1987; Young 1991; Hibbitts & Fitzgerald 2005; Van Wassenbergh et al. 2010). As the hydrodynamic drag force is proportional to the surface area of the object that moves perpendicularly to the flow, a reduction in both length, width and surface area of the mouth likely decreases the drag associated with the open-mouth capture typically observed in these animals as suggested by the lower projected frontal surface area (Van Wassenbergh et al. 2010; Taylor 1987). In contrast, the head of aquatic snakes is proportionally larger posteriorly. This may ensure an efficient ‘pterygoid walk’ in aquatic snakes despite their reduced jaw length. According to Young (Young 1991), the width of the posterior part of the head impacts the length of the lever arm which is involved in the pterygoid walk; the larger the width the more

efficient the swallowing. Moreover, this ensures a smooth head-neck transition in aquatic snakes. The jaw tips (i.e. landmarks 4 and 5) are not prominent which could possibly be an advantage during swimming as this may avoid the detachment of the flow behind the head.

As the nostrils are more dorsally positioned in aquatic snakes, this could allow them to breathe at the surface of the water while remaining submerged (Somaweera 2004). Likewise, the more dorsal position of the eyes could allow them to target prey or to see predators that are positioned above (Trapp & Mebert 2011; Povel & Van Der Kooij 1997). Eyes in predators generally tend to have a more frontal position to increase their binocular overlap, allowing them to better judge the distance to the prey. In contrast, species that tend to have a more laterally positioned eyes have a wider visual field (Walls 1942). As most aquatic snakes rely on visual cues to detect and capture prey (Drummond 1985; Schaeffel & Mathis 1991; Schaeffel & de Queiroz 1990; Shine et al. 2004; Brischoux & Lillywhite 2011) their eyes may have moved closer together to allow a better perception of depth and distance (Hibbitts & Fitzgerald 2005).

Our results show that the head shape of snakes that capture elusive prey under water has indeed converged. Nevertheless, the shape observed does not exactly correspond to our *a priori* predictions. Most of previous work on this subject predicted that the hydrodynamic forces should favor an elongated snout (Hibbitts & Fitzgerald 2005), a smaller or narrower head (Young 1991) and a decrease of the overall head width (Herrel et al. 2008), at least in frontal strikers. The head of the 'aquatic' snakes in our study is indeed proportionally narrower, but only in the anterior part. The enlargement of the posterior part of the head and the smaller size of the jaw is in contrast with the prediction of prior studies. However, simulation studies showed that an increase in head width is not likely to impair the strike speed of a snake (Van Wassenbergh et al. 2010). As such the head shape observed in aquatic snakes combines a narrow anterior part which will reduce drag, and a wide posterior head which allow an efficient prey transport. Direct measurements of the hydrodynamic forces and bow wave generation are needed, however, to test these ideas.

Interestingly, a considerable amount of variation in head shape is present among the snakes that capture elusive prey under water suggesting that multiple solutions to the same problem may exist. Snakes that capture elusive aquatic prey are known to use mostly one of two types of behaviors: frontally versus laterally directed strikes (Herrel et al. 2008). The strike behavior greatly influences the flow of water around the head and the associated drag forces during a prey capture event (Young 1991). Moreover, similarity in shape does not *per se* result in a similarity in performance (Miles 1994) and the ecological relevance of variation in shape remains to be tested. The exploration of the relationship between morphology, the behavior, and the hydrodynamics of prey capture is a promising avenue to better understand how the physical environment may constrain the evolution of form in aquatic species.

Acknowledgments

We thank the herpetological collections of the Field Museum of Natural History, the American Museum of Natural History, the Museum of Comparative Zoology and the California Academy of Sciences and their respective curators Alan Resetar (FMNH), David A. Kizirian (AMNH), Jens Vindum (CAS) and Jose P. Rosado (MCZ) for their help in the choice of specimens and the loans. We especially wanted to thank the staff of the Laboratoire Reptiles et Amphibiens of the National Museum of Natural History of Paris for their help, patience and effectiveness. The ‘plate-forme de morphométrie’ of the UMS 2700 (CNRS, MNHN) is acknowledged for allowing us to use the surface scanner.

Chapter 2

Hydrodynamics of the frontal strike in aquatic snakes: drag, added mass and the consequences for prey capture success.

Hydrodynamics of the frontal strike in aquatic snakes: drag, added mass and the possible consequences for prey capture success.

2017, submitted

Abstract

Natural selection favors animals that are the most successful in their fitness-related behaviors, such as foraging. Secondary adaptations pose the problem of re-adapting an already 'hypothetically optimized' phenotype to new constraints. When animals forage underwater, they face strong physical constraints, particularly when capturing a prey. The capture requires the predator to be fast and to generate a high acceleration to catch the prey. This involves two main constraints due to the surrounding fluid: drag and added mass. Both of these constraints are related to the shape of the animal. We experimentally explore the relationship between shape and performance in the context of an aquatic strike. As a model, we use 3D-printed snake heads of different shapes and frontal strike kinematics based on *in vivo* observations. By using direct force measurements, we compare the drag and added mass generated by aquatic and non-aquatic snake models during a strike. Our results show that drag is optimized in aquatic snakes. Added mass appears less important than drag for snakes during an aquatic strike. The flow features associated to the hydrodynamic forces measured allows us to suggest a mechanism rendering the shape of the head of aquatic snakes well adapted to catch prey underwater.

Key words: snakes, fluid mechanics, forces, morphology, prey capture

Introduction

Aquatic animals have to overcome the strong viscous and inertial constraints associated with underwater movement (Webb 1988). Physically, these constraints are related to the kinematics of movement and the morphology of an animal (i.e. the shape of the object that is facing the flow). For most aquatic vertebrates, viscous effects are confined to a thin boundary layer surrounding the body, which couples the motion of the animal with that of the surrounding fluid, and gives rise to the skin friction that penalizes aquatic locomotion. In addition, fluid inertia causes the boundary layer to separate from the animal's body, creating the recirculation zones associated to pressure drag (Vogel 1994). The specifics of the flow separation determine the relative importance of pressure to skin friction drag (Hoerner 1965). In addition to drag, which depends on the velocity of the animal, the hydrodynamics are also dependent on acceleration of the added mass (Daniel 1984; Brennen 1982). This corresponds to the mass of fluid that is accelerated together with the animal and which exerts a reaction force. Both drag and added mass also depend on the size and shape of the body (Daniel 1984), and it can thus be expected that the morphology of aquatic animals is optimized to reduce drag and added mass. However, organisms have a morphology that is also constrained by evolutionary history, functional trade-offs, and developmental programs thus restricting the range of possible morphological adaptations. Environmental and biological constraints act in parallel on an organism and may all impact their evolution, sometimes leading to convergent phenotypes (Bilcke et al. 2007; Kelley & Motani 2015; Howell 1971; Winemiller et al. 1995). These convergences are numerous across the animal kingdom, yet their impact on function has only rarely been tested (Van Wassenbergh et al. 2010; Stayton 2011; Young 1991; Herrel et al. 2008; Hibbitts & Fitzgerald 2005). We here use the case of convergence in head shape in aquatic snakes (Segall et al. 2016) to provide an experimental test of the suggested functional advantages of observed similarities in the head shape of aquatic snakes.

Snakes are an ideal model to study convergence as they have invaded the aquatic medium multiple times independently throughout their evolutionary history. However, they do not show any of the usual adaptations to aquatic prey capture (e.g. they cannot perform suction feeding due to their reduced hyoid) (Herrel et al. 2008). This lack of

suction feeding capacity likely results in an even stronger selective pressure on their head shape as the shape of the head will determine the magnitude of the hydrodynamic constraints (Webb 1984; Webb 1988; Young 1991). Convergence of the head shape in aquatic snakes has been demonstrated previously (Esquerré & Keogh 2016; Hibbitts & Fitzgerald 2005; Vincent et al. 2009; Herrel et al. 2008; Segall et al. 2016), and a hydrodynamic advantage of this convergence in shape has been suggested (Herrel et al. 2008; Segall et al. 2016; Fabre et al. 2016; Young 1991). Here we explore whether this convergence in head shape (Segall et al. 2016) can be explained as an 'optimization' for the capture of mobile prey under water. The hydrodynamic constraints involved during a strike, namely pressure drag - skin friction being negligible in the regimes of interest here (Van Wassenbergh et al. 2010) - and added mass, are related to the shape of an object (Brennen 1982; Daniel 1984). Thus, we should be able to detect a difference between the hydrodynamic forces associated with the head shape of snakes that capture elusive prey underwater and the non-aquatically foraging species.

Another constraint related with the capture of prey under water is the mechanosensitivity of aquatic prey like fish. The lateral line system of fish is composed of mechanoreceptors that can detect very small pressure variations –with an estimated threshold of 0.1 to 1mPa at 1mm (van Netten 2006; McHenry et al. 2009). This system triggers a reflex escape response in the prey once a pressure threshold has been reached. Previous studies have suggested that a snake moving underwater generates a bow wave that might be able to trigger the reflex response of the prey (Herrel et al. 2008; Van Wassenbergh et al. 2010). We decided to test this hypothesis and we predict that aquatic snakes should be stealthier than the non-aquatic snakes during the strike maneuver such that the detection of the predator by the prey would be delayed.

We use direct force measurements on different models of snake heads derived from a previous analysis based on the comparison of 83 species of snakes (Segall et al. 2016). We compared models with the mouth open, as aquatic snakes keep their mouth opened during frontal strikes (Vincent et al. 2009; Fabre et al. 2016; van Netten 2006; McHenry et al. 2009; pers. obs). Our experimental setup mimics a 'sit-and-wait' frontal strike under water, meaning that the model remains motionless before the strike and is then suddenly accelerated to reach an almost constant speed for a short time. The force

applied on the head during the strike was recorded to characterize the added mass and drag, which determine the hydrodynamic efficiency of a strike. In addition, another sensor was placed at the end of the strike track to assess the distance at which a prey is likely to detect the presence of the snake during capture. Particle Image Velocimetry (PIV) was used to visualize the fluid flow around the different shapes during a strike. We also characterized the evolution of the vortex intensity during a strike for each shape, as it is closely related to the hydrodynamic force generation by a moving object (Thiria et al. 2006; Saffman 1992; Ringuette et al. 2007).

Material & Methods

3D models

We used two models of head shape of snakes corresponding to two ecological groups, the “aquatic” group, which captures prey under water, and the non-aquatic group, which does not forage under water. The shapes associated with these two groups were extracted from a 3D geometric morphometric published previously (Segall et al. 2016) in which the head shape of 62 species of aquatic snakes were compared to 21 non-aquatically foraging species. To extract size from shape a Generalized Procrustes Analysis was performed resulting in the two model being at the same scale. Next a linear discriminant analysis was performed to extract the shapes that best discriminate between groups. The models were then 600 times enlarged. Next, the mouth of our models was opened to an angle of 70° to be biologically relevant in a prey capture context (Herrel et al. 2008; Bilcke et al. 2006; Vincent et al. 2005). This was done by dividing the heads into three parts corresponding to the ‘skull’ and the jaw that are the parts that are opened during a strike and the rest of the head. We used the same landmarks to divide in a homologous way the head in both models. Then, a rotation of 35° for the jaw and skull parts was performed in Blender™. The models were elongated at the level of the neck by approximately 10 cm, in order to avoid an artificial flow separation near the back of the head that could impact the measurements. The two models were then 3D printed using Stratasys Fortus 250 MC 3D printer with ABS P430 as material (Fig. 13a.).

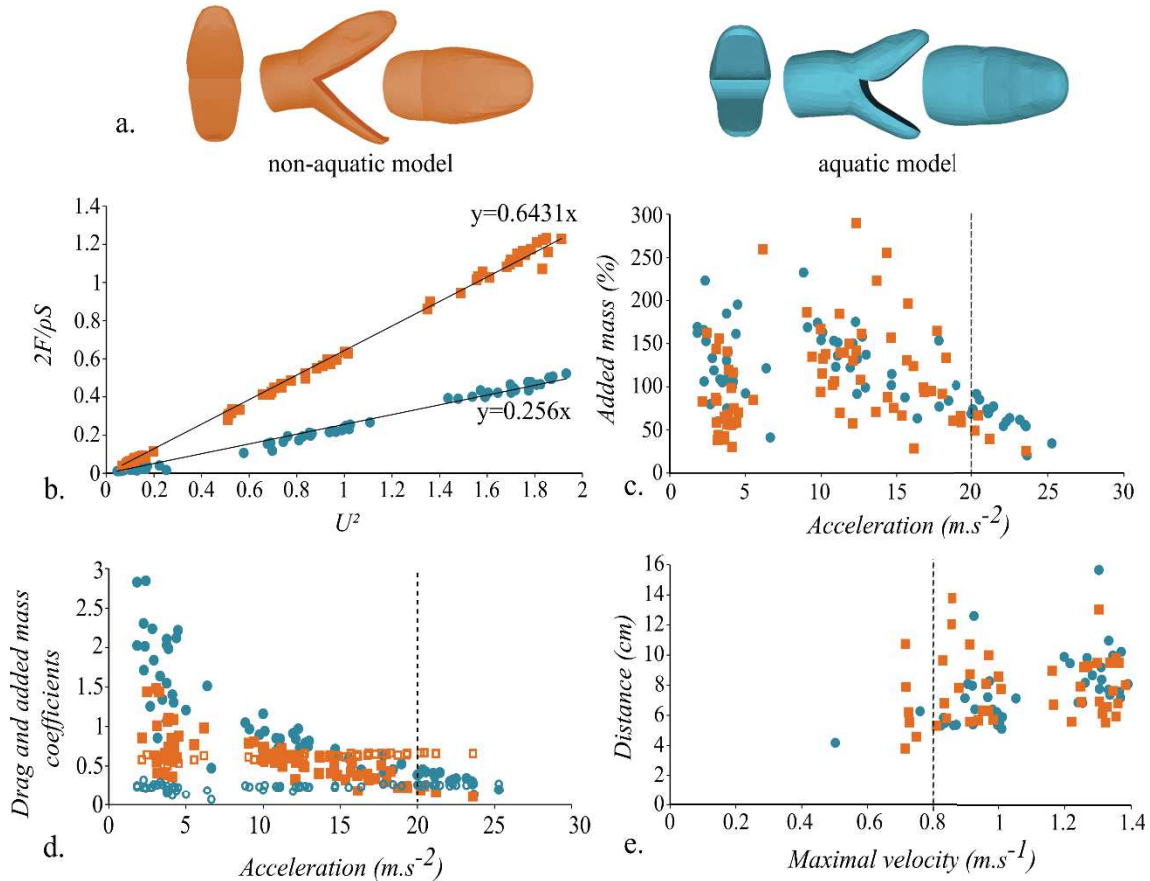


Figure 13: *a.* Frontal, side and top views of the 3D models of head shape of aquatic and non-aquatic snakes used during the experiments. *b.* Drag term $2F_d/\rho S$ depending on the velocity term of the strike (U^2) for the two head models tested. Linear regression lines are drawn. The y coefficients correspond to the drag coefficient of each shape. *c.* Comparison of the added mass associated with the two different head shapes depending on the acceleration of the strike ($m.s^{-2}$). The added mass is the amount of water that is pulled along with the head relative to the volume of the model (ρV_{model}). *d.* Comparison of the respective contribution of the added mass and drag during the acceleration phase depending on the head shape and the acceleration during the strike. Drag coefficient: open symbols, added mass coefficient: closed symbols. For each graph: squares: non-aquatic model, circles: aquatic model. *e.* Distance (cm) at which the prey could potentially detect the snake depending on the maximal velocity of the strike ($m.s^{-1}$). The dashed lines represent the lowest velocity or acceleration found in the literature for an aquatic strike in snakes. Squares: non-aquatic model, circles: aquatic model.

Experimental setup

The same setup was used for the force measurements and PIV. The 3D printed models were positioned horizontally in a water tank. A force sensor FUTEK LSB210+/- 2 Lb was attached to the 3D printed head using an aluminum rod and recorded the axial forces applied to the head during a strike. The other side of the sensor was attached to a bracket (sensor 1, Fig. 14) that was itself hooked on the movable part of an airborne rail. Springs were used to simulate the head acceleration during a frontal strike. We applied different compressions of the springs to generate a range of strike velocities and accelerations. The length of the path was 20cm. A position sensor (optoNCDT1420, Micro-Epsilon) was set at the end of the path to record the position and extract the head displacement. In addition, another more sensitive force sensor FUTEK LSB210 100g was set at the end of the path (sensor 2, Fig. 14). We monitored the pressure fluctuations that occur at the end of the strike path in front of the snake head using a round plastic plate of 7cm of diameter attached to a force sensor. This sensor provided information about the distance at which a prey could potentially detect the presence of a snake during a strike. The force and position sensors were synchronized and recorded at 1kHz. Approximately 60 trials were done for each model.

Drag coefficient and added mass

The profile of the force exerted on the head (red line in the Fig. 14) presents a first peak, which corresponds to the rapid acceleration phase driven by the decompression of the spring, followed by a plateau-like phase that signals a nearly constant velocity between the release of the spring and the end of the track. The latter appearing clearly as a negative peak on the force measurement when the moving cart of the rail hits the stop. The plateau phase of the first force sensor provides a measure of the drag force (Fig. 14) as it corresponds to the nearly constant speed phase during which drag is the major element of the measured force. The drag coefficient (C_d) of our models was calculated using the standard definition (Vogel 1994):

$$C_d = \frac{2F_d}{\rho U^2 S} \quad (4)$$

where F_d is the drag force, ρ is the density of water, U the velocity of the object and S its projected frontal surface area, which was measured at 12.89cm² for the aquatic model and 14.72cm² for the non-aquatic model. The term $2F_d/\rho S$ was plotted against U^2 and the coefficient of the linear regression corresponds to the drag coefficient of the models (Fig. 13).

The added mass was calculated from the peak force that corresponds to the acceleration phase during which the spring is pushing the cart of the air-bearing rail (Fig. 14). During this phase the force measured by the sensor includes not only the hydrodynamic drag, but also an inertial contribution given by $F_i = (m + M)\ddot{x}$, where \ddot{x} is the acceleration, m is the mass of the 3D printed models and M is the added mass. Using a quasi-steady assumption for the drag term, a reasonable estimate of the drag contribution to the force peak measured by the sensor during the acceleration phase is $\frac{1}{2}F_d$ (the drag being zero at the beginning when the velocity is zero and reaching a value of F_d when the cart detaches from the spring at the beginning of the plateau; see Fig. 14). The peak force F_p is thus equal to the sum of the inertial force F_i and half of the drag force measured at the beginning of the plateau F_d . Using an average value for the acceleration $a = \langle \ddot{x} \rangle$ obtained from the $x(t)$ data of the position sensor, we obtain this equation to estimate the added mass M (Fig. 13):

$$M = \frac{F_p - \frac{1}{2} F_d - ma}{a} \quad (5)$$

To compare the respective contributions of the added mass and the drag during the acceleration phase (see Fig. 13), we defined a dimensionless added mass as:

$$C_{AM} = \frac{2 Ma}{S \rho U^2} \quad (6)$$

It should be noted that the previous equation is different from the traditional definition of the coefficient C_a appearing in the added mass expression $C_a \rho V$ (Vogel 1994).

Detection distance

To compare the effect of the head shape on the detection by a possible prey we used the output of the second force sensor (sensor 2, Fig. 14). This sensor can detect pressure variations of approximately 0.3Pa. To estimate the position at which the prey could detect the predator, we defined the detection distance d (plotted in Fig. 13e as a function of the maximum velocity of the strike) as the position at which the force in sensor 2 deviates from the unperturbed value by more than one standard deviation of the sensor output before the strike (Fig. 14).

Particle Image Velocimetry

We used 2D Particle Image Velocimetry (PIV) with a high-speed camera, Dantec Dynamics SpeedSense M, to obtain a time-resolved recording of the strike from the bottom of the tank (Fig. 14). Water was seeded with polyamid particles of 20 μm in diameter and a Quantronix® Darwin-Duo laser was used to produce the light sheet. Image acquisition was performed at 733Hz. We choose to record three different planes on each head to obtain a complete picture of the fluid flow around the head during the attack (see Appendix 7). We applied the same compression to the springs (i.e. maximal compression) in order to get a fair comparison for the different shapes. Acquisition was performed using the Dantec DynamicStudio 2015a software. The PIV vector computation was performed using LaVision 7.2 with a 16 x 16 pixel² interrogation window and 50% overlap. Additional post-processing and analysis was done in Matlab using the PIVMat toolbox (Moisy 2006). A more quantitative analysis has been performed by computing the overall primary circulation $\Gamma = \int \omega^+ dA$ in each PIV plane (ω^+ being the positive vorticity in Fig. 15b.). The evolution of the dimensionless circulation Γ/UL as a function of time, where L is the characteristic length scale of the acceleration regime of the strike maneuver (that is constant for all experiments) and U is the velocity of the strike has been plotted in Fig. 15b.

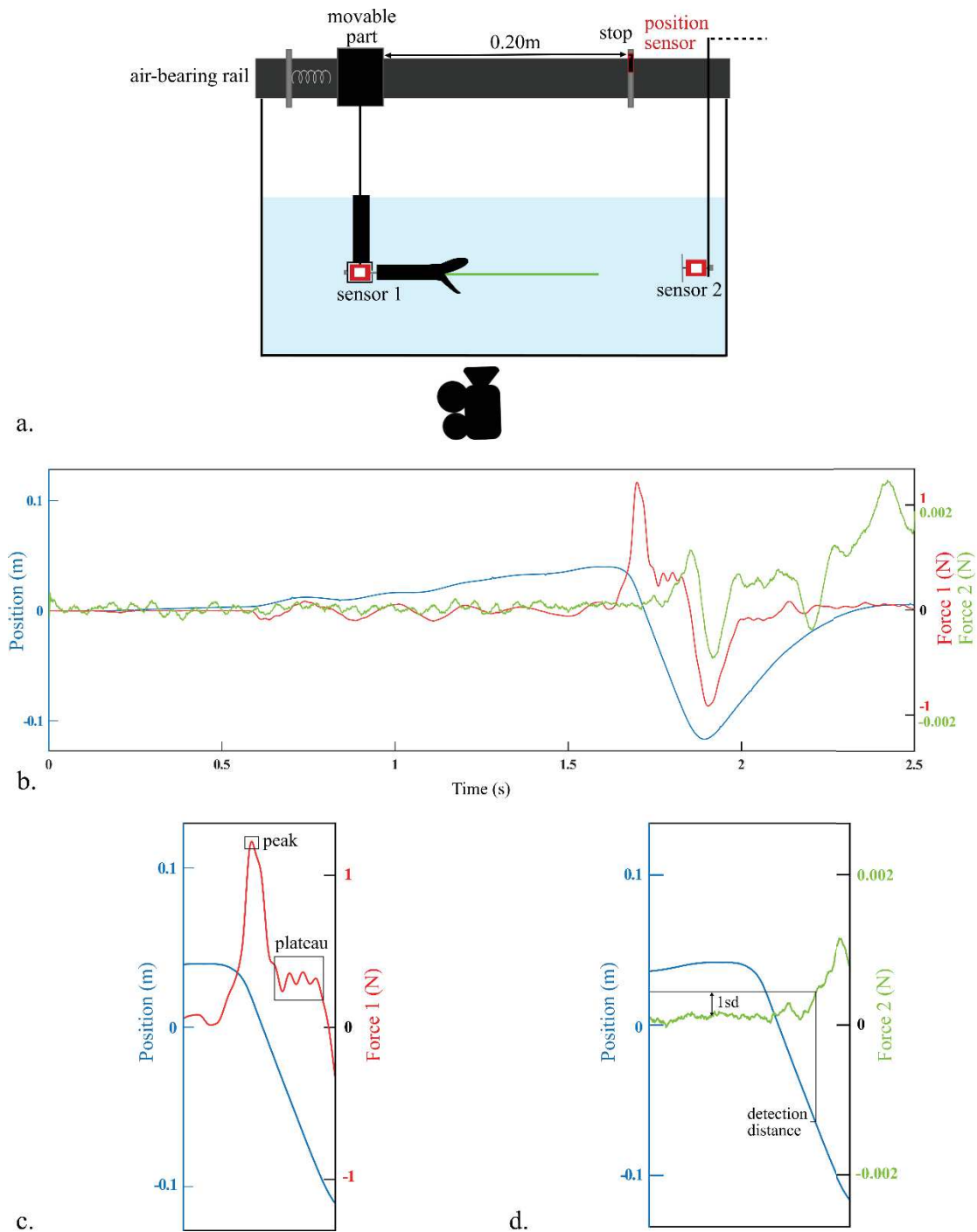


Figure 14: *a.* Experimental setup used to simulate the frontal attack of a snake towards a prey. *b.* Example of the output of the position sensor (blue), force sensor 1 (red) and force sensor 2 (green) from one strike. *c.* Zoom in on the output of the force sensor 1 showing the peak and plateau phases that were used to measure drag and added mass. *d.* Zoom in on the prey sensor output highlighting the method we used to determine the detection distance, using the 1sd (standard deviation) threshold (not at scale here).

Statistical analyses

To test for differences between the drag coefficients of the two shapes, we ran a Pearson correlation on the force component of the drag coefficient ($2F_d/\rho S$) with the square velocity (U^2). An ANCOVA with mass as a co-variate was performed to test for statistical differences in the drag coefficient between the two models. We also ran an ANCOVA with the added mass as the response variable, the acceleration as covariate and the model as factor. Finally, to compare the detection distance, we ran an ANCOVA with the distance as the response variable, the model as a factor, and the velocity as covariate. All the variables were Log_{10} -transformed and the statistical analyses were performed using R (R Development Core Team 2014). The significance level was set at 5%.

Results*Drag and added mass*

The drag coefficient of the non-aquatic shape is higher than the coefficient of the aquatic model, respectively 0.64 and 0.26 (Pearson's correlation: nonaq: $df = 67$, $P < 0.001$, $R^2 = 0.996$; aq: $df=64$, $P < 0.001$, $R^2 = 0.995$; ANCOVA: $F_{2,132} = 671.1$, $P < 0.001$) (Fig. 13b). The added mass measurements show a large scatter at low accelerations (between 0 and $10\text{m}\cdot\text{s}^{-2}$) for both models: the measured added mass ranged between 25% and almost 250% of the mass of water occupied by the model. At higher accelerations, between 10 to $25\text{m}\cdot\text{s}^{-2}$, there is less scatter and the added mass decreases slowly towards a value of $\sim 50\%$ of the volume occupied by the model for both shapes (Fig. 13c).

The statistical analysis shows that the added mass is slightly larger for the aquatic model than for the non-aquatic one ($M'_{\text{aq}}: 112 \pm 46\%$; $M'_{\text{nonaq}}: 108 \pm 57$) and that it is dependent on the acceleration (ANCOVA: $F_{2,132} = 5.36$, $P = 0.005$; shape: $P = 0.01$; acceleration: $P = 0.024$). Due to the observed scatter at low accelerations we performed an additional ANCOVA taking into account only the added mass values corresponding to accelerations above $10\text{m}\cdot\text{s}^{-2}$. When doing so there is no longer any statistical difference

between the two shapes but still a significant effect of acceleration (ANCOVA: $F_{2,74} = 23.38$, $P < 0.001$; model: $P = 0.107$; acceleration: $P < 0.001$).

Both added mass and drag are involved during the acceleration phase of a strike, however, their respective contribution changes depending on the acceleration and the shape of the head. For the non-aquatic shape, between 0 and $10\text{m}\cdot\text{s}^{-2}$, the added mass is more important than the drag but beyond $10\text{m}\cdot\text{s}^{-2}$, the drag is more important than the added mass (Fig. 13d). Whereas, for the aquatic shape, the added mass is very important at very low accelerations and it decreases rapidly beyond $5\text{m}\cdot\text{s}^{-2}$. For the aquatic shape, the added mass is almost equivalent to the drag beyond $15\text{m}\cdot\text{s}^{-2}$.

Detection distance

We were not able to get any accurate measures of the detection distance for low velocities (i.e. $U > 0.5\text{m}\cdot\text{s}^{-1}$). There is moreover no statistical difference between the distance at which the prey could detect the presence of the snake depending on their head shape. However, this distance depends on the maximal velocity of the strike, the faster the strike, the earlier the detection of the predator (ANCOVA: $F_{2,84} = 5.05$, $P = 0.008$; model: $P = 0.65$; U_{max} : $P = 0.008$) (Fig. 13e).

Flow characterization

The frontal strike maneuver involves strong flow separations due to the high shear produced by the impulsive acceleration (Fig. 15). The flow features can be characterized by examining the vortex structures formed at the corner of the mouth and on both tips of the jaw and of the skull. We created videos of the vortex formation during a strike, obtained from PIV on three planes around the snake heads (Appendix 6), in order to compare both models (see [video 1](#), [video 2](#), [video 3](#)). The PIV measurements show the formation of vortices during the strike maneuver. In Fig. 15a. we compare the vorticity field at the end of the acceleration phase (at $t \approx 0.8\text{s}$) in the three measurement planes; bottom view, jaw view, and skull view (Appendix 7) for the aquatic and non-aquatic heads. Looking at the bottom view, the difference of the flow pattern between the two models is clearly observable; the advantage of the aquatic model seems to be related to a

smaller primary vortex. The picture is not as straightforward considering the jaw and skull view, where opposite observations on the primary vorticity production can be pointed out qualitatively: on the jaw view the primary vorticity patch appears slightly more detached from the jaw in the non-aquatic case, whereas in the skull view this observation can be made for the aquatic case. Fig. 15b. shows the quantitative analysis of the primary circulation. First, we can see that the bottom view the aquatic model induces a slightly ($\sim 10\%$) lower overall circulation over the whole acceleration phase. Second, on the jaw view, it can be remarked that a much lower overall circulation is produced by the vorticity detached from the tip of the jaw in the aquatic case (around 40% of the non-aquatic value at the end of the acceleration phase). The picture in the skull view is the opposite, the aquatic case generating more overall circulation. We note also for the skull view that the computed value for the circulation fluctuates much more.

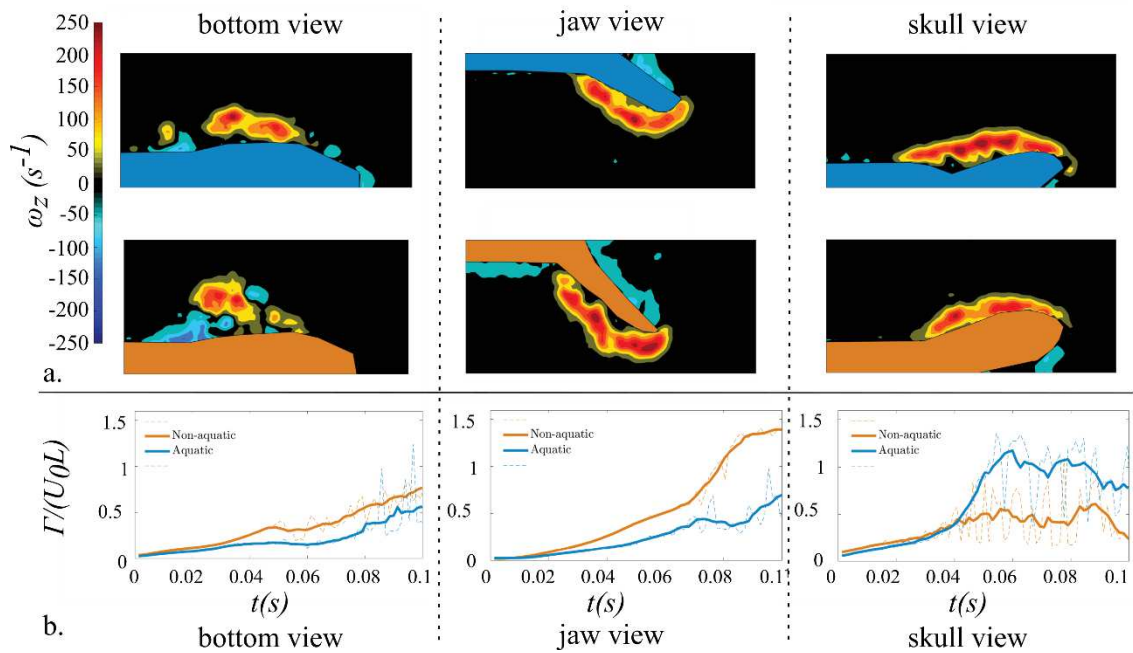


Figure 15: **a.** Snapshots of the vorticity field ω_z around the snake head models at the end of the acceleration phase for the aquatic (first line) and non-aquatic (second line) models, in the three measurement planes: bottom, jaw and skull views are shown on the first to third columns, respectively. The color bar for the vorticity field is given in s^{-1} . **b.** Evolution of the dimensionless integrated positive circulation during the acceleration phase depending on the time for both models in each of the three views considered.

Discussion

The foraging success of an aquatic snake is at least partly related to the response of the potential prey. Contrary to our predictions, our results show that the relative distance at which a prey can possibly detect a snake does not depend on the snake's head shape. Yet, this distance does increase with velocity for both models. However, we cannot conclude on the biological relevance of the absolute distance measured in the present experiment in terms of prey capture success for several reasons. First, the threshold of pressure detection of a fish depends on the species, and it is also difficult to compare to the threshold that can be defined from our force sensor. Second, our setup is based on a very idealized strike, different from a real frontal strike, especially because most of aquatic snakes strike when they are very close to their targeted prey (e.g. 0.5-0.8cm *Erpeton tentaculatum* (Catania 2009); *T. couchii* 4.87cm; *T. rufipunctatus* 2.81cm (Alfaro 2002); less than 3cm *Hydrophis schistosus* (Voris et al. 1978)). The detection distance measured here is around 6 to 10cm, so we could consider that the prey detects the snake almost instantaneously when the strike is initiated. Capture success is thus likely more related with the hydrodynamic profile of the snake head shape than being dependent on the reaction of the prey.

Drag is well known for its role in steady locomotion such as cruising, however, it is also involved in transient behaviors such as the capture maneuver studied here. Certainly, the aquatic model appears more adapted to capture aquatic prey using a frontal strike than the non-aquatic model in terms of drag. The drag coefficient of both models with the mouth closed is smaller or equivalent to the drag coefficients reported for aquatic mammals in the literature (Fish 1993) (Appendix 6). These coefficients are close to those of streamlined bodies (Koehl 1996) and practically equivalent for both models, which means that the cruising regime is not so much constrained by the shape of the head. However, during prey capture, when the mouth is open, the drag coefficient increases dramatically. Despite this, the aquatic model has a drag coefficient that is almost 3 times smaller than the non-aquatic model. As mentioned above, drag in this fast impulsive maneuver is mainly pressure drag, which is intimately linked to the flow separation in the near wake of the snake head as it moves. Through the PIV measurements, we can observe the vortices that are formed very early during the strike (see videos).

However, the relationship between the drag coefficient and the vortex profile is not straightforward. A full time-resolved 3D reconstruction of the flow would be needed to compute a total force that could be compared quantitatively to the output of the direct force measurements. This is however beyond the scope of the present paper. The planar PIV data allows us nonetheless to conjecture on the possible fluid dynamic origin of the differences in drag coefficient measured between the two models. Looking at the bottom view in Fig. 15, the advantage of drag of the aquatic model could to be related to a smaller primary vortex, the non-aquatic case showing a more fluctuating and disordered field. Moreover, the vorticity production at the tip of the jaw shows a clear quantitative difference and is consistently higher for the non-aquatic model. However, the skull view shows the opposite pattern of vorticity; the non-aquatic snake produces fewer vortices with an integrated primary circulation that is less important than for the aquatic model. However, the involvement of jaw and skull vorticity could be under or overestimated with a 2D view given that in reality it is a 3D phenomenon. Further analysis should explore the 3D pattern of the fluid flow as the results of such an experiment would allow to make a more direct link between drag and the vorticity profile of the flow around the head. From the present results we can only conjecture that a reduction of the recirculation bubble behind the jaw appears to be the main physical mechanism explaining the physical advantage of the head shape in aquatically foraging snakes.

The added mass depends on the acceleration; the higher the acceleration, the smaller the added mass for both models. The non-aquatic model generates slightly less added mass than the aquatic model for lower accelerations, but this difference disappears at higher accelerations (i.e. $a > 10\text{m}\cdot\text{s}^{-2}$). Thus, theoretically, aquatic snakes should strike at high acceleration to reduce the added mass generated by their motion. Only few data are available on underwater strike kinematics in snakes but it appears that accelerations during frontal strikes are typically higher than $20\text{ m}\cdot\text{s}^{-2}$ in aquatic snakes (Smith et al. 2002; Vincent et al. 2005; Alfaro 2002). Beyond $20\text{ m}\cdot\text{s}^{-2}$, the added mass is very small for both models and there is no longer any difference between the models, meaning that the shape does not affect the added mass at such high accelerations.

Interestingly, aquatic snakes appear optimized in terms of drag but not so much with respect to the added mass. This could be the result of opposite requirements to

optimize added mass and drag in animals. It is possible that the reduction of both hydrodynamic constraints involves morphological features that are mutually exclusive as has been highlighted for fish (Webb 1984). Alternatively, the head shape of snakes may already minimize added mass within the context of the anatomical and phylogenetic constraints acting on these animals. Webb (1984; 1988) showed that an optimal body shape for transient propulsion, such as a snake strike, would be an elongated, streamlined, and flexible body along with skin and “dead weight” reduction, which corresponds to a snake-like configuration. However, to our knowledge, no study has focused on the shape of the head and its role. Drag increases with acceleration whereas added mass decreases suggesting that snakes may have adapted their body form to facilitate transient propulsion (elongated, streamlined body, paddle-like tail...) and their head shape to reduce the drag at high accelerations, resulting in an overall optimized morphology for underwater prey capture.

Additionally, drag and added mass do not contribute equally during a strike depending on the kinematics. Based on our observations, we assume that drag is more important than added mass. As Daniel (1984) mentioned, in the case of animals accelerating from rest, as during a strike, both drag and added mass are acting and it is possible to evaluate the relative importance of each. We did so by looking at their respective coefficients. The results show that at high accelerations, which are biologically relevant for snakes striking (Vincent et al. 2005; Smith et al. 2002; Alfaro 2002; Alfaro 2003; Drummond 1983), the added mass coefficient decreases until it reaches the drag coefficient values, which remain constant. However, there is no difference in the added mass between the two shapes. This suggests that drag is more largely impacted by the difference in shape than the added mass coefficient, which mainly depends on the acceleration of the strike itself. An optimal evolutionary strategy for an aquatically foraging snake could thus be to reduce its drag coefficient by adapting head shape and to reduce its added mass coefficient by adapting its body to generate high accelerations.

Acknowledgments

We thank Olivier Brouard, Amaury Fourgeaud and Tahar Amorri from the PMMH lab for their precious help in the experimental design as well as Xavier Benoit-Gonin for his help with the 3D printer. Thierry Darnige and especially Justine Laurent are acknowledged for their help with the sensors and computer coding. MS thanks the Région Ile de France for funding this research project and the doctoral school Frontières du Vivant (FdV) – Programme Bettencourt.

Chapter 3

**The complexity of convergence: from
one-to-one mapping of form to
function to many-to-one mapping of
function to ecology.**

The complexity of convergence: from one-to-one mapping of form to function to many-to-one mapping of function to ecology.

2017, submitted

Abstract

We explored the morphological diversity in a group of animals that has converged in head shape to circumvent strong physical constraints: the aquatically foraging snakes. Despite the observed convergence considerable variability in head shape across species was still detected. Given the importance of head shape on fitness, we hypothesized that this may be an example of many-to-one mapping of form to function. Thus, the different head shapes of aquatic species are expected to result in equivalent hydrodynamic performance. We also investigated features that could drive the evolution of this diversity, such as diet, presence of glands, and habitat use. We used 3D geometric morphometrics on a large sample of species to extract five shapes that are representative of the variability. We 3D printed these shapes and measured the drag coefficient of each shape using an experiment that mimics a snake strike. We found that prey shape is partly constraining the head shape. However, instead of a many-to-one mapping of form to function, we highlight a one-to-one mapping of form to function and a many-to-one mapping of function to ecology as these snakes are all successful at catching aquatic prey despite the variation in head shape leading to different hydrodynamic efficiencies.

Key words: evolution, convergence, function, shape, snakes, ecology

Introduction

The goal of evolutionary biology is to understand the origins and evolution of biological systems. By documenting patterns across evolutionary time, insights can be gained on the selective forces that drive the evolution of a given phenotype (Greene 1983; Howell 1971). Related species may resemble each other more than distantly related species because of their shared evolutionary history (Darwin 1859). However, some distantly related species resemble each other more due to the convergent evolution of certain phenotypes in similar ecological contexts (Winemiller et al. 1995). This convergence is often driven by strong extrinsic constraints driving the phenotype towards a limited number of solutions (e.g. streamlined animals) (Howell 1971; Hosoi et al. 2007; Esquerré & Keogh 2016; Kelley & Motani 2015). Yet, phenotypes may also functionally converge (i.e. many-to-one mapping) with many different phenotypes giving rise to the same function (e.g. the 4-bar linkage in fish) (Wainwright et al. 2005). Predicting evolutionary trajectories is further complicated because of functional trade-offs imposing conflicting demands on a single structure (e.g. transient and burst swimming; speed and stamina) (Webb 1988; Vanhooydonck et al. 2001; Webb 1984).

We propose here to study the head shape in aquatically foraging snakes to address the question of whether this system shows a many-to-one mapping of form to function. It has been demonstrated previously (Segall et al. 2016) that the shape of the head in snakes that capture prey under water has converged. This shape convergence was suggested to help minimize drag and thus optimize prey capture success in these animals (Segall et al. n.d.). We further demonstrated that this convergent shape does indeed provide snakes with a functional advantage (i.e. drag reduction).

Unexpectedly, however, the variability in head shape in aquatically foraging snakes is rather large ranging from relatively long and thin to more short and bulky heads. Consequently we asked ourselves whether many-to-one mapping of form to function occurs in aquatically foraging snakes; i.e. do these different head shapes all result in the same hydrodynamic profile. Moreover, we ask ourselves how this variability is structured? Apart from the hydrodynamic constraints, what other factors may drive the evolution of head shape in aquatically foraging snakes?

Head shape variability could, for example, be driven by the habitat of the species, i.e. the media in which they spend most of their time (Savitzky 1983; Esquerré & Keogh 2016). The morphospace overlap between aquatic and non-aquatic foragers could be related to the more terrestrial habits of some species. We defined ‘aquatic foragers’ as species that capture elusive prey underwater. According to this definition, a terrestrial species that occasionally but actively hunts fish is considered as an aquatic forager. It seems pretty intuitive that the selective pressures acting on an entirely aquatic snake are different from those acting on a terrestrial snake that occasionally forages underwater. Thus, we predict the species in our morphological space to be, at least partly different based on their habitat use.

Another hypothesis that could explain the variability among the aquatic foragers is their diet and more precisely the shape of their preferred prey. Indeed, snakes are gape-limited predators that swallow large prey whole (Gans 1961). Thus their head shape may be related to their prey shape given that several studies have previously demonstrated an effect of dietary preference on the shape of the head of snakes (Vincent et al. 2007; Forsman 1991; Camilleri & Shine 1990; Queral-Regil & King 1998). Here we predict that whereas elongated prey should not impose specific constraints on head shape, bulky prey eaters would benefit from wide heads and long jaws (Forsman 1991; Fabre et al. 2016; Brecko et al. 2011). Finally, the presence of glands such as Duvernoy’s or venom glands could impact the overall head shape of snakes. The Duvernoy’s gland is also a venom gland but is less complex in structure (Fry et al. 2008). However, marked differences between both types of glands exist in terms of their size, shape and position in the head. Moreover, true venom glands show a specialized musculature that allows to compress the gland (Fry et al. 2008; Fry et al. 2003) and that may impact head shape. In addition, gland secretions may facilitate prey handling by tranquilizing and, in some cases, killing the prey (Kardong 2002; Weinstein et al. 2009). However, venomous snakes tend to have long handling times and sometimes chew or reposition prey before swallowing (Weinstein et al. 2009; Mori 1998). This may require larger muscles and venomous snakes may thus be expected to have bulkier heads.

Despite its importance, functional diversity has rarely been empirically tested (Collar & Wainwright 2006). We here propose an experimental approach to assess

whether the morphological variability observed in the shape of the head has functional consequences in terms of underwater prey capture. Specifically, we measure the drag that is generated by different head shapes under water. We hypothesize that the different head shapes result in similar functional features given that they all capture elusive prey under water. We expect the drag coefficient, which is the most important constraint during aquatic locomotion and foraging (Segall et al. n.d.) to be similar in animals with differently shaped heads foraging on elusive aquatic prey thus providing an example of many-to-one mapping of form to function (Wainwright et al. 2005).

To address these questions, we gathered a large dataset containing the head shape of 62 species of snakes that forage underwater. We used 3D geometric morphometrics and comparative analysis to test for effects of ecological factors on head shape evolution. Next, we extracted a set of head shapes that we 3D printed to measure the drag coefficient that is associated with each shape; drag being the main constraint involved during an underwater prey capture event in snakes.

Material & Methods

Specimens

3D scans of the heads of 316 snakes were obtained using a high resolution surface scanner: a Stereoscan3D Breuckmann white light fringe StereoSCAN3D with a camera resolution of 1.4 megapixels, available at the Museum National d'Histoire Naturelle, Paris. Only specimens with a well-preserved head and closed mouth were scanned to allow shape comparisons. Five specimens per species were used in this study where possible (Appendix 1). Our sample consists of 62 species of snake species that consume elusive aquatic prey (e.g. fish, amphibians, crustaceans...) (Appendix 1). We chose at least one aquatic species among each family of snakes in which a return to an aquatic lifestyle has occurred. The phylogenetic tree of Pyron (Pyron et al. 2013) was pruned in Mesquite 3.03 (Maddison & Maddison 2015) to only keep the species we included in our data set (Fig. 16).

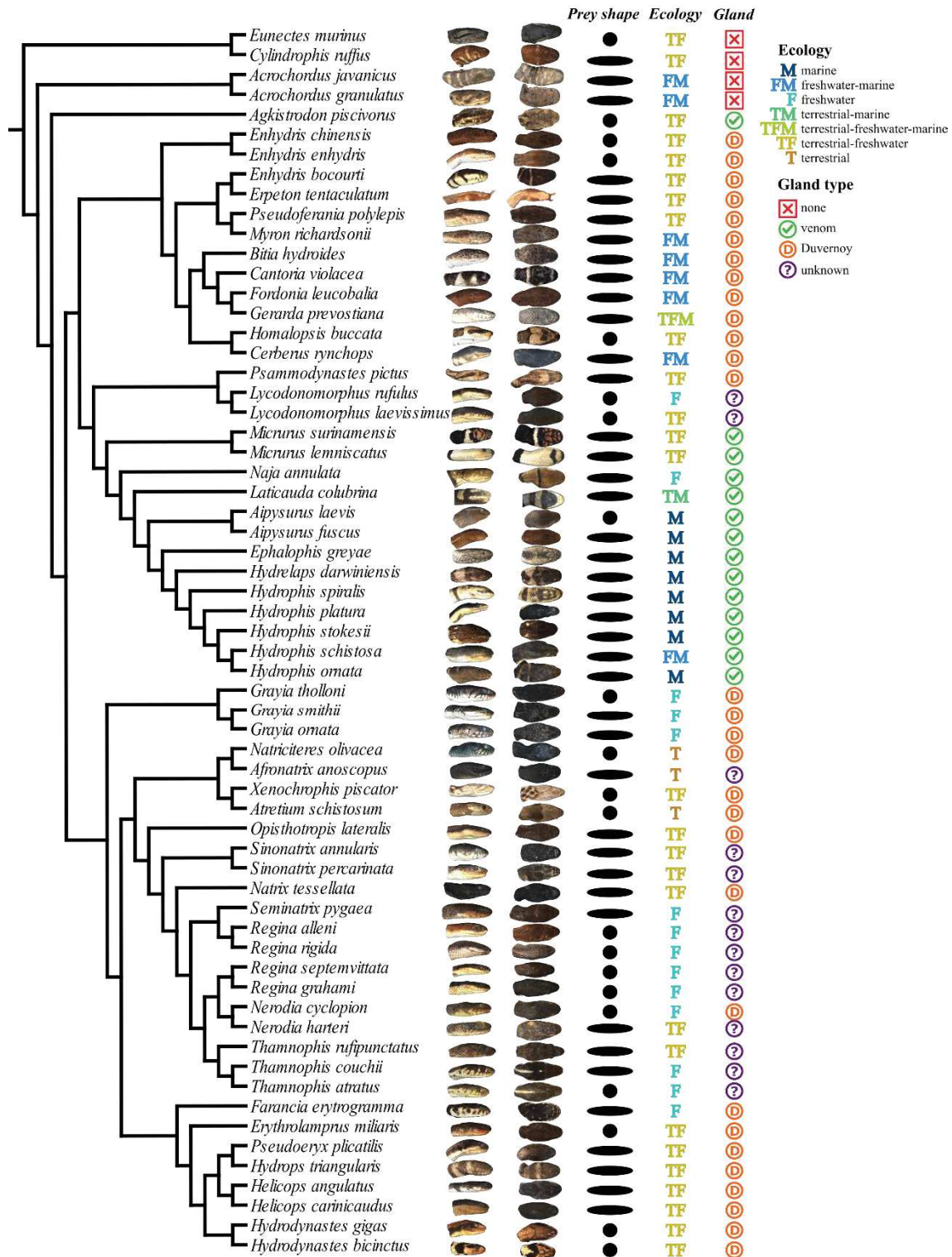


Figure 16: Phylogeny of the selected species based on Pyron et al. 2013. For each species is associated a side and top view of their head, the shape of their most common prey, their ecology, and the gland type.

Geometric morphometrics

To quantify shape variation between species, we recorded the 3D coordinates of 10 landmarks, both anatomical landmarks and maxima of curvature, and 6 curves using the 'Landmark' software package (Wiley et al. 2005). A template consisting of 921 landmarks, including 10 anatomical landmarks, 74 sliding-landmarks on curves and 837 sliding-landmarks on the surface of the head was created (Fig. 11, Appendix 3) to obtain an accurate description of the head shape of the snakes (Gunz & Mitteroecker 2013). The template was positioned on each specimen, semi-landmarks were projected onto the surface of the specimen and allowed to slide while minimizing the bending energy between the template and the specimen using the Morpho package in R (Botton-Divet et al. 2015; Gunz & Mitteroecker 2013; Schlager 2015; R Development Core Team 2014). Next, MorphoJ (Klingenberg 2011) was used to render all landmarks symmetrical, a Procrustes superimposition was run (Rohlf & Slice 1990) and an average head shape per species was calculated. A PCA was run to evaluate the overall shape variation in the dataset. The first 7 principal components (PC) accounting for more than 90% of the shape variability were used for further statistical analyses (Table 4).

3D models

We chose to test five models of head shape of snakes, which correspond to the extremes of the two first axes of the principal component analysis and the mean shape; PC1 and PC2, representing respectively 53% and 11% of the overall variability. The models were enlarged to a length of approximately 5cm. Next, the mouth of our models was opened to an angle of 70° to be biologically relevant in a prey capture context (Herrel et al. 2008; Bilcke et al. 2006; Vincent et al. 2005). This was done by dividing the heads into three parts corresponding to the 'skull' and the jaw, which are the parts that are opened during a strike and the rest of the head. The same landmarks were used to divide the head in all models. Then, a rotation of 35° for the jaw and skull parts was performed in Blender™. The models were elongated at the level of the neck by approximately 10 cm, in order to avoid an artificial flow separation near the back of the head that could impact the measurements. The five models were then 3D printed using Stratasys Fortus 250 MC 3D printer with ABS P430 as material (Fig. 17).

Experimental setup

Force measurements were obtained for each 3D printed model using an experiment that simulates the attack maneuver. The snake head model was positioned horizontally in a water tank. A force sensor FUTEK LSB210+/-2 Lb was attached to the 3D printed head using an aluminum rod and recorded the axial forces applied to the head during a strike. The other side of the sensor was attached to a bracket (sensor 1, Fig. 14a) that was itself hooked on the movable part of an airborne rail. Springs were used to simulate the head acceleration during a frontal strike. We applied different compressions of the springs to generate a range of strike velocities and accelerations. The length of the path was 20cm. A position sensor (optoNCDT1420, Micro-Epsilon) was set at the end of the path to record the position and extract the head displacement. Approximately 60 trials were done for each model.

Drag coefficient

The profile of the force exerted on the head (red line in the Fig. 14b,c) presents a first peak, which corresponds to the rapid acceleration phase driven by the decompression of the spring, followed by a plateau-like phase. The plateau phase of the force sensor provides a measure of the drag force (Fig. 14b,c) as it corresponds to a phase during which only drag constrains the motion. As in the previous chapter, the drag coefficient (C_d) of our models was calculated using the standard definition (Vogel 1994):

$$C_d = \frac{2F_d}{\rho U^2 S} , \quad (4)$$

where F_d is the drag force, ρ is the density of water, U the velocity of the object and S its projected frontal surface area, which was measured as 13.57cm², 13.68cm², 15.17cm², 14.23cm², 14.41cm² respectively for the PC1min, PC1max, PC2min, PC2max, mean shape models. The term $2F_d/\rho S$ was plotted against U^2 and the coefficient of the linear regression corresponds to the drag coefficient of the models.

Statistical analyses

Before exploring our hypotheses, we wanted to know if the overall variability on our dataset (90% of the total variability) could be divided in several sub-distributions using the Gaussian Mixture Model (GMM) in the *mclust* package in R (Fraley et al. 2012). Next, we tested three *a priori* hypotheses of features that could impact head shape: 1) namely the presence or absence of a venom gland, 2) habitat use (aquatic, semi-aquatic and terrestrial), and 3) prey shape (bulky vs. elongated). Phylogenetic statistical tests were used as our species cannot be considered as independent from one another given their common evolutionary history. Thus, we ran phylogenetic MANOVAs on the first seven PC axes to test whether head shape is impacted by these features. Subsequently we ran phylogenetic ANOVAs to evaluate which axes contributed to the differences in shape. To highlight a statistical difference between drag coefficients of the five shapes, we ran Pearson's correlation tests on the force component of the drag coefficient ($2F_d/\rho S$) with the square velocity (U^2). An overall ANCOVA was performed to test for statistical differences in of the drag coefficient between the five models with model mass as a covariate. Then, pairwise ANCOVAs were ran to compare the models two-by-two, a sequential Bonferroni correction was applied to the P-values of each comparison. The statistical analyses were performed using R (R Development Core Team 2014) with a significance level set at 5%.

Results

Morphometry

The distribution of the species in the morphospace described by the first two principal components representing 64.5% of the overall variability revealed no obvious patterns (Fig. 17). To test whether any natural groups are present we applied a Gaussian Mixture Model on 90% of the variability. This analysis returns a unique component suggesting little or no structure within the shape data.

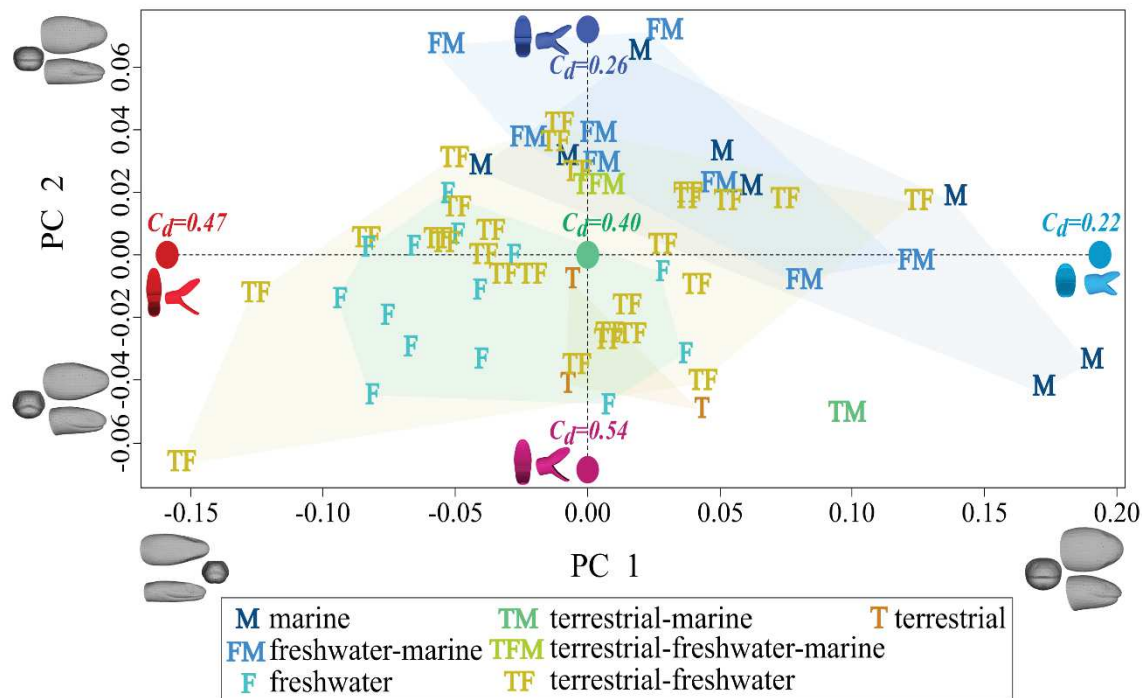


Figure 17: Scatter plot of the principal components one and two (PC1 & PC2) representing respectively 53.4% and 11.1% of the head shape variance among the 62 aquatically foraging snake species. Each letter represents a single species, the letter indicates the ecology of the species as illustrated on the figure. The shape associated with each extreme of the PC axes is represented in grey. Illustrated in color are the extreme shapes with the mouth opened that were used for the drag experiment and their resulting drag coefficients (C_d).

The phylogenetic signal is significant in our dataset ($P = 0.005$, $K_{mult} = 0.34$) meaning that the head shape is partly constrained by the evolutionary relationships between the species. Unexpectedly, neither habitat use (Wilk's lambda = 0.17, $F_{6,55} = 2.49$, $P_{phy} = 0.64$) nor the type of gland (Wilk's lambda = 0.36, $F_{3,58} = 3$, $P_{phy} = 0.98$) appear to drive head shape evolution in aquatically foraging snakes. The effect of prey shape was, however, significant (Wilk's lambda = 0.69, $F_{1,60} = 3.34$, $P_{phy} = 0.03$). Univariate analyses show that this difference is significant on PC6 which carries 3.4% of the overall variability in head shape (Table 4). This axis does not carry any phylogenetic signal suggesting that the difference in head shape described by this axis is entirely due to differences in prey shape. Unexpectedly, the linear discriminant analysis shows that

elongated prey eaters have a shorter and bulkier head with smaller eyes, and with the eyes and nostrils being more dorsally positioned. The bulky prey eaters, in contrast, have a more elongated head that is relatively narrower anteriorly (Fig. 18).

	Proportion of variance (%)		Univariate K statistic		Phylogenetic ANOVA	
	Proportion	Cumulative proportion	K	P-value	F _{1,60}	P-value
PC1	53.4	53.4	0.40	0.002	2.26	0.25
PC2	11.1	64.5	0.36	0.0009	4.33	0.10
PC3	7.9	72.4	0.42	0.0009	0.01	0.94
PC4	7.1	79.5	0.24	0.03	3.71	0.11
PC5	5.1	84.6	0.17	0.32	0.20	0.72
PC6	3.4	88	0.31	0.12	8.74	0.02
PC7	2.6	90.7	0.48	0.02	0.58	0.55

Table 4: Results of the statistical analyses performed on the first seven principal components. The proportion of variance explained by each axis is indicated along with the cumulative variance. To assess the strength of the phylogeny in each component we use a K statistic. Phylogenetic ANOVAs are used to evaluate whether a statistical difference can be detected between snakes that eat bulky prey and those that eat elongated prey. Statistical differences are indicated in bold.

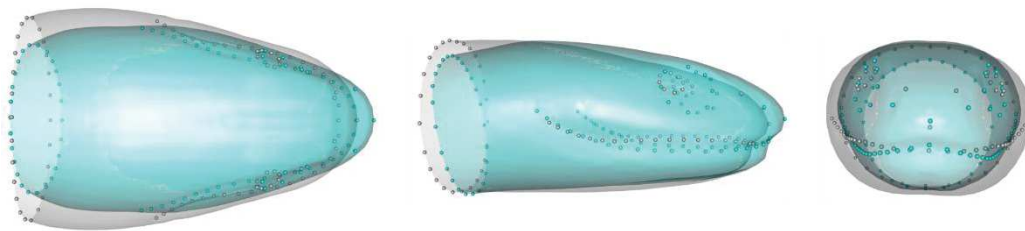


Figure 18: Results of the linear discriminant analysis performed on the 7 first principal components illustrating the head shapes associated with species eating preferentially bulky prey (in blue) and elongated prey (in grey) in top view, side view, and frontal view. Dots are the semi-landmarks associated with the eyes, nostrils, mouth and neck.

Drag coefficients

We printed five 3D models of snake heads corresponding to the maxima and minima of the first and second principal components as well as the mean shape. The drag coefficients of the different shapes are represented in Fig. 19 and the Pearson correlation coefficients for all shapes are significant (all $P < 0.001$). All head shapes are different in terms of the drag they generate (ANCOVA: $F_{5,323} = 981$, $P < 0.001$; pairwise ANCOVAs: $P < 0.001$ for all comparisons). The shapes corresponding to the maxima of PC1 and PC2 are the ones with the smallest drag coefficients (around 0.2) whereas the coefficients of the minima are both two times higher (around 0.5). The two maxima (PC1max and PC2max) have a drag coefficient very close to the value obtained for the convergent shape characterizing aquatic snakes and the minima are closer to non-aquatically foraging snakes (Segall et al. n.d.).

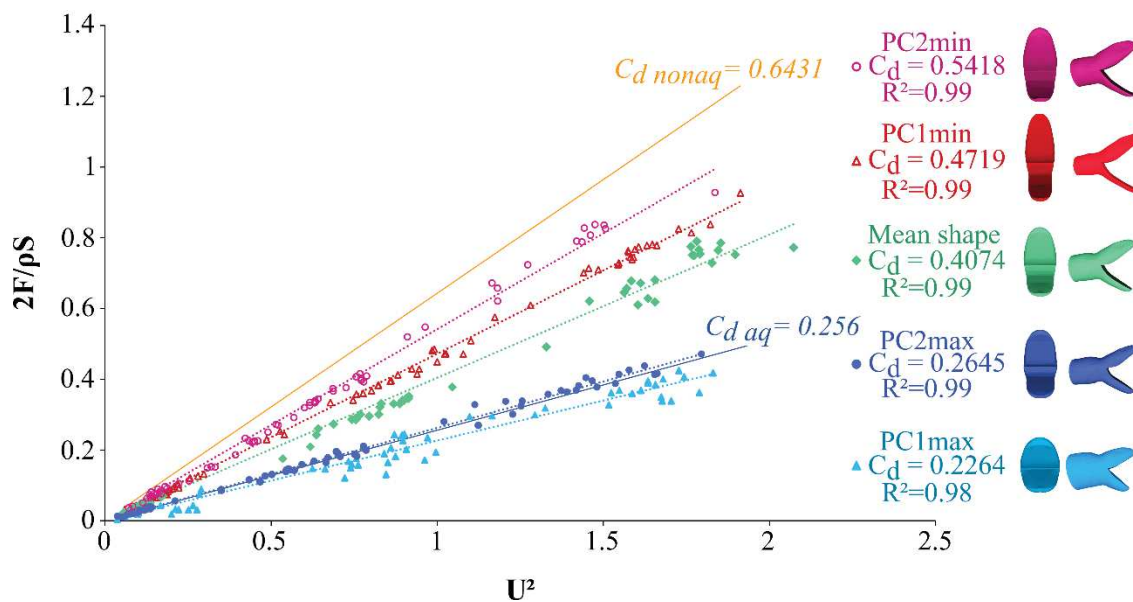


Figure 19: Drag term $2F/\rho S$ depending on the velocity term of the strike (U^2) for the five head models tested. The caption is on the right side of the figure. Linear regression lines are drawn using dashed lines, the regression coefficients correspond to the drag coefficient (C_d) of each shape and are indicated on the right side of the figure next to the associated shape. R^2 indicate the strength of the regression. To compare with our previous work, the drag coefficient of the non-aquatically (C_d nonaq) and aquatically (C_d aq) foraging snakes are added using solid lines.

Discussion

The morphological variability we observe among aquatically foraging species does not show any obvious sub-group structure. This could be related to the strength of the convergence that has been highlighted previously (Segall et al. 2016). Neither habitat use, nor the presence of glands seems to explain the variability in the head shape of aquatically foraging snakes. The absence of a significant effect of habitat use on the head shape of species could indicate that the constraints related with the underwater prey capture are stronger than other ecological requirements. In the same way, the presence of a gland does not seem to affect head shape.

However, prey shape does seem to be related with head shape in aquatically foraging snakes. However, the axis that discriminates between the two shapes represents less than 4% of the overall variability. The shapes associated with the two categories considered are in contradiction to our *a priori* predictions and the results of previous studies (Forsman 1991; Fabre et al. 2016; Brecko et al. 2011): bulky prey eaters have elongated heads whereas elongated prey eaters have a bulky head (Fig. 18). From a biomechanical perspective, however, the shape associated with the bulky eaters versus the elongated prey eaters can make sense. The function of ingestion in snakes is accomplished by a maneuver where the head of the snake advances over the prey using a series of alternating steps of the skull which ultimately allows swallowing the prey (i.e. the so-called pterygoid walk). The lever arm formed by the palato-maxillary complexes and the vertebral column (Young 1991) is likely to be modified along with the shape of the head. The example of a trade-off highlighted by Wainwright in his review (Wainwright 2007) perfectly fits the snake system: a large and short head means a small ratio between the input lever and output lever, which means less steps to cover the length of the prey, even though each step will need more muscle force. This configuration allows thus to reduce the number of “lever cycles” needed to swallow a prey and, as snakes are quite vulnerable to predators while eating, they can reduce their handling time when feeding on elongated animals. Actually, when swallowing a prey of the same relative mass, the viperids (i.e. bulky head species) perform better than colubrid snakes (i.e. elongated head species) by reducing the number of jaw cycles (Lillywhite 2014). Moreover, *Laticauda colubrina* which has a very bulky head only needs 7 seconds to swallow an entire eel (Radcliffe & Chiszar 1980).

Hydrophis schistosa, a catfish specialist, needs on average 1.2 min to swallow a catfish and 2.5 min for puffer fish, which is bulkier (Vorlis et al. 1978). However, this hypothesis that remains to be tested as we lack data about the skull morphology and we do not know how reliable the external head shape represents the length of the bones that compose the skull of a snake.

The morphological variability in head shape is difficult to explain with the ecological traits tested here despite the fact that they should be strong drivers of morphological diversity. If selection on morphology is not as strong as we thought and as the species still have to deal with the same strong physical constraint, we were expecting a many-to-one mapping of form to function. Among the five shapes we tested, two have a drag coefficient that is very close to the coefficient of the “average” aquatic forager (Segall et al. n.d.). These species correspond to the part of the morphospace that comprises the Acrochordidae, Homalopsidae and marine Elapidae which are the most aquatic species of our dataset. The three others have higher drag coefficients, one being close to the “non-aquatically” foraging snakes (Fig. 19). A large drag coefficient means that the strike will be more energetically costly for the snake and reduces its chances to capture its prey. However, many species with a high drag coefficient have a diet that is mainly composed of aquatic prey. All the species included in our dataset are successful in aquatic foraging despite the hydrodynamic constraints. This means that, instead of a classical many-to-one mapping of form to function, we have here an example of one-to-one mapping of form to function followed by a many-to-one mapping of function to ecology.

It would be of interest to map the fitness features related to prey capture behavior onto the morphospace of the head shape of aquatically foraging snakes. Prey capture success could, for example, be a good indicator of fitness. This would require an extensive further study that would nevertheless be very informative and even essential to understand whether the observed morphological and functional diversity is related to fitness. This would then allow us to create an adaptive landscape that could open up new avenues for further study. Finally, future investigations should focus on the role of behavior as a buffer between shape, function, and ecology (Wainwright 2007). Previous studies have highlighted two main behavioral strategies employed by aquatic feeding snakes; the

frontal strike and the lateral strike (Herrel et al. 2008). It seems intuitive that snakes that have a head that is associated with a high drag coefficient would prefer to capture their prey using a lateral strike whereas the ones with a small drag coefficient should probably use a frontal strike. Unfortunately, we are not able to test this hypothesis due to a lack of behavioral data for most of the species of our dataset. However, from what is known on the literature, it seems that high drag coefficient species preferably use a frontal strike and *vice versa* (Herrel et al. 2008; Franz 1977; Voris et al. 1978; Smith et al. 2002; Jayne et al. 1988).

In conclusion, the narrow relationship between form function and fitness is not as straightforward as proposed by Arnold (Arnold 1983). In our study, morphological diversity is directly associated with functional diversity. Yet this functional diversity does not correspond to a single functional 'optimum' as would have been expected in the case of a many-to-one mapping of form to function. The resulting diversity of phenotypes all have to deal with the same strong hydrodynamic constraints without any obvious functional advantages associated with some head shapes. Despite this conundrum, all species studied are successful aquatic predators managing to deal effectively with the physical obstacle in order to succeed in their ecological task: feeding.

Acknowledgments

We thank the herpetological collections of the FMNH, the AMNH, the MCZ and the CAS and their respective curators Alan Resetar (FMNH), David A. Kizirian (AMNH), Jens Vindum (CAS) and Jose P. Rosado (MCZ) for their help in the choice of specimens and the loans. We especially want to thank the staff of the Laboratoire Reptiles et Amphibiens of the National Museum of Natural History of Paris for their help, patience and effectiveness. The 'plateforme de morphometrie' of the UMS 2700 (CNRS, MNHN) is acknowledged for allowing us to use the surface scanner. We thank Olivier Brouard, Amaury Fourgeaud and Tahar Amorri from the PMMH lab for their precious help in the experimental design as well as Xavier Benoit-Gonin for his help with the 3D printer. Justine Laurent is especially acknowledged for their help with the sensors and computer coding.

Chapter 4

**Morphology, function and behavior:
a complex relationship**

Morphology, function and behavior: a complex relationship.

Abstract

The morphology of the head of aquatically foraging snakes is shaped by the hydrodynamic forces that apply during a strike. Some shapes appear to be more advantageous when performing a frontal strike than others. However, whereas some aquatic snakes strike at their prey using a frontal strike, others use lateral strikes. In this study, we hypothesize that each behavioral strategy is associated with a specific head shape. We hypothesize that the couple shape-strategy is optimized and thus that the performance of the strike should not be different between frontal and lateral strikers. We first used high-speed video analysis to quantify performance in three previously unstudied species of aquatic snakes. Next we used 3D geometric morphometrics to quantify head shape in lateral and frontal strikers. A comparative analysis in a phylogenetic framework was then conducted by completing our data set with behavioral and performance data available in the literature. Our results show that the behavioral strategies are associated with different head shapes but that there are no differences in performance between the two strategies.

Key words: aquatic snake, behavioral strategy, frontal striker, lateral striker, kinematics, head shape

Introduction

Feeding under water is a challenge for animals, particularly when they prey on elusive aquatic animals that present efficient anti-predatory systems (Chivers & Jan 1998; Feminella & Hawkins 1994; Faber et al. 1989; Zottoli 1977; Zeddies & Fay 2005). Not only does the predator have to deal with the escape response of the prey but also with the hydrodynamic constraints that act against its strike (Young 1991). Moreover, they are constrained by their morphology, which is the result of their evolutionary history plus any adaptations that have occurred over evolutionary time (Taylor 1987). The acquisition of an aquatic lifestyle has at least in part driven the evolution of the head shape of aquatic snakes (Chapter 1, Segall et al. 2016). This adaptation appears to be quite original as it has actually resulted in a variety of head shapes. Furthermore, these head shapes are associated with variability in the hydrodynamics (i.e. drag coefficient) which are thought to be intimately linked to capture performance and ultimately fitness (Chapter 3). This variability in hydrodynamic streamlining is ultimately related to an evolutionary success as all the species, independently of their head shape, manage to capture elusive aquatic prey. The main hypothesis explaining why animals with differently shaped heads and different drag profiles are still successful is a behavioral adaptation of the prey capture strategy in aquatic snakes.

Indeed, previous studies have highlighted different prey capture behavior in aquatic snakes, namely a frontal and a lateral strike (Herrel et al. 2008). These strategies seem to be dependent on the species (Alfaro 2003; Alfaro 2002; Bilcke et al. 2006). The hydrodynamic constraints related with prey capture, namely drag and added mass are both in some way related to the shape of the head (Chapter 2 & 3). Thus, the constraints related with a frontal strike and a lateral strike should not be the same for a given shape (Young 1991). Drag has been shown to have a major contribution to the hydrodynamics of a strike and is related to the surface that is opposed to the movement (Eq. 4). In Fig 19, both frontal and lateral surfaces of different head shapes are presented and it is quite obvious that, for each shape, lateral and frontal strikes are not likely to result in the same hydrodynamic profile. Although the hydrodynamic constraints of a lateral strike remain to be characterized, the behavioral adaptations of the prey capture strategy in

aquatic snakes could potentially explain their evolutionary success despite the morphological variability that has been observed. The aim of the present study is to link morphology and prey capture behavior in aquatic snakes. The main hypothesis is that the species using a frontal strike strategy have a different head shape than the species that strike laterally. We expect that the frontal strikers present a head shape that allows a reduction of the frontal area as it is related to drag. The second prediction is that, as the head shape-strategy couple is supposedly optimized for each species, the performance of the strike (here velocity and acceleration) should not be different for the species performing frontal or lateral strike. We propose to explore this question by comparing the head shape and the behavior, both strategy and kinematics, of aquatic snakes species.

However, as mentioned in the conclusion of the previous chapter, the prey capture behavior and kinematics remain poorly known in aquatic snake species thus preventing a proper comparative analysis of the relationship between form, function (i.e. kinematics) and the behavior. Most of the studies in the literature focus on natricine species (Herrel et al. 2008; Bilcke et al. 2006; Alfaro 2002; Alfaro 2003; Hibbitts & Fitzgerald 2005). To be able to perform a comparative analysis in an evolutionary framework, we here describe and compare the behavior and kinematics of the strike in three species of aquatic snakes: a sea snake, *Hydrophis platura* and two homalopsid snakes, *Cerberus schneiderii* and *Enhydris bocourti*. We recorded several strikes on aquatic elusive prey in several individuals of these three species using high speed cameras to quantify the kinematics of the strike but also obtained regular speed videos to understand the general foraging behavior. Next, we gathered information on the kinematics and behavior of species for which the head shape has been characterized in Chapter 1 and for which data are available in the literature. We ran a comparative analysis in a phylogenetic context to understand the link between the morphology and the behavior of aquatic snakes.

Material & Methods

Experimental setups and tracking

Experimental setups were built to gather information on three aquatic snake species for which no quantitative data on aquatic strikes exist; *Hydrophis platura*, *Enhydria (Subessor) bocourti* and *Cerberus schneiderii*. A similar experimental setup was used for both *H. platura* and *E. bocourti*, it consisted in a tank filled with 10cm of water. Several fish were put in the tank before putting the snake inside. Two cameras were positioned above in order to have a view of the entire tank. A camera Canon EOS 1100D was used to continuously record the snakes while in the tank to get the behavioral features associated with the prey capture. A high speed camera (Phantom Miro M110) was also set above the tank to record the strike at 500fps for *H. platura* and 1000fps for *E. bocourti*. The experimental setup for *C. schneiderii* consisted in a water tank with only a high speed camera RedLake MotionMeter that recorded the strikes at 250fps.

Hydrophis platura experiments

15 individuals of the yellow morph of *H. platura* from Golfo Dulce, Costa Rica, were captured and brought to the field lab to be filmed while foraging. They were kept in a tank with fresh ocean water and they were moved to the study tank for the experiment. The tank dimensions were 80x30x50cm. After the experiment, the snakes were put back with the other individuals in the housing tank. They were not fed while in the housing tank as the experiments were ran over a short time period (less than two weeks). The fish were captured in the mangrove of Golfito bay and were kept in a tank with fresh ocean water. Several fish were put in the tank before the snake was introduced. All individuals were tested at least three times. Among the 15 individuals, six attempted to catch a fish at least once and five succeeded at least once, resulting in a total amount of 19 successful strikes that were recorded among which 10 videos were usable for tracking.

Enhydris bocourti experiments

Thirteen individuals of *E. bocourti* kept at Amneville Zoo were used in the experiments. They are housed either in separate tanks or by groups of two or three individuals. The experimental tank dimensions were 75x50x50cm. The snakes were usually fed with cyprinid fish kept in a housing tank with *ad libitum* food. One to four fishes were put in the experimental tank before the tested individual was introduced. All snakes were tested at least two times. Among the 13 individuals tested, four were recorded capturing fish, resulting in 20 videos among which 13 videos were suitable for the tracking.

Cerberus schneiderii experiments

Fourteen individuals were captured in the wild and brought to the field lab. Six individuals successfully captured fish resulting in 12 films that were used for the behavioral analysis and eight that were used for tracking.

Video analysis

The tip of the snout of the snakes was manually tracked on each high speed video using the plugin MTrackJ of ImageJ (Meijering & Dzyubachyk 2012). All tracks were filtered using a butterworth low pass data noise filter with a cutoff frequency of 25Hz. The maximal velocity and maximal acceleration of each successful strike were extracted from the filtered data. These variables are commonly used in studies on prey capture thus making the comparison with previous work possible. Both variables were calculated in two ways; using the international system of units, respectively $\text{m}\cdot\text{sec}^{-1}$ and $\text{m}\cdot\text{sec}^{-2}$, and using a relative unit based on the head length (hl) of each individual, respectively $\text{hl}\cdot\text{sec}^{-1}$ and $\text{hl}\cdot\text{sec}^{-2}$. The use of relative units allows comparing the kinematics of the species while taking into account the differences that are related to size. As behavioral characteristics, we chose to record the capture strategy; either if the snake attack the prey frontally or laterally (Herrel et al. 2008). Along with the mouth position before the initiation of the strike; either open or closed and the relative size of the prey (in hl). The handling time was recorded whenever possible along with the

number of pterygoid walks used to swallow the prey. We defined the handling time as the time between the first contact with the prey and the time when the prey was completely swallowed. This definition of the handling time is based on an ecological concept; the snake likely wants to reduce the time spent with a prey in the mouth as during that time they are vulnerable to predators.

Data from literature

The maximal velocity and maximal acceleration were gathered from the literature along with the preferred strategy of the species (Table 5). Whenever a conflict of data occurred, we averaged published data. Some quantitative measurements were taken directly from published graphs using WebPlotDigitizer (Rohatgi 2017) when further information was not directly indicated in the text.

Species	Strategy	Maximal velocity (m.s ⁻¹)	Maximal acceleration (m.s ⁻²)	Reference
<i>Acrochordus javanicus</i>	lateral	3.04	1520	Brecko unpub.
<i>Agkistrodon piscivorous</i>	frontal	1.62	75.5	Vincent et al. 2005
<i>Enhydryis bocourti</i>	lateral	1.34	64.81	this study
<i>Erpeton tentaculatum</i>	lateral	1.70	234.44	Smith et al. 2002
<i>Homalopsis buccata</i>	frontal			pers. obs
<i>Cerberus rynchops</i>	lateral			Jayne et al. 1988
<i>Hydrophis platura</i>	lateral	1	40.77	this study
<i>Hydrophis schistosa</i>	lateral			Voris et al. 1978
<i>Natrix tessellata</i>	frontal	0.93	8.3	Bilcke et al. 2006
<i>Nerodia cyclopion</i>	lateral	0.24		Bilcke et al. 2006
<i>Nerodia harteri</i>	frontal			Bilcke et al. 2006
<i>Thamnophis rufipunctatus</i>	frontal	7.92	30.05	Alfaro 2002
<i>Thamnophis couchii</i>	frontal	1.14	39.4	Alfaro 2002
<i>Thamnophis atratus</i>	frontal			pers. obs

Table 5: Summary of the strategy and kinematics of the strike of aquatic snakes available in the literature along with their phylogenetic relationship (left).

Statistical analyses

To compare the performance of the strike between the three species, a MANOVA was ran using the species and the strategy used (lateral or frontal) as factors and the velocity and acceleration in head length as response variables. A MANCOVA was ran to compare the performances of the strike in the international system of unit using the size as a covariate and the species and the strategy as factors. If need, post hoc tests with a reduced dataset to compare the species two-by-two, a sequential Bonferroni correction was used.

To highlight a link between the behavioral strategy and the shape in the 14 species for which we were able to get data, we used the scatter plot resulting from a PCA on the 62 aquatic species studied in Chapter 3 (Fig. 16). On this scatter plot, we assigned color to the species for which we had data on the behavior. This figure will allow us not only to see if there is a relationship between the strategy and the behavior of the 14 species, but also to make prediction on the behavior of other species. Next, we extracted the mean shape associated with both strategies and compared these morphologies.

We performed a new principal component analysis with only the 14 species for which we have behavioral data to test for differences in morphology. We used all the components that represent more than 1% of the variability of the dataset namely the four first components. To test for a relationship between head shape and behavior, we ran a phylogenetic MANOVA on 14 species (Table 5). The phylogenetic relationship between the species plays an important role in the evolution of their phenotype and thus it should be considered. Then, we ran subsequent phylogenetic ANOVAs to highlight which axis differentiates between the two strategies. A MANCOVA was ran on 8 species for which the kinematics of the strike have been characterized (Table 5) to test whether the strategy, the shape and the size affected the strike performance. Velocity and acceleration were used as response variables. The centroid size was used as an indicator of overall size. All the continuous variables were log-transformed to ensure normality, which was tested using Shapiro tests. As data on acceleration were missing for *Nerodia cyclopion*, another ANCOVA with only velocity was performed to test for a

potential effect of the strategy, the size and the shape in this 9 species dataset. The statistical analyses were performed using R (R Development Core Team 2014) with a significance level set at 5%.

Results

*Description of the behavior and kinematics of *Hydrophis platura**

Despite their captive conditions and the probable stress of the manipulation, the captured specimens of *H. platura* showed quite rapidly an interest in the fish when placed in the experimental tank. Different sizes of prey were proposed among which some were quite big (4-5 hl). None of the individuals showed an interest or attempted to catch the bigger fish, although one individual did bite one of the big fish but subsequently released it. The fish died some time later, probably from an injection of venom during the bite. This bite was most probably defensive. The snakes caught a range of prey sizes ranging from 0.8hl to 1.9hl, with an average of 1.2 ± 0.3 hl. The ingestion was always head first, sometimes requiring a repositioning of the prey either performed only with the mouth for the small prey or with help of the body, for the bigger prey. The smallest specimens were ingested alive, directly after the strike without any apparent pterygoid walk but mostly by movement of the mandibles. The handling time was quite short, around 1-2 sec from the first contact with the prey until the prey was completely swallowed ([Movie 1](#)). It was not rare that the snake chewed several times the fish before or during ingestion. The bigger prey, however, were kept in the mouth until they died and were subsequently swallowed using a few pterygoid walks (3-4 cycles) ([Movie 2](#)). When struck near the head, the prey was immediately ingested after the strike independent of the size of the prey ([Movie 3](#)). Unfortunately, we did not get enough videos of ingestion to perform a proper statistical analysis. Directly after ingestion, most snakes continued to forage and capture fish. The mean capture success for *H. platura* was 33%, with a high inter-individual variability, from 25% to 100%, with the exception of one individual that attempted once to capture a fish and failed, but never tried again.

The prey capture behavior was quite stereotyped, the snake was floating at the surface, and the body adopting an L-shape, the part of the L with the tail was used to generate the movement while the other part was targeting the prey. The head hung below the surface, slightly laterally orientated. When a fish entered in the field of vision of the snake, either the snake attacked immediately or engaged a pursuit by a backward swimming generated by the tail ([Movie 4](#)). The average distance at which the snakes engaged in the capture behavior by orienting their head in the direction of the targeted fish was quite short, $0.87 \pm 0.93hl$. The L-shape behavior was part of a foraging sequence initiated when the snake detected a fish and chased it over a short distance. However, it happened that a fish approached a snake that remained motionless or explored the tank which resulted often in the snake opportunistically capturing the fish without adopting the L position ([Movie 5](#)). Strikes were always lateral, either in the horizontal plane ([Movie 6](#)) or in an almost vertical plane ([Movie 4](#)). *Hydrophis platura* open their mouth at the very beginning of the strike. If the prey was missed, they tended to keep their mouth open for an “open-mouth searching” behavior.

Description of the behavior and kinematics of Enhydris bocourti

The mean capture success for *E. bocourti* was 74%, only few capture attempts failed. However, it was not rare that a successful strike was decomposed in two phase: a first strike toward the prey that failed then a redirection resulting in a successful capture ([Movie 7](#)). Unlike *H. platura*, *E. bocourti* did not present a preferred prey capture behavior. They are “sit-and-wait” foragers (i.e. they do not chase their prey) and struck only once the prey was at a short distance, $0.70 \pm 0.92hl$. They struck laterally and frontally in equal proportions for the successful attempts (Appendix 8, [Movie 7](#) is an example of the different strategies used by *E. bocourti*). Like *H. platura*, *E. bocourti* opened its mouth when initiating the strike and kept the mouth open when they failed at capturing a target. The mean size of the prey captured was $1.8 \pm 0.2hl$. The handling time was quite long, from 26s to almost 20min. Most of the time, they kept their prey in the mouth for up to several minutes until the prey was immobilized, probably by the action of the oral secretions. Then, they repositioned the prey and swallowed the prey head first using 4 to 7 cycles of pterygoid walks. We recorded two attempts to swallow the prey tail first which all resulted in the regurgitation of the prey. One individual

recaptured its regurgitated prey and repositioned it for a head first ingestion, the others just abandoned their prey. We noticed that if the prey was captured at the head region, the ingestion began rapidly after the strike resulting in a total handling time of 26s for the fastest individual. However, when bitten at mid-body or around the tail region, the snake waited for the fish to be calm in order to be able to reposition it. As for *H. platura*, we lack data on the ingestion phase to perform a statistical analysis.

Description of the behavior and kinematics of Cerberus schneiderii

Cerberus schneiderii, unlike the two other species, tended to strike from farther away, 2.23 ± 2.31 hl. The capture tracks were quite long for this species (Appendix 9) and thus we can consider *C. schneiderii* as a more active predator in comparison of *H. platura* and *E. bocourti* who used a “sit-and-wait” strategy.

The strike performance of the three species is reported in Table 6.

	<i>H. platura</i> N = 10	<i>E. bocourti</i> N = 13	<i>C. schneiderii</i> N = 8
Mean maximal velocity (hl.s ⁻¹)	36.47 ± 11.82	29.20 ± 12.55	52.41 ± 14.29
Mean max acceleration (hl.s ⁻²)	1505.49 ± 645.23	1398.54 ± 976.1	2287.04 ± 910.98
Mean maximal velocity (m.s ⁻¹)	1.00 ± 0.38	1.34 ± 0.57	1.09 ± 0.3
Mean max acceleration (m.s ⁻²)	40.77 ± 17.46	64.81 ± 46.58	47.67 ± 18.99

Table 6: Kinematics of the strike of the three species studied. The mean maximal velocity and acceleration are presented in both head length and meters along with their respective standard error. N represents the number of strikes analyzed.

Strike performance

The strike performance in SI is not statistically different between species (MANCOVA: *Pillai*: 0.1; $P = 0.3$) or strategies (MANCOVA: *Pillai*: 0.03; $P = 0.66$). However, the relative performance in head length is statistically different between species (MANOVA: *Pillai*: 0.39; $P = 0.01$) but it is not between strategies (MANOVA: *Pillai*: 0.05; $P = 0.48$). The only statistically significant difference between the performances in head length is between *Cerberus schneiderii* and *Enhydris bocourti* (MANOVA: *Pillai*: 0.43; $P = 0.005$).

Meta-analysis

When the behavioral strategy is plotted on the two first principal components (Fig. 20), we can see that the species for which we know the behavior are distributed along the PC2 axis. The species that use a lateral strike are on the positive part of the axis while the species that are located around the mean and negative part appear to use frontal strikes (Fig. 20). We colored the morphological space occupied by both groups and it appears that there is no overlap.

The statistical analysis performed on the 14 species shows a significant difference in head shape between lateral and frontal strikers (Wilk's lambda = 0.27, $F_{1,12} = 5.83$, $P_{\text{phy}} = 0.03$). When looking at the first four axes separately, it appears that only the PC3 shows a significant difference ($F_{1,12} = 9.33$, $P_{\text{phy}} = 0.03$). This axis accounts for 14% of the overall variability in head shape between these 14 species. We took the average shape for each of the groups to compare the specific features associated with the two strategies (Fig. 21). The difference between the two shapes is subtle. The heads are approximately of the same width, except that the neck region of the frontal striker shows a narrowing whereas the lateral striker keeps the same, maximal cross-sectional area. The two shapes are about the same length but the anterior part of the head that carries the eyes, nostrils and mouth is a bit shorter for the lateral strikers. The pattern of the mandible for the lateral strikers is particular, it is almost rectangular whereas the frontal striker jaw shape is curvier. The eyes are laterally positioned and a bit bigger in

the frontal strikers. The lateral strikers show some similarities with the general head shape of aquatic species described in the first chapter; the eyes are small and dorsally positioned as well as the nostrils. The head of the lateral striker seems laterally compressed whereas the head of the frontal striker is more dorso-ventrally compressed (Fig. 21). The head shape was opened to an angle of 70° between the jaws to estimate the frontal and lateral surfaces that will be opposed to the flow during a frontal strike (Fig. 21). It appears that the frontal strikers have a frontal surface area that is 6.8% greater than the frontal surface of the lateral strikers. Moreover, the lateral surface is slightly larger (0.5%) for lateral strikers than for frontal strikers.

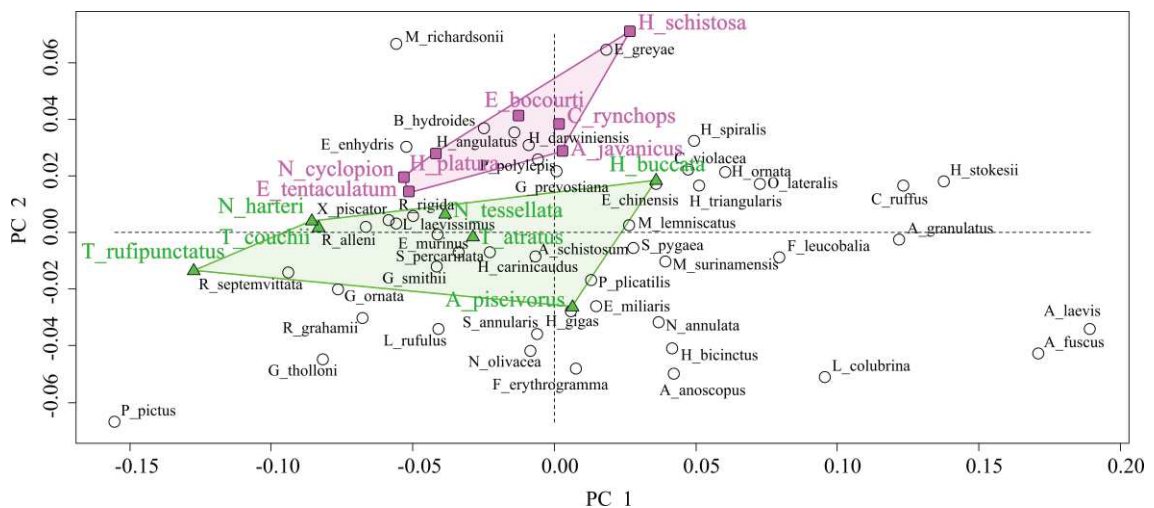


Figure 20: Scatter plot of the principal components one and two (PC1 & PC2) representing respectively 53.4% and 11.1% of the head shape variance among the 62 aquatically foraging snake species. The species that are lateral strikers are colored in pink and the frontal strikers are colored in green, the behavior of the species without any color is unknown. It should be noticed that there is no overlap between the morphological areas occupied by frontal and lateral strikers.

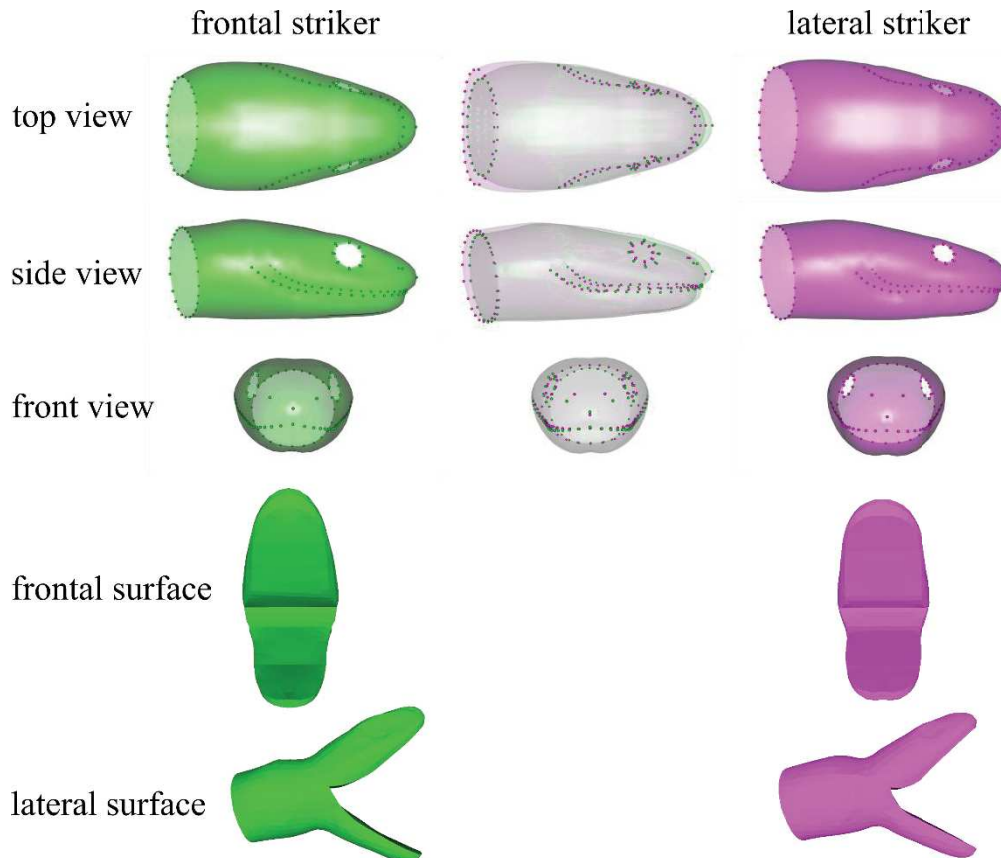


Figure 21: Mean head shapes corresponding to frontal (left, green) versus lateral strikers (right, pink). The middle column represents the two shapes superimposed. Dots represents the landmarks corresponding to the eyes, the nostrils, the mouth and the head-neck limit. The two last rows represent the frontal and lateral surfaces that faces the flow during a frontal strike. The opened models are at the same scale.

There is no statistical difference between the performance of lateral and frontal strikers, and neither the shape (PC3) nor the size seem to impact significantly the performance (MANCOVA: $F_{1,4} > 0.1$, $P > 0.3$; ANCOVA: $F_{1,5} > 0.07$, $P > 0.4$).

Discussion

Comparison of the prey capture behavior of H. platura, E. bocourti and C. schneiderii

The three species are highly aquatic and all managed to catch fish in captivity. The performances of the strike were not different between the species except between

Cerberus schneiderii and *Enhydris bocourti* when considering the relative velocity and acceleration. This could be due to their different foraging behavior. Indeed, *C. schneiderii* tend to strike from farther away and is the most active forager among the three species whereas *E. bocourti* tend to strike when the prey is very close. As the prey is more likely to detect a predator that is striking from far away, the species using this strategy should perform better than the other to ensure the success of the strike.

Some similarities can be noted in the foraging behavior of *E. bocourti* and *H. platura*, such as their tendency to immediately ingest their prey when the bite was located on the head. However, when the bite was located elsewhere, and if the prey was too big, the two species kept it in the mouth until they calm down. This can be explained for *E. bocourti* as the secretions of the Duvernoy's glands are used to tranquilize the prey (Kardong 2002; Weinstein et al. 2009) but the process takes quite a long time. Consequently, the risk of losing the prey is high if released too early. However, *H. platura* is truly venomous and thus one would expect them to inject venom into the prey and release it after death as described for *Laticauda* (Radcliffe & Chiszar 1980) and most terrestrial venomous snakes. The venom of marine Elapids has been shown to have a different composition from their terrestrial relatives which could be related to their specific piscivorous diet (Fry et al. 2003). However, the size and dangerousness of the prey has to be taken into account and counterbalanced with the probability of escape if released (Glaudas et al. 2017). As *H. platura* seems to feed repeatedly on small prey which are not likely to harm the snake, the best strategy could be to hold it. *Laticauda* feeds on relatively large eels that represents a possible danger and as such the best strategy could be to release them. Moreover, it seems that this species stays around its prey until the venom acts but remaining very careful and avoiding any contact during that time (Radcliffe & Chiszar 1980). Plus, *H. platura* is a pelagic snake thus the chances of losing the prey are higher than for *L. colubrina* which mainly forages in crevices. Surprisingly, the prey capture success of *H. platura* is lower than for *E. bocourti*. This difference could be due to the experimental setup. Indeed, while *E. bocourti*, although wild caught specimens, were used to the experimental conditions, *H. platura* seemed not able to realize its foraging behavior correctly. Most of the failed attempts were due to their habit of following their prey by swimming

backward which made them hit the wall of the tank with their tail during the capture phase. Additional experiments should be done with a larger tank and two high speed cameras to record the strike in 3D. Additionally, the experimental setup used for *E. bocourti* can be improved by adding a dry area and some obstacles allowing the animals to anchor their tail. During the experiment, we observed that they used to swim backwards and appeared to try to grab something with their tail, probably to allow them to be more balanced and thus to be able to more firmly maintain the prey or to pull it outside of the water.

Relationships between form, function and behavior

The performance of the strike does not seem to be affected by the strategy used by the species. The frontal strike is thought to be hydrodynamically disadvantageous in comparison with the lateral strike (Young 1991), however, the species manage to perform it at equivalent speeds and accelerations irrespective of the behavior. This can be explained by if the shape and the strategy are related. Indeed the coupling of head shape and strategy was one of the main hypothesis of this study. Given that head shape is in part constrained by the evolutionary history of the species, the strategy should be adapted to reduce to the hydrodynamic constraints, and mainly the drag, associated with a strike. Thus, species with a head shape that performs badly with a frontal strike should use a lateral strike and *vice versa*. When looking at the distribution of the species along PC2 (Fig. 20), the lateral strikers occupy the positive part of the axis while the frontal striker are on the more located around the mean or the negative part of the axis. This means that the shape associated with PC2min should be more adapted to perform a frontal strike. Thus, it should be associated with a smaller drag coefficient (Chapter 2). However, the drag coefficient associated with the positive part of PC2 has a smaller drag coefficient than the mean and the negative part of the axis, respectively 0.26, 0.40 and 0.54. The drag is associated with the project surface that is opposed to the motion, the larger the surface the larger the drag. In figure 21, the frontal surface of the frontal striker is larger and the lateral surface of the lateral strikers is larger which is counterintuitive. Although the drag is related to the frontal surface (Eq. 4), it should be noted that this relationship is not straightforward as in Chapter 3 there is no correlation between the frontal surface and the drag coefficient. Furthermore, the hydrodynamic

constraints associated with the frontal and lateral striker shapes have not been tested and, as seen in Chapter 3, even what appears as a slight difference in shape resulted in a different hydrodynamic profile. Consequently, it appears difficult to predict the hydrodynamic constraints associated with each shape. Force measurements are necessary to characterize the hydrodynamic constraints associated with frontal and lateral striker head shape during frontal and lateral maneuvers.

To summarize, our results show that head shape and capture behavior are indeed related; the lateral strikers and frontal strikes show specific head morphologies. However, the behavior-shape association does not follow the results of the previous chapter; the shape that is closer to a small drag coefficient when performing a frontal strike are actually lateral strikers. This is quite counterintuitive. However, it is possible that the drag coefficient of the frontal strikers when performing a lateral strike is larger and that the drag coefficient of the lateral strikers is even smaller when striking laterally. However, the strike performance is not statistically different for species striking laterally or frontally, meaning that the frontal strikers manage to compensate their hydrodynamic 'disadvantage'. In addition, we do not understand the possible consequences of a 'sub-optimal' strategy on the fitness of the species. For now, data are too sparse on fitness relevant indicators such as the prey capture success of aquatic snakes but further investigations would be of great interest to assess whether the behavior and morphology of frontal strikers are really sub-optimal in terms of fitness.

General conclusion

General conclusion

The main goal of this thesis was to shed light on how the physical properties of water may drive the evolution of species by focusing on snakes as a model system. The hypothesis that has driven this work was that a complex network of relationships exists between hydrodynamic constraints and the biological features of aquatically foraging snakes (Fig. 9).

First, we tackled the question of whether foraging on elusive prey under water has driven the evolution of the head shape of snakes. The main assumption was that hydrodynamic constraints are critical during a strike. Indeed, the strike is the fast transient maneuver that involves not only hydrodynamic drag but also an added mass effect due to the acceleration reaction of the surrounding fluid. Thus, species that are successful aquatic predators should have evolved in a way to circumvent or minimize these constraints as they likely impact the efficacy and success of underwater foraging. To test this hypothesis, we scanned a large sample of heads of snakes in 3D involving more than 400 collection specimens, belonging to 21 species that do not forage under water and compared to 62 species that forage, to some extent, on aquatic elusive prey. This broad sample of species allowed us to compare the non-aquatically foraging snakes to the aquatically foraging ones in an evolutionary context by using analyses that take into account the relationship between the species (i.e. the phylogeny). The results from these analyses showed that snakes that catch elusive prey under water have a head shape that is different from species that do not, irrespective of the phylogenetic relationships between species. In other words, the aquatic species look more similar to one another than they resemble to their close non-aquatic relatives. This analysis provided us with a shape that best characterized the aquatic species. This ‘aquatic shape’ indeed shows some features related to an aquatic lifestyle such as dorsally positioned eyes and nostrils. We thus confirmed that the ability to capture elusive aquatic prey was associated with a convergence in the morphology of the head of snakes. However, we did not assess whether this convergence actually resulted in a hydrodynamic advantage.

In a second chapter we tried to characterize the hydrodynamic constraints associated with a frontal underwater strike and to demonstrate that the head shape of the aquatically foraging species allows reducing the drag imposed upon the head during rapid striking. To do so, we built an experimental setup that measured the forces that are applied to the head of a snake during a frontal strike under water. The flow around the head was visualized using a Particle Image Velocimetry system. The mean characteristic head shapes associated with aquatic and non-aquatic foragers were 3D-printed and mounted on the setup. For both heads, we calculated the drag and the added mass coefficient and their respective contribution during a strike depending on the kinematics (i.e. strike speed and acceleration). It appeared that the added mass coefficient decreases when the acceleration increases. For accelerations larger than $15\text{m}\cdot\text{s}^{-2}$, the added mass coefficient is smaller than the drag coefficient. As most aquatic snake species strike with an acceleration that is higher than $15\text{m}\cdot\text{s}^{-2}$, the drag seems to be the most important hydrodynamic constraint for them. Afterwards, we demonstrated that the drag coefficient is higher for the non-aquatic shape compared to the aquatic one. Thus, we here highlighted not only that head shape does indeed impact the hydrodynamics of striking, but also that the convergent head shape characterized in the first chapter is related to a hydrodynamic advantage during a frontal strike.

At this point we have demonstrated that head shape and hydrodynamics are linked and that the convergence occurred in the evolutionary history of snakes and conferred a reduction in the drag coefficient of aquatically foraging species. Despite this convergence, there was, however, a high variability of head shape in our dataset which led us to raise the question of a potential many-to-one mapping of form to function (i.e. drag coefficient) in this group. In other words, is it possible that different shapes led to the same hydrodynamic advantage? We tested hypothesis was tested by measuring the resistive forces applied on 5 head shape models during frontal striking. It appears that the different head shapes did not converge in term of function; their drag coefficients were very different from one another. Thus, some shapes appear to be more efficient to capture prey under water using a frontal strike. The highest drag coefficients were very close to the drag coefficient of the non-aquatic species. This was quite interesting as we are facing a case of morphological variability that led to performance variability.

Nevertheless that latter variability must result in successful aquatic prey capture as all these species are known to feed on elusive aquatic prey. This puzzling case led us to investigate the behavioral strategy of aquatic snakes.

In previous works, we only investigated the hydrodynamic constraints related with a frontal strike. However, snakes also use another prey capture strategy: a lateral strike. Thus, hypothesized that what appeared as a sub-optimal shape during a frontal strike could be due to the use by the species presenting this phenotype of a lateral strike strategy. To test this idea we gathered information on the prey capture strategy of as many species as we could for which we had the associated head shape. However, aquatic snakes are rather shy and are quite difficult to observe on the field as they forage under water. Thus, the literature data are quite sparse, making it difficult to perform a proper comparative analysis. Consequently we decided to collect data on three additional species from previously under studied groups (sea snakes and homalopsids). Our results highlighted that frontal and lateral strikers presented specific head shapes that are quite different. After crossing these results with the previous analysis we performed, it appeared that hydrodynamically good frontal strikers are actually performing lateral strike whereas bad frontal strikers are using frontal strikes. However, when looking at the performance associated with their strikes, we showed that, despite what appeared to be sub-optimal strategies/shape relationship, the velocity and acceleration of the strike were not different between frontal and lateral strikers. Thus, in some way, all species manage to compensate their hydrodynamic disadvantage to achieve the same levels of performance. Additionally, the hydrodynamics of a lateral strike have not been characterized to date, and thus our conclusions are based on the assumption that the frontal strike is more constrained than a lateral strike. Yet, differently shaped heads will probably also show different hydrodynamic characteristics (i.e. drag coefficient) when performing a lateral strike. In this context, it is possible that the frontal strikers, which show a shape that seems highly constrained for this strategy, are actually even more constrained during a lateral strike. Conversely, lateral strikers which appeared more streamlined to perform a frontal strike, may be even better at striking laterally.

The characterization of the hydrodynamic forces of a lateral strike and the comparison of the different head shape of aquatic snakes during a lateral strike was explored by an intern that I co-supervised (Appendix 10). The experiments mimicked a lateral strike by using a spring that pulls the head of the snake through a water tank. As in Chapters 2 and 3, a force sensor was inserted inside the head to measure the forces applied to the head during a lateral strike. The same five head shapes as in Chapter 3 were used for comparison. However, the experimental setup presents some important differences with the one used in Chapter 2 & 3 as the motion is here driven by a spring pulling during the entire strike whereas in the other experiment, the compression spring released the moving part after a short accelerating phase and the system was then free of the spring. The lateral experiment is, however, more similar to a real snake strike. Thus, to be able to make a proper comparative analysis of the hydrodynamics of the two strategies and to compare the head shape, the lateral strike setup was also adapted to mimic a frontal strike. The inertial part of the strike cannot be neglected with this setup and thus we cannot calculate directly the drag coefficient and the added mass as both are at play. However, the global hydrodynamic forces can be compared. To do so, the maximal force recorded was extracted for each strike and used for the comparison. To make a fair comparison between the head shape and as inertia cannot be neglected, the maximal force was divided by the mass of each model (Fig. 22)

As predicted in the literature (Young 1991; Taylor 1987), the hydrodynamic constraints that apply on the head of a snake during a lateral strike are less important than during frontal strike for every model. However, contrary to our initial prediction, the bad “frontal striker shapes”, namely PC1min and PC2min are also “bad lateral strikers”. Still, the forces resisting the movement of the head are less important during the lateral strike. The results of this experiment are preliminary and require further analysis to extract the hydrodynamic properties of the different shapes such as the drag coefficient or the added mass. Yet, we can conclude that it would be preferable for snakes to perform a lateral strike, independent from their head shape. The frontal strike strategy does not make sense in terms of hydrodynamics and thus, of energetic optimization. Further investigations will focus on the impact of these head shape-behavior-hydrodynamics on fitness related traits such as the prey capture success of the

different species. Indeed, it is possible that the differences observed in the hydrodynamic pattern between the different shapes are not as deleterious as it seems in terms of fitness.

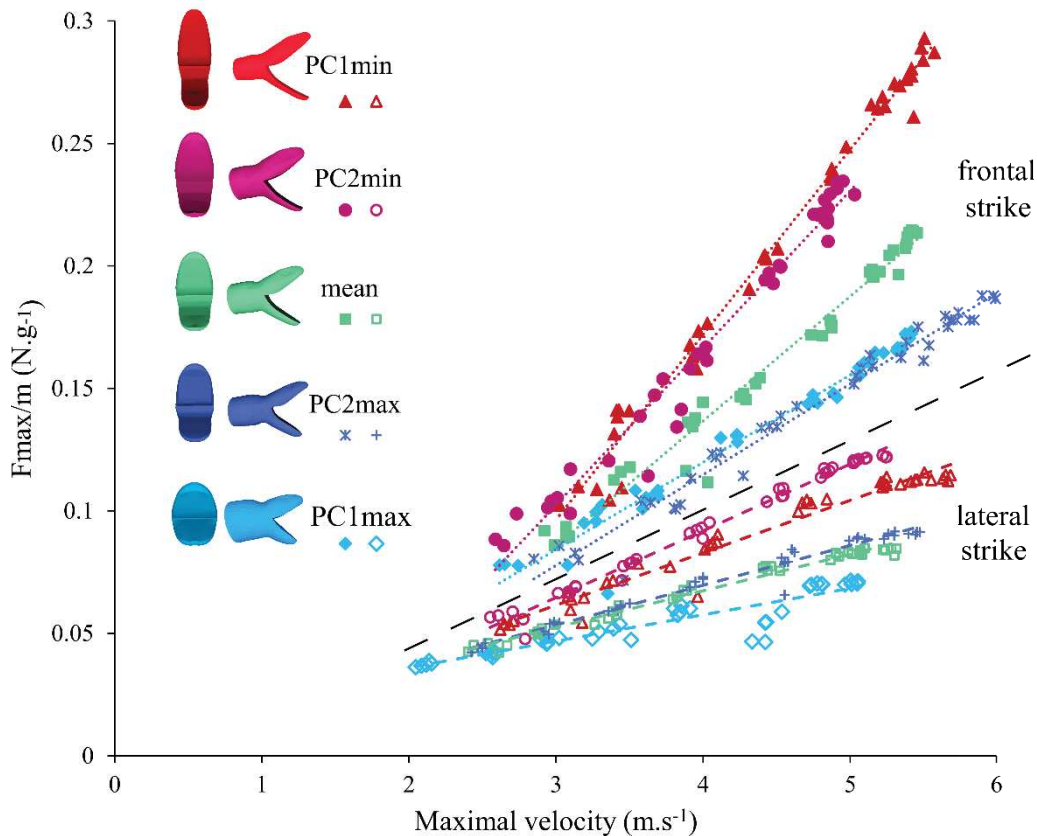


Figure 22: Comparison of the maximal force applied on five 3D printed models of head of snakes during either a lateral or a frontal strike under water depending on the velocity. The force was divided by the mass of the models as these were highly variable and as inertia cannot be ignored.

The frontal strike strategy has been observed in several snake species despite its poor hydrodynamic performance. This could potentially be explained by other hypotheses: first, we could have underestimated the already quite good hydrodynamic profile of a snake and their ability to generate high power accelerations. Second, the impact of the hydrodynamic forces on the outcome of a strike could have been overestimated and it is, as mentioned previously, needs to be investigated further. Another hypothesis is related to the sensory systems. Indeed, foraging is highly related

to the senses of an animal and to be able to accurately locate and strike at a prey, a triangulation system is often the more useful, and this involves a pair of sensory organs such as the eyes, the nostrils or the forked tongue of snakes. Thus, the frontal strike can be advantageous in the way that it potentially allows the predator to be more accurate during the prey capture. This hypothesis requires further analysis and is part of what will be explored in a future project. Indeed, personal observations of *H. platyura* trying to capture its shadow or striking at a rock highlighted, first, the use of vision to detect a prey and second a potentially poor visual system as it does not allow the animal to make the difference between its shadow and a prey.

In conclusion, water and its physical properties have indeed highly impacted the evolution of species, and snakes are not the exception. The laws of physics are universal, which is striking when looking at the many convergent events that have occurred in aquatic animals. However, other ecological, anatomical, physiological and evolutionary constraints are also acting and jointly drive the evolution of species. If we return to figure 9 and adapt it with what has been highlighted in the present work and what remains to be done, without mentioning the new questions that have emerged, my final conclusion would look like figure 23. Several questions have emerged, yet others require a deeper analysis. The behavioral analysis of the prey capture of aquatic snake species should be encouraged as we know so little about them despite the fascinating biological and hydrodynamic issues they raise.

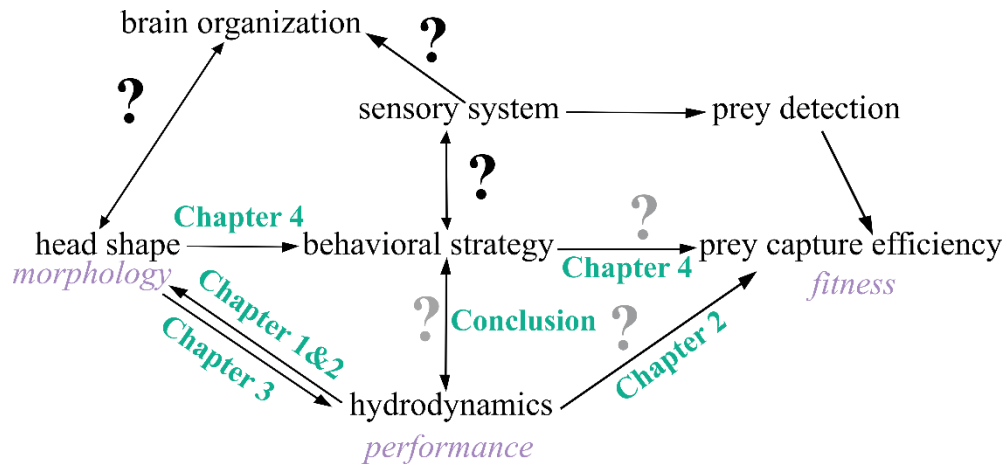


Figure 23: Scheme of the hypothetical relationships between the hydrodynamic constraints, the morphology of the head shape and the behavior of aquatically foraging snakes. In italic and purple are represented the components of Arnold's paradigm. Closed to the arrow are the chapter in which we tried to highlight the relationship represented by the arrow. Light question marks are things that were slightly explored but that require further investigation. Dark question marks are what have been opened and is going to be explore in a close future.

General conclusion

References

References

- Adams, D.C. & Otarola-Castillo, E., 2013. Geomorph: an R package for the collection and analysis of geometric morphometric shape data. *Methods in Ecology and Evolution*, 4, pp.393–399.
- Adams, D.C., 2014. A Generalized K Statistic for Estimating Phylogenetic Signal from Shape and Other High-Dimensional Multivariate Data. *Systematic Biology*, 63(5), pp.685–697.
- Alfaro, M.E., 2002. Forward attack modes of aquatic feeding garter snakes. *Functional Ecology*, 16(2), pp.204–215.
- Alfaro, M.E., 2003. Sweeping and striking: a kinematic study of the trunk during prey capture in three thamnophiine snakes. *Journal of Experimental Biology*, 206(14), pp.2381–2392.
- Arnold, S.J., 1983. Morphology, performance and fitness. *American Zoologist*, 23, pp.347–361.
- Baylac, M., 2012. Rmorph: a R geometric and multivariate morphometrics library. Available from the author: baylac@mnhn.fr.
- Bennett, A.F., 1980. The metabolic foundations of vertebrate behavior. *Bioscience*, 30(7), pp.452–456. Available at: <http://www.jstor.org/stable/10.2307/1307946>.
- Bilcke, J., Herrel, A. & Aerts, P., 2007. Effect of prey and predator size on the capture success of an aquatic snake. *Belgian Journal of Zoology*, 137(2), pp.191–195.
- Bilcke, J., Herrel, A. & Van Damme, R., 2006. Correlated evolution of aquatic prey-capture strategies in European and American natricine snakes. *Biological Journal of the Linnean Society*, 88(1), pp.73–83.
- Blomberg, S.P., Garland, T.J. & Ives, A.R., 2003. Testing for phylogenetic signal in comparative data: behavioral traits are more labile. *Evolution; international journal of organic evolution*, 57(4), pp.717–745.
- Bolt, R.E. & Ewer, R.F., 1964. The functional anatomy of the head of the puff adder,

- Bitis arietans*. *Journal of Morphology*, 114(1), pp.85–105.
- Botton-Divet, L. Houssaye, A., Herrel, A., Fabre, A-C. & Cornette, R., 2015. Tools for quantitative form description; an evaluation of different software packages for semi-landmark analysis. *PeerJ*, 3, p.e1417.
- Brecko, J., Vervust, B., Herrel, A. & Van Damme, R., 2011. Head morphology and diet in the dice snake (*Natrix tessellata*). *Mertensiella*, 18(September), pp.20–29.
- Brennen, C.E., 1982. A Review of Added Mass and Fluid Inertial Forces.
- Brischoux, F. & Lillywhite, H.B., 2011. Light- and flotsam-dependent “float-and-wait” foraging by pelagic sea snakes (*Pelamis platurus*). *Marine Biology*, 158(10), pp.2343–2347.
- Camilleri, C. & Shine, R., 1990. Sexual Dimorphism and Dietary Divergence: Differences in Trophic Morphology between Male and Female Snakes. *Copeia*, 1990(3), pp.649–658.
- Catania, K.C., 2009. Tentacled snakes turn C-starts to their advantage and predict future prey behavior. *Proceedings of the National Academy of Sciences of the United States of America*, 106(27), pp.11183–7.
- Chivers, D.P. & Jan, F.S., 1998. Chemical alarm signalling in aquatic predator-prey systems: A review and prospectus. *Ecoscience*, 5(3), pp.338–352.
- Collar, D.C. & Wainwright, P.C., 2006. Discordance between Morphological and Mechanical Diversity in the Feeding Mechanism of Centrarchid Fishes. *Evolution*, 60(12), pp.2575–2584.
- Crowe-Riddell, J.M., Snelling, E.P., Watson, A.P., Suh, A.K. Partridge, J.C. & Sanders, K.L., 2016. The evolution of scale sensilla in the transition from land to sea in elapid snakes. *Open Biology*, 6, p.160054.
- Cundall, D. & Gans, C., 1979. Feeding in watersnakes: an electromyographic study. *Journal of Experimental Zoology*, 209(2), pp.189–209.
- Daniel, T.L. & Webb, P.W., 1987. Physical determinants of locomotion. In P. Dejours, Bolis, L., Taylor, C. R., Weibel, E. R., eds. *Comparative Physiology: Life in Water and on Land*. New York, pp. 343–369.

References

- Daniel, T.L., 1984. Unsteady Aspects of Aquatic Locomotion. *American Zoologist*, 24(1), pp.121–134.
- Darwin, C., 1859. *On the origin of species*, John Murray.
- Deban, S.M. & Wake, D.B., 2000. Aquatic feeding in Salamanders. In K. Schwenk, ed. *Feeding: Form, Function and Evolution in Tetrapod Vertebrates*. San Diego, p. 537.
- Drummond, H., 1983. Aquatic Foraging in Garter Snakes : A Comparison of Specialists and Generalists. *Behavior*, 86(1), pp.1–30.
- Drummond, H., 1985. The role of vision in the predatory behaviour of natricine snakes. *Animal Behaviour*, 33, pp.206–215.
- Dunson, W.A. & Dunson, M.K., 1973. Convergent evolution of sublingual salt-glands in marine file snake and true sea snakes. *Journal of Comparative Physiology*, 86(3), pp.193–208.
- Eckhardt, R.C., 1979. The adaptive syndromes of two guilds of insectivorous birds in the Colorado Rocky Mountains. *Ecological Monographs*, 49(2), pp.129–149.
- Esquerré, D. & Keogh, J.S., 2016. Parallel selective pressures drive convergent diversification of phenotypes in pythons and boas. *Ecology Letters*, 19, pp.800–809. Available at: <http://doi.wiley.com/10.1111/ele.12620>.
- Faber, D.S., Fetcho, J.R. & Korn, H., 1989. Neuronal networks underlying the escape response in goldfish. General implications for motor control. *Annals of the New York Academy of Sciences*, 563, pp.11–33.
- Fabre, A.-C., Bickford, D., Segall, M. & Herrel, A., 2016. The impact of diet, habitat use, and behavior on head shape evolution in homalopsid snakes. *Biological Journal of the Linnean Society*, 118, pp.634–647.
- Feminella, J.W. & Hawkins, C.P., 1994. Tailed frog tadpoles differentially alter their feeding behavior in response to non-visual cues from four predators. *Journal of the North American Benthological Society*, 13(2), pp.310–320.
- Fish, F.E., 1993. Influence of hydrodynamic design and propulsive mode on mammalian swimming energetics. *Australian Journal of Zoology*, 42, pp.79–101.

- Forsman, A., 1991. Adaptive variation in head size in *Vipera berus*. *Biological Journal of the Linnean Society*, 43(4), pp.281–296.
- Fraley, C., Raftery, A.E., Murphy, T.B. & Scrucca, L., 2012. mclust Version 4 for R: Normal Mixture Modeling for Model-Based Clustering, Classification, and Density Estimation.
- Franz, R., 1977. Observations on the food, feeding behavior, and parasites of the striped swamp snake, *Regina alleni*. *Herpetologica*, 33(1), pp.91–94.
- Fry, B.G., Wuster, W., Ramjan, S.F.R., Jackson, T., Martelli, P. & Kini, R.M., 2003. Analysis of Colubroidea snake venoms by liquid chromatography with mass spectrometry: evolutionary and toxinological implications. *Rapid Communications in Mass Spectrometry*, 17, pp.2047–2062.
- Fry, B.G., Scheib, H., van der Weerd, L., Young, B.A., McNaughtan, J., Ramjan, S.F.R., Vidal, N., Poelmann, R.E. & Norman, J.A., 2008. Evolution of an arsenal: structural and functional diversification of the venom system in the advanced snakes (Caenophidia). *Molecular & Cellular Proteomics*, 7(2), pp.215–246.
- Gans, C., 1961. The Feeding Mechanism of Snakes and Its Possible Evolution. *American Zoologist*, 1(2), pp.217–227.
- Gans, C., 1969. Comments on inertial feeding. *Copeia*, 1969(4), pp.855–857.
- Gazzola, M., Argentina, M. & Mahadevan, L., 2014. Scaling macroscopic aquatic locomotion. *Nature Physics*, 10(10), pp.758–761.
- Glaudas, X., Kearney, T.C. & Alexander, G.J., 2017. To hold or not to hold? The effects of prey type and size on the predatory strategy of a venomous snake. *Journal of Zoology*, pp.1–8.
- Glodek, G.S. & Voris, H.K., 1982. Marine snake diets : prey composition, diversity and overlap. *Copeia*, 1982(3), pp.661–666.
- Greene, H.W., 1983. Dietary correlates of the origin and radiation of snakes. *American Zoologist*, 23(2), pp.431–441.
- Gunz, P. & Mitteroecker, P., 2013. Semilandmarks: A method for quantifying curves and surfaces. *Hystrix*, 24(1), pp.103–109.

References

- Heatwole, H., 1987. *Sea snakes*, Kensington, NSW, Australia: University of New South Wales Press Ltd.
- Heiss, E., Natchev, N., Gumpenberger, M., Weissenbacher, A. & Van Wassenbergh, S., 2013. Biomechanics and hydrodynamics of prey capture in the Chinese giant salamander reveal a high-performance jaw-powered suction feeding mechanism. *Journal of the Royal Society, Interface*, 10(82), p.20121028.
- Herrel, A., Vincent, S.E., Alfaro, M.E., Van Wassenbergh, S., Vanhooydonck, B. & Irschick, D.J., 2008. Morphological convergence as a consequence of extreme functional demands: Examples from the feeding system of natricine snakes. *Journal of Evolutionary Biology*, 21(5), pp.1438–1448.
- Hibbitts, T.J. & Fitzgerald, L.A., 2005. Morphological and ecological convergence in two natricine snakes. *Biological Journal of the Linnean Society*, 85, pp.363–371.
- Hoerner, S.F., 1965. *Fluid Dynamic Drag*, Bakersfield, California.
- Hoso, M., Asami, T. & Hori, M., 2007. Right-handed snakes: convergent evolution of asymmetry for functional specialization. *Biology letters*, 3(2), pp.169–172.
- Houssaye, A. & Fish, F.E., 2016. Functional (Secondary) Adaptation to an Aquatic Life in Vertebrates: An Introduction to the Symposium. *Integrative and Comparative Biology*, 56(6), pp.1266–1270. Available at: <https://academic.oup.com/icb/article-lookup/doi/10.1093/icb/icw129>.
- Howell, A.B., 1971. *Aquatic mammals*, New York, USA: Dover Publications Inc.
- Huey, R.B. & Pianka, E.R., 1981. Ecological Consequences of Foraging Mode. *Ecology*, 62(4), pp.991–999.
- Jayne, B.C., Voris, H.K. & Heang, K.B., 1988. Diet, feeding behavior, growth and numbers of a population of *Cerberus rynchops* (Serpentes: Homalopsinae) in Malaysia., Chicago: Field Museum of Natural History.
- Kardong, K.V., 2002. Colubrid snakes and Duvernoy's "venom" glands. *Journal of Toxicology : Toxin Reviews*, 21(1), pp.1–15.
- Kelley, N.P. & Motani, R., 2015. Trophic convergence drives morphological convergence in marine tetrapods. *Biology Letters*, 11(1), p.5.

- Kembel, S.W., Cowan, P.D., Helmus, M.R., Cornwell, W.K., Morlon, H., Ackerly, D.D., Blomberg, S.P. & Webb, C.O., 2010. Picante: R tools for integrating phylogenies and ecology. *Bioinformatics*, 26(11), pp.1463–1464.
- Klingenberg, C.P., 2011. MorphoJ: an integrated software package for geometric morphometrics. *Molecular Ecology Resources*, 11(2), pp.353–357.
- Koehl, M.A.R., 1996. When Does Morphology Matter? *Annual Review of Ecology and Systematics*, 27, pp.501–542.
- Landau, L.D. & Lifshitz, E.M., 1959. *Fluid Mechanics* Pergamon P.
- Langebartel, D.A., 1968. The hyoid and its associated muscles in snakes. In *Illinois biological monographs*, 38. Urbana, University of Illinois Press, p. 180.
- Lauder, G. V. & Prendergast, T., 1992. Kinematics of aquatic prey capture in the snapping turtle *Chelydra serpentina*. *Journal of Experimental Biology*, 164, pp.55–78.
- Lemell, P., Lemell, C., Snelderwaard, P., Gumpenberger, M., Wochesländer, R. & Weisgram, J., 2002. Feeding patterns of *Chelus fimbriatus* (Pleurodira: Chelidae). *The Journal of experimental biology*, 205, pp.1495–1506.
- Lewontin, R.C., Rose, S. & Kamin, L.J., 1984. *Not in our genes: biology, ideology, and human nature*, Pantheon Books.
- Lillywhite, H.B., 1996. Husbandry of the little file snake, *Acrochordus granulatus*. *Zoo Biology*, 15(3), pp.315–327.
- Lillywhite, H.B., 2014. *How snakes work: structure, function and behavior of the World's snakes*, New York, New York: Oxford University Press.
- Maddison, W.P. & Maddison, D.R., 2015. Mesquite: a modular system for evolutionary analysis. Version 3.04. Available at: <http://mesquiteproject.org>.
- Marx, H. & Rabb, G.B., 1972. Phyletic analysis of fifty characters of advanced snakes. *Fieldiana (Zoology)*, 63(2), pp.1–321.
- McHenry, M.J., Feitl, K.E., Strother, J.A. & Van Trump, W.J., 2009. Larval zebrafish rapidly sense the water flow of a predator's strike. *Biology letters*, 5(4), pp.477–9.

References

- Meijering, O. & Dzyubachyk, I.S., 2012. Methods for Cell and Particle Tracking. *Methods in Enzymology*, 504, pp.183–200.
- Miles, D.B., 1994. Covariation between morphology and locomotory performance in Sceloporine lizards. In L. J. Vitt & E. R. Pianka, eds. *Lizard Ecology: Historical and Experimental Perspectives*. Princeton University Press, pp. 207–236.
- Moisy, F., 2006. A PIV Post-processing and data analysis toolbox : PIVMat 4.00 27 Apr 2006 (Updated 26 Apr 2016).
- Mori, A., 1998. Prey-Handling Behavior of Three Species of Homalopsine Snakes: Features Associated with Piscivory and Duvernoy's Glands. *Journal of herpetology*, 32(1), pp.40–50.
- Muller, M. & Osse, J.W.M., 1984. Hydrodynamics of suction feeding in fish. *Transaction of the Zoological Society of London*, 37(March 1983), pp.51–135.
- Murphy, J.C., 2007. *Homalopsid snakes: Evolution in the mud*, Malabar, Florida: Krieger Publishing Company.
- Murphy, J.C., 2012. Marine invasions by non-sea snakes, with thoughts on terrestrial-aquatic- marine transitions. *Integrative and Comparative Biology*, 52(2), pp.217–226.
- Oufiero, C.E., Holzman, R.A., Young, F.A. & Wainwright, P.C., 2012. New insights from serranid fishes on the role of trade-offs in suction-feeding diversification. *Journal of Experimental Biology*, 215, pp.3845–3855.
- Povel, D.E. & Van Der Kooij, J., 1997. Scale sensillae of the File Snake (Serpentes: Acrochordidae) and some other aquatic and burrowing snakes. *Netherlands Journal of Zoology*, 47(4), pp.443–456.
- Pyron, R.A., Burbrink, F.T. & Wiens, J.J., 2013. A phylogeny and revised classification of Squamata, including 4161 species of lizards and snakes. *BMC evolutionary biology*, 13(1), p.93.
- Queral-Regil, A. & King, R.B., 1998. Evidence for Phenotypic Plasticity in Snake Body Size and Relative Head Dimensions in Response to Amount and Size of Prey. *Copeia*, 1998(2), pp.423–429.

- R Development Core Team, 2014. *R: A language and environment for statistical computing*. R Foundation, Vienna, Austria.
- Radcliffe, C.W. & Chiszar, D.A., 1980. A Descriptive Analysis of Predatory Behavior in the Yellow Lipped Sea Krait (*Laticauda colubrina*). *Journal of Herpetology*, 14(4), pp.422–424.
- Ringuette, M.J., Milano, M. & Gharib, M., 2007. Role of the tip vortex in the force generation of low-aspect-ratio normal flat plates. *Journal of Fluid Mechanics*, 581(2007), p.453.
- Rohatgi, A., 2017. WebPlotDigitizer. Available at: <http://arohatgi.info/WebPlotDigitizer>.
- Rohlf, F.J. & Slice, D., 1990. Extensions of the Procrustes method for the optimal superimposition of landmarks. *Systematic Zoology*, 39(1), pp.40–59.
- Saffman, P.G., 1992. *Vortex dynamics*, Cambridge, UK: Cambridge University Press.
- Savitzky, A.H., 1983. Coadapted character complexes among snakes: fossoriality, piscivory, and durophagy. *American Zoologist*, 23(2), pp.397–409.
- Schaeffel, F. & de Queiroz, A., 1990. Alternative Mechanisms of Enhanced Underwater Vision in the Garter Snakes *Thamnophis melanogaster* and *T. couchii*. *Copeia*, 1990(1), pp.50–58.
- Schaeffel, F. & Mathis, U., 1991. Underwater Vision in Semi-Aquatic European Snakes. *Naturwissenschaften*, 78, pp.373–375.
- Schlager, S., 2013. Morpho: Calculations and visualizations related to Geometric Morphometrics. Available at: <http://sourceforge.net/projects/morpho-rpackage/>.
- Schlager, S., 2015. Package “Morpho.”
- Schluter, D., 2000. *The ecology of adaptive radiation*, Oxford: Oxford University Press.
- Schwenk, K., 1994. Why snakes have forked tongues. *Science*, 263, pp.1573–1577.
- Segall, M., Cornette, R., Fabre, A-C, Godoy-Diana, R. & Herrel, A., 2016. Does aquatic foraging impact head shape evolution in snakes? *Proceedings of the Royal Society of London, B Biological Sciences*, 283(1645).

References

- Segall, M., Herrel, A. & Godoy-Diana, R., Hydrodynamics of the frontal strike in aquatic snakes: drag, added mass and the consequences for prey capture success, submitted.
- Sfakiotakis, M., Lane, D.M. & Davies, J.B.C., 1999. Review of fish swimming modes for aquatic locomotion. *IEEE Journal of Oceanic Engineering*, 24(2), pp.237–252.
- Shine, R., Brown, G.P. & Elphick, M.J., 2004. Field experiments on foraging in free-ranging water snakes *Enhydris polylepis* (Homalopsinae). *Animal Behaviour*, 68, pp.1313–1324.
- Smith, T.L., Povel, D.E. & Kardong, K. V., 2002. Predatory strike of the tentacled snake (*Erpeton tentaculatum*). *Journal of Zoology*, 256, pp.233–242.
- Somaweera, R., 2004. Sri Lankan Colubrid Snakes. *Sri Lanka Naturalist*, 5, pp.32–46.
- Stayton, C.T., 2011. Biomechanics on the half shell: Functional performance influences patterns of morphological variation in the emydid turtle carapace. *Zoology*, 114(4), pp.213–223.
- Taylor, M.A., 1987. How tetrapods feed in water: a functional analysis by paradigm. *Zoological Journal of the Linnean Society*, 91, pp.171–195.
- Thiria, B., Goujon-Durand, S. & Wesfreid, J.E., 2006. The wake of a cylinder performing rotary oscillations. *Journal of Fluid Mechanics*, 560(1988), pp.123–147.
- Trapp, B. & Mebert, K., 2011. Upward Position of Eyes and Nostrils of the Dice Snake to Break the Water Surface ? *Mertensiella*, 18(September 2011), p.440.
- Tytell, E.D., 2004. The hydrodynamics of eel swimming: I. Wake structure. *Journal of Experimental Biology*, 207(11), pp.1825–1841.
- Van Damme, J. & Aerts, P., 1997. Kinematics and functional morphology of aquatic feeding in Australian snake-necked turtles (Pleurodira;Chelodina). *Journal of morphology*, 233(2), pp.113–25.
- van Netten, S.M., 2006. Hydrodynamic detection by cupulae in a lateral line canal: functional relations between physics and physiology. *Biological Cybernetics*, 94(1), pp.67–85.

- van Valen, L., 1973. A new evolutionary law. *Evolutionary Theory*, 1, pp.1–30.
- Van Wassenbergh, S., Brecko, J., Aerts, P., Stouten, I., Vanheusden, G., Camps, A., Van Damme, R. & Herrel, A., 2010. Hydrodynamic constraints on prey-capture performance in forward-striking snakes. *Journal of the Royal Society, Interface*, 7(46), pp.773–785.
- Vanhooydonck, B., Van Damme, R. & Aerts, P., 2001. Speed and Stamina Trade-Off in Lacertid Lizards. *Evolution*, 55(5), pp.1040–1048.
- Varon, E., 2017. *Contrôle réactif d'écoulements décollés en 2D ou 3D à l'aide de capteurs visuels*.
- Videler, J.J., Müller, U.K. & Stamhuis, E.J., 1999. Aquatic vertebrate locomotion: wakes from body waves. *The Journal of experimental biology*, 202(Pt 23), pp.3423–3430.
- Vincent, S.E., Dang, P.D., Herrel, A. & Kley, N.J., 2006. Morphological integration and adaptation in the snake feeding system: A comparative phylogenetic study. *Journal of Evolutionary Biology*, 19(5), pp.1545–1554.
- Vincent, S.E., Moon, B.R., Herrel, A. & Kley, N.J., 2007. Are ontogenetic shifts in diet linked to shifts in feeding mechanics? Scaling of the feeding apparatus in the banded watersnake *Nerodia fasciata*. *The Journal of experimental biology*, 210, pp.2057–2069.
- Vincent, S.E., Brandley, M.C., Herrel, A. & Alfaro, M.E., 2009. Convergence in trophic morphology and feeding performance among piscivorous natricine snakes. *Journal of Evolutionary Biology*, 22(6), pp.1203–1211.
- Vincent, S.E., Herrel, A. & Irschick, D.J., 2004. Sexual dimorphism in head shape and diet in the cottonmouth snake (*Agkistrodon piscivorus*). *Journal of Zoology*, 264(1), pp.53–59.
- Vincent, S.E., Herrel, A. & Irschick, D.J., 2005. Comparisons of aquatic versus terrestrial predatory strikes in the pitviper, *Agkistrodon piscivorus*. *Journal of Experimental Zoology Part A: Comparative Experimental Biology*, 303(6), pp.476–488.

References

- Vitt, L.J. & Congdon, J.D., 1978. Body shape, reproductive effort, and relative clutch mass in lizards: resolution of a paradox. *The American Naturalist*, 112(985), p.595.
- Vogel, S., 1994. *Life in moving fluids: the physical biology of flow*, Princeton: Princeton University Press.
- Voris, H.K., Voris, H.H. & Liat, L.B., 1978. The Food and Feeding Behavior of a Marine Snake, *Enhydrina schistosa* (Hydrophiidae). , 1978(1), pp.134–146.
- Wainwright, P.C., Sanford, C.P., Reilly, S.M., & Lauder, G.V., 1989. Evolution of motor patterns: aquatic feeding in salamanders and ray-finned fishes. *Brain, behavior and evolution*, 34(6), pp.329–341.
- Wainwright, P.C., Alfaro, M.E., Bolnick, D.I., & Hulsey, C.D., 2005. Many-to-One Mapping of Form to Function: A General Principle in Organismal Design? *Integrative and Comparative Biology*, 45(2), pp.256–262.
- Wainwright, P.C., 2007. Functional Versus Morphological Diversity in Macroevolution. *Annual Review of Ecology, Evolution, and Systematics*, 38(1), pp.381–401.
- Walls, G.L., 1942. *The Vertebrate Eye And Its Adaptive Radiation*, New York, New York: Hafner Publishing Company.
- Webb, P.W., 1971a. The swimming energetics of trout. I. Thrust and power output at cruising speeds. *Journal of Experimental Biology*, 55, pp.489–520.
- Webb, P.W., 1984. Body form, locomotion and foraging in aquatic vertebrates. *American Zoologist*, 24(1), pp.107–120.
- Webb, P.W., 1988. Simple physical principles and vertebrate aquatic locomotion. *Integrative and Comparative Biology*, 28(2), pp.709–725.
- Weinstein, S.A., Smith, T.L. & Kardong, K. V., 2009. Reptile venom glands : form, function, and future. In S. P. Mackessy, ed. *Handbook of Venoms and Toxins of Reptiles*. CRC Press Taylor & Francis Group, pp. 65–92.
- Werth, A.J., 2006. Odontocete Suction Feeding: Experimental Analysis of Water Flow and Head Shape. *Journal of Morphology*, 267, pp.1415–1428.
- Wiley, D.F., Amenta, N., Alcantara, D.A., Ghosh, D., Kil, Y.J., Delson, E., Harcourt-

- Smith, W., Rohlf, F.J., St John, K. & Hamann, B., 2005. Evolutionary morphing. *Proceedings of IEEE Visualization 2005 (VIS'05)*.
- Winemiller, K.O., Kelso-Winemiller, L.C. & Brenkert, A.L., 1995. Ecomorphological diversification and convergence in fluvial cichlid fishes. *Environmental Biology of Fishes*, 44(1–3), pp.235–261.
- Young, B.A., 1991. The influences of the aquatic medium on the prey capture system of snakes. *Journal of Natural History*, 25(2), pp.519–531.
- Zeddies, D.G. & Fay, R.R., 2005. Development of the acoustically evoked behavioral response in zebrafish to pure tones. *The Journal of experimental biology*, 208, pp.1363–1372.
- Zottoli, S.J., 1977. Correlation of the startle reflex and Mauthner cell auditory responses in unrestrained goldfish. *The Journal of experimental biology*, 66(1), pp.243–54.

References

Appendices

Appendices

Appendix 1: List of species included in the analysis, their respective ecology, and the number of specimens scanned per species (N).

Species	Ecology	Specimen number and collection	N	References
<i>Acrochordus granulatus</i>	Aquatic	0000.7200, MNHN 0000.5196, MNHN 0000.7201, MNHN 0000.6155, MNHN 1900.0356, MNHN 1900.0357, MNHN	6	1–4
<i>Acrochordus javanicus</i>	Aquatic	0000.3294, MNHN MS45, Anthony Herrel MS52, Anthony Herrel 0000.5370, MNHN 0000.1145, MNHN	5	4–6
<i>Afronatrix anoscopus</i>	Aquatic	1921.0391, MNHN 1916.0215A, MNHN 1960.0139, MNHN 1943.0079, MNHN 1951.0008, MNHN	5	7,8
<i>Agkistrodon piscivorus</i>	Aquatic	0000.4252, MNHN R3979, AMNH R46913, AMNH R50493, AMNH R64620, AMNH	5	9–12
<i>Aipysurus fuscus</i>	Aquatic	R23488, MCZ R23485, MCZ R23483, MCZ R23482, MCZ R23481, MCZ	5	13
<i>Aipysurus laevis</i>	Aquatic	1990.4513, MNHN 1990.4507, MNHN 1990.4514, MNHN 1990.4515, MNHN 1999.6566, MNHN	5	13
<i>Atretium schistosum</i>	Aquatic	0000.3519, MNHN 1946.0064, MNHN 0000.7000, MNHN 1999.8089, MNHN 0000.7414, MNHN	5	14–16
<i>Bitia hydroides</i>	Aquatic	229793, FMNH 229795, FMNH 198701, FMNH 229791, FMNH 211898, CAS 211899, CAS 211902, CAS	7	17–20
<i>Cantoria violacea</i>	Aquatic	206912, FMNH 250116, FMNH 250118, FMNH 204970, CAS 204971, CAS 211909, CAS	7	17,21

<i>Cerberus rynchops</i>	Aquatic	1996.0258, MNHN 1900.0417, MNHN 1946.0078, MNHN 1946.0078A, MNHN 1946.0077, MNHN	5	17,21–23
<i>Cylindrophis ruffus</i>	Aquatic	0000.3280, MNHN 2007.2452, MNHN 0000.0440, MNHN 0000.3281, MNHN 0000.6362, MNHN	5	24,25
<i>Enhydris bocourti</i>	Aquatic	1988.3768, MNHN 1970.0556, MNHN 1970.0558, MNHN 1970.0559, MNHN 1885.0333, MNHN	5	17,26
<i>Enhydris chinensis</i>	Aquatic	1911.0014, MNHN 1911.0015, MNHN 0000.8777, MNHN 0000.8778, MNHN 1906.0217, MNHN	5	17,21,27– 29
<i>Enhydris enhydris</i>	Aquatic	0000.3749, MNHN 0000.5567, MNHN 1970.0544, MNHN 1970.0550, MNHN 0000.5528, MNHN	5	17,21,26,3 0,31
<i>Ephalophis greyae</i>	Aquatic	212348, FMNH 212362, FMNH 212351, FMNH 212361, FMNH 212367, FMNH	5	32,33
<i>Erpeton tentaculatum</i>	Aquatic	1970.0564, MNHN 1970.0568, MNHN 0000.5458, MNHN 0000.0924, MNHN 0000.0924A, MNHN	5	17,34
<i>Erythrolamprus miliaris</i>	Aquatic	15426, FMNH 15427, FMNH 15432, FMNH 15433, FMNH 217389, FMNH	5	35
<i>Eunectes murinus</i>	Aquatic	0000.7190, MNHN 1996.7897, MNHN 1996.7898, MNHN 1994.1539, MNHN 1994.1538, MNHN	5	35
<i>Farancia erythrogramma</i>	Aquatic	1903.0325, MNHN 0000.3397, MNHN 1991.1666, MNHN 0000.3396, MNHN R128620, AMNH	5	36–38
<i>Fordonia leucobalia</i>	Aquatic	1974.1331, MNHN 1885.0128, MNHN 1892.0270, MNHN 1885.0545, MNHN 217450, FMNH 218887, FMNH	6	17,21,31,3 9–41

Appendices

<i>Gerarda prevostiana</i>	Aquatic	1946.0079, MNHN 1946.0271, MNHN 204972, CAS 211971, CAS	4	17,21,41,42
<i>Grayia ornata</i>	Aquatic	1996.6644, MNHN 1995.9679, MNHN 1994.3383, MNHN 1994.8079, MNHN 1995.9672, MNHN	5	7
<i>Grayia smithii</i>	Aquatic	1998.0603, MNHN 1995.3401, MNHN 1996.6446, MNHN 1994.3393, MNHN 1995.3406, MNHN	5	43
<i>Grayia tholloni</i>	Aquatic	1996.6450, MNHN 1996.6451, MNHN 1988.2341, MNHN 1988.2345, MNHN 1994.8085, MNHN	5	7
<i>Helicops angulatus</i>	Aquatic	0000.3609, MNHN 0000.1542, MNHN 1997.2097, MNHN 1997.2032, MNHN 1997.2034, MNHN	5	35
<i>Helicops carinicaudus</i>	Aquatic	0000.5237, MNHN 1887.0447, MNHN 87097, CAS	3	44
<i>Homalopsis buccata</i>	Aquatic	1970.0516, MNHN 1970.0518, MNHN 1974.1333, MNHN 1970.0517, MNHN 1884.0123, MNHN	5	17,20,45–47
<i>Hydrelaps darwiniensis</i>	Aquatic	R86165, AMNH R86166, AMNH R86167, AMNH R86169, AMNH R86172, AMNH	5	48,49
<i>Hydrodynastes bicinctus</i>	Aquatic	1974.0854, MNHN 1889.0398, MNHN 1902.0271, MNHN 0000.8665, MNHN R88401, AMNH	5	35
<i>Hydrodynastes gigas</i>	Aquatic	1989.3093, MNHN 0000.A301, MNHN 0000.A302, MNHN 1997.2121, MNHN 1999.8322, MNHN 1997.2347, MNHN	6	35
<i>Hydrophis ornata</i>	Aquatic	0000.0851, MNHN 1977.0807, MNHN R66586, AMNH R66588, AMNH R161770, AMNH	5	1

<i>Hydrophis platura</i>	Aquatic	0000.5137, MNHN 1922.0005, MNHN 1922.0002, MNHN 1994.0659, MNHN 1893.0064, MNHN	5	1,50,51
<i>Hydrophis schistosa</i>	Aquatic	198586, FMNH 202102, FMNH 202103, FMNH 199488, FMNH 218842, FMNH	5	1,13
<i>Hydrophis spiralis</i>	Aquatic	0000.4260A, MNHN 0000.4260, MNHN 0000.3988, MNHN 0000.7723, MNHN R161772, AMNH	5	52
<i>Hydrophis stokesii</i>	Aquatic	212320, FMNH 213063, FMNH 16774, CAS	3	13
<i>Hydrops triangularis</i>	Aquatic	1973.0296, MNHN 0000.3438, MNHN 1978.2500, MNHN 1986.0565, MNHN 1989.3052, MNHN	5	35
<i>Laticauda colubrina</i>	Aquatic	0000.5180, MNHN 0000.7702, MNHN 0000.5881, MNHN 0000.5766, MNHN 0000.9053, MNHN	5	1,53–55
<i>Lycodonomorphus laevisissimus</i>	Aquatic	R18223, AMNH 156721, CAS	2	56
<i>Lycodonomorphus rufulus</i>	Aquatic	205893, FMNH 205889, FMNH 0000.3377, MNHN 0000.1210, MNHN 0000.0563, MNHN	5	57
<i>Micrurus lemniscatus</i>	Aquatic	1897.0006, MNHN 1989.3151, MNHN 0000.7658, MNHN 1996.7849, MNHN 0000.0201, MNHN	5	35
<i>Micrurus surinamensis</i>	Aquatic	1996.7874, MNHN 1978.2312, MNHN 0000.3926, MNHN 1873, Antoine Fouquet 1999.8313, MNHN	5	35
<i>Myron richardsonii</i>	Aquatic	R86236, AMNH R111790, AMNH R111792, AMNH R111793, AMNH 114105, CAS 135489, CAS 135491, CAS	7	13
<i>Naja annulata</i>	Aquatic	1967.0455, MNHN 1899.0294, MNHN 1892.0098, MNHN 1967.0452, MNHN 0000.8222, MNHN	5	7

Appendices

<i>Natriciteres olivacea</i>	Aquatic	1896.0518, MNHN 0000.6507A, MNHN 1896.0520, MNHN 0000.6508, MNHN 1994.8215, MNHN	5	8,58,59
<i>Natrix tessellata</i>	Aquatic	2000.5145, MNHN 1989.0698, MNHN 0000.0641, MNHN 1884.0155, MNHN 0000.0642, MNHN	5	60,61
<i>Nerodia cyclopion</i>	Aquatic	0000.0121, MNHN 0000.3482, MNHN 1955.0058, MNHN R159217, AMNH R159218, AMNH	5	62,63
<i>Nerodia harteri</i>	Aquatic	R64408, AMNH R72686, AMNH R72690, AMNH R85314, AMNH R162252, AMNH	5	62,64–67
<i>Opisthotropis lateralis</i>	Aquatic	R172664, MCZ R172665, MCZ R175987, MCZ R172654, MCZ R172653, MCZ	5	68
<i>Psammodynastes pictus</i>	Aquatic	1891.0077, MNHN 1891.0045, MNHN 1891.0046, MNHN 128402, FMNH 148906, FMNH 148926, FMNH	6	47
<i>Pseudoeryx plicatilis</i>	Aquatic	0000.3402, MNHN 0000.3401, MNHN 0000.3401A, MNHN 1962.0423, MNHN 1978.2550, MNHN	5	35,69
<i>Pseudoferania polylepis</i>	Aquatic	R35067, MCZ R140183, MCZ R129135, MCZ R141689, MCZ 1937.0082, MNHN	5	17,70
<i>Regina grahami</i>	Aquatic	29565, FMNH 30428, FMNH 7791, FMNH 17033, FMNH 17609, FMNH	5	62,71
<i>Regina septemvittata</i>	Aquatic	3074, FMNH 35881, FMNH 3076, FMNH 3077, FMNH 35880, FMNH 0000.3492, MNHN	6	72–74
<i>Regina alleni</i>	Aquatic	11047, FMNH 22591, FMNH 48360, FMNH R159307, AMNH R170180, AMNH	5	75–77

<i>Regina rigida</i>	Aquatic	0000.1101, MNHN R159322, AMNH R159323, AMNH R160211, AMNH R162319, AMNH	5	62,63,78
<i>Seminatrix pygaea</i>	Aquatic	53688, FMNH 53693, FMNH 53687, FMNH 53691, FMNH 95347, FMNH	5	79
<i>Sinonatrix annularis</i>	Aquatic	1902.0080, MNHN 1989.0215, MNHN 1989.0206, MNHN 1999.9017, MNHN 1999.9016, MNHN	5	80
<i>Sinonatrix percarinata</i>	Aquatic	1935.0449, MNHN 1935.0449A, MNHN 1812.0321, MNHN 2007.2443, MNHN 1812.0319, MNHN	5	80
<i>Thamnophis atratus</i>	Aquatic	R57421, AMNH R162404, AMNH R162405, AMNH 212664, CAS 212709, CAS 212720, CAS 220684, CAS	7	81–85
<i>Thamnophis couchii</i>	Aquatic	R57423, AMNH R66544, AMNH R108191, AMNH R108192, AMNH R108194, AMNH	5	81,86
<i>Thamnophis rufipunctatus</i>	Aquatic	R64376, AMNH R64402, AMNH R68286, AMNH R85996, AMNH R162440, AMNH	5	81,87–89
<i>Xenochrophis piscator</i>	Aquatic	1991.1628, MNHN 0000.7323, MNHN 1991.1627, MNHN 1998.8543, MNHN 1998.8553, MNHN R34085, AMNH	6	28,90,91
<i>Achalinus rufescens</i>	Non-aquatic	1935.0439, MNHN 1935.0441, MNHN 1935.0051A, MNHN 1935.0051B, MNHN 1935.0440, MNHN	5	92
<i>Agkistrodon contortrix</i>	Non-aquatic	1996.2762, MNHN 0000.0884, MNHN 1973.0072, MNHN 1973.0077, MNHN 0000.1762, MNHN	5	93

Appendices

<i>Boaedon lineatus</i>	Non-aquatic	1988.2109, MNHN 1994.8159, MNHN 1994.8131, MNHN 1994.8134, MNHN 1990.4591, MNHN	5	94
<i>Bungarus caeruleus</i>	Non-aquatic	0000.4259, MNHN 2007.2454, MNHN 1962.0237, MNHN 1962.0238, MNHN 0000.3952, MNHN	5	95
<i>Diadophis punctatus</i>	Non-aquatic	0000.8593, MNHN 1894.0061, MNHN 1894.0062, MNHN 0000.3379, MNHN 0000.3379A, MNHN	5	96
<i>Echiopsis curta</i>	Non-aquatic	0000.0951, MNHN 0000.7675, MNHN	2	97
<i>Epicrates cenchria</i>	Non-aquatic	1955.0037, MNHN 1991.1492, MNHN 0000.3335, MNHN 1973.1196, MNHN 0000.3291, MNHN	5	98
<i>Erythrolamprus aesculapii</i>	Non-aquatic	1978.2515, MNHN 1978.2516, MNHN 1887.0391, MNHN 0000.3686, MNHN 1980.1115, MNHN	5	99
<i>Micrurus corallinus</i>	Non-aquatic	1883.0260, MNHN 1962.0468, MNHN 1962.0469, MNHN 0000.7653, MNHN 0000.3909, MNHN	5	100
<i>Naja haje</i>	Non-aquatic	1999.8836, MNHN 1990.4629, MNHN 1990.4660, MNHN 1988.2485, MNHN 1988.2486, MNHN 1988.3931, MNHN	6	101,102
<i>Philodryas nattereri</i>	Non-aquatic	1908.0245, MNHN 1967.0136, MNHN 1967.0133, MNHN 1967.0134, MNHN 0000.3744, MNHN	5	103
<i>Prosymna meleagris</i>	Non-aquatic	0000.8807, MNHN 1916.0176, MNHN 1962.0007, MNHN 1977.0380, MNHN 1908.0062, MNHN	5	104
<i>Psammophis sibilans</i>	Non-aquatic	1921.0471, MNHN 1921.0470, MNHN 1905.0215, MNHN 1891.0184, MNHN 1902.0014, MNHN	5	105

<i>Pseudaspis cana</i>	Non-aquatic	1912.0494, MNHN 0000.3529, MNHN 0000.8592, MNHN 1896.0391, MNHN 2007.2457, MNHN	5	106,107
<i>Pseudechis porphyriacus</i>	Non-aquatic	0000.7672, MNHN 0000.7673, MNHN 0000.7674, MNHN 0000.3945, MNHN 2007.2453, MNHN	5	108
<i>Pseudonaja textilis</i>	Non-aquatic	1900.0521, MNHN 1900.0522, MNHN 0000.1027, MNHN 2007.2479, MNHN 0000.1303, MNHN	5	109
<i>Sibynophis collaris</i>	Non-aquatic	1919.0144, MNHN 1919.0145, MNHN 1946.0285, MNHN 1928.0055, MNHN 1928.0053, MNHN	5	110,111
<i>Storeria dekayi</i>	Non-aquatic	0000.3439, MNHN 1994.0077, MNHN 1994.0765, MNHN 0000.1326, MNHN 0000.1023, MNHN	5	112
<i>Tachymenis peruviana</i>	Non-aquatic	0000.3907, MNHN 1961.0575, MNHN 1961.0576, MNHN 1905.0350, MNHN 1996.2732, MNHN	5	113
<i>Thamnophis scaliger</i>	Non-aquatic	1975.0190, MNHN 1901.0305, MNHN 1894.0081, MNHN 1901.0306, MNHN R88724, AMNH	5	114
<i>Uroptelis ceylanicus</i>	Non-aquatic	1895.0099, MNHN 1895.0100, MNHN 1848.0265, MNHN 1848.0266, MNHN 1897.0258, MNHN	5	115

References:

1. Glodek GS, Voris HK. Marine Snake Diets: Prey Composition, Diversity and Overlap. *Copeia*. 1982;1982(3):661–6.
2. Voris HK, Glodek GS. Habitat, Diet, and Reproduction of the File Snake, *Acrochordus granulatus*, in the Straits of Malacca. *J Herpetol*. 1980;14(1):105–8.
3. Lillywhite HB. Husbandry of the little file snake, *Acrochordus granulatus*. *Zoo Biol*. 1996;15(3):315–27.
4. Lillywhite HB. File snakes (Acrochordidae). In: Hutchins M, Murphy JB, Schlager N, editors. *Grzimek's Animal Life Encyclopedia*, 2nd Edition, Volume 7, Reptiles. Farmington Hills, MI: Gale Group; 2003. p. 439–44.
5. Dowling HG. The curious feeding habits of the Java Wart Snake. *Anim Kingdom*. 1960;63:13–5.

6. Boo-Liat L. Notes on the elephant's trunk snake and the puff-faced water snake in Kuala Lumpur. *Malayan Nat J.* 1964;18:179–83.
7. Pacini N, Harper DM. Tropical Stream Ecology [Internet]. *Tropical Stream Ecology*. Elsevier; 2008 [cited 2014 Oct 20]. 147-197 p. Available from: <http://www.sciencedirect.com/science/article/pii/B978012088449050008X>
8. Chippaux J-P. Les serpents d'Afrique occidentale et centrale. *Faune et Flore Tropicales*. 2006. 1-300 p.
9. Vincent SE, Herrel A, Irschick DJ. Sexual dimorphism in head shape and diet in the cottonmouth snake (*Agkistrodon piscivorus*). *J Zool.* 2004 Sep;264(1):53–9.
10. Lillywhite HB, McCleary RJR. Trophic Ecology of Insular Cottonmouth Snakes: Review and Perspective. *South Am J Herpetol.* 2008;3(2):175–85.
11. Mitchell J. *The Reptiles of Virginia*. Washington and London: Smithsonian Institution Press; 1994.
12. Mitchell J. Snakes. *Biol Dig.* 1991;52(6):17–22.
13. Heatwole H. *Sea Snakes*. Sydney, Australia: University of New South Wales Press Ltd; 1999. 148 p.
14. De Silva A. *Atretium schistosum*. The IUCN Red List of Threatened Species. Version 2014.2. 2010.
15. Daniels RRJ. *Amphibians of Peninsular India*. Press U, editor. Orient Blackswa; 2004. 284 p.
16. Somaweera R. Sri Lankan Colubrid Snakes. *Sri Lanka Nat.* 2004;5:32–46.
17. Murphy JC. *Homalopsid snakes. Evolution in the mud*. Malabar, Florida: Krieger Publishing Company; 2007.
18. Boulenger GA. *Reptilia and Batrachia. The Fauna of British India, including Ceylon and Burma*. Kessinger Publishing, LLC; 1890. 564 p.
19. Jayne BC, Ward TJ, Voris HK. Morphology, reproduction, and diet of the marine homalopsine snake *Bitia hydroides* in Peninsular Malaysia. *Copeia.* 1995;1995(4):800–8.
20. Cantor T. *Catalogue of reptiles inhabiting the Malayan peninsula and islands*. Calcutta: Printed by J. Thomas; 1847. 182 p.
21. Voris HK, Murphy JC. The prey and predators of Homalopsine snakes. *J Nat Hist.* 2002;36(13):1621–32.
22. Auffenberg W. The Herpetofauna of Komodo, with notes on adjacent areas. *Bull Florida State Museum, Biol Sci.* 1980;25(2):40–156.
23. Jayne BC, Voris HK, Heang KB. Diet, feeding behavior, growth and numbers of a population of *Cerberus rynchops* (Serpentes: Homalopsinae) in Malaysia. *Fieldiana Zoology*. Chicago: Field Museum of Natural History; 1988. 36 p.
24. O'Shea M, Halliday T. *Reptiles and amphibians*. Dorling Kindersley Ltd; 2001. 256 p.
25. Kupfer A, Gower DJ, Himstedt W. Field observations on the predation of the caecilian amphibian, genus *Ichthyophis* (Fitzinger, 1826), by the red-tailed pipe snake *Cylindrophis ruffus* (Laurenti, 1768). *Amphibia-Reptilia.* 2003;24(June 2001):212–5.
26. Saint Girons H. *Les serpents du Cambodge*. Muséum Nat. 1972. 170 p.
27. Mori A. Prey-Handling Behavior of Three Species of Homalopsine Snakes: Features Associated with Piscivory and Duvernoy's Glands. *J Herpetol.* 1998;32(1):40–50.
28. Pope CH. Notes on Reptiles from Fukien and other Chinese Provinces. *American Museum of Natural History*; 1929. 153 p.
29. Pope CH. *The Reptiles of China*. (Scientific Books: Natural History of Central Asia, Vol. X, the

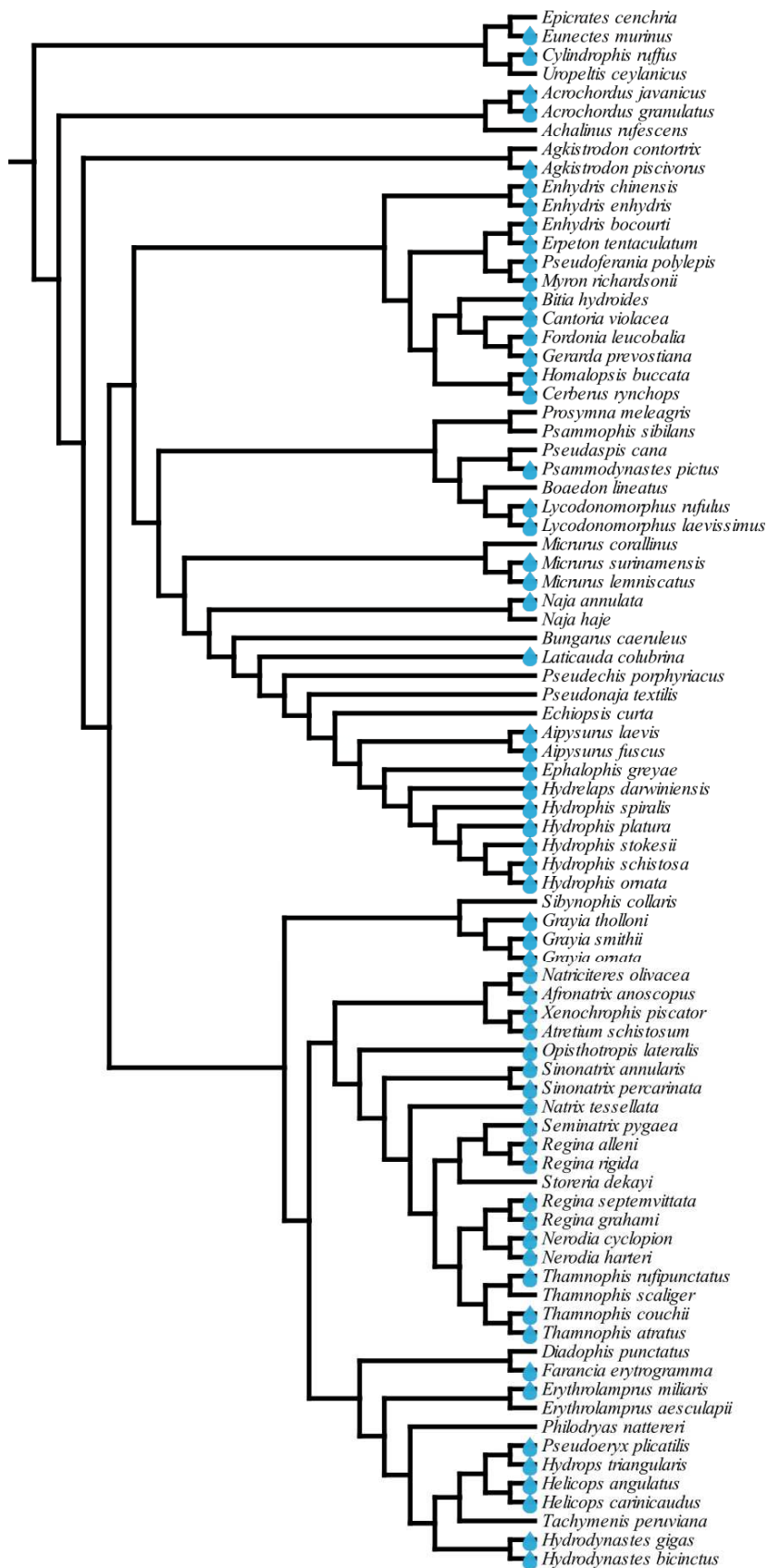
- Reptiles of China). *Science* (80-). 1935;82:303–4.
30. Karns DR, Murphy JC, Voris HK, Suddeth JS. Comparison of Semi-aquatic Snake Communities Associated with the Khorat Basin , Thailand. *Nat Hist J Chulalongkorn Univ.* 2005;5(October):73–90.
 31. Murphy JC, Voris HK, Karns DR, Chan-ard T, Suvunrat K. The Ecology of the Water Snakes of Ban Tha Hin, Songkhla Province, Thailand. *Nat Hist Bull Siam Soc.* 1999;47(2):129–47.
 32. Voris HK, Voris HH. Feeding Strategies in Marine Snakes: An Analysis of Evolutionary, Morphological, Behavioral and Ecological Relationships. *Am Zool.* 1983;23(2):411–25.
 33. Tomascik T, Mah AJ, Nontji A, Mossa MK. The ecology of the Indonesian seas. Oxford University Press; 1997. 656 p.
 34. Shaw CE. Tentacled fishing snake. *ZooNooz.* 1965;38:3–5.
 35. Starace F. Guide des serpents et amphibènes de Guyane. *Ibis Rouge.* 1998. 452 p.
 36. Haltom WL. Alabama reptiles, (Alabama museum of natural history. Museum paper). University. 1931. 145 p.
 37. Cochran TT. A Review and Synthesis of Existing Literature on Rainbow Snakes, *Farancia erytrogramma*. *Bull Chicago Herpetol Soc.* 2011;46(12):157–61.
 38. Richmond ND. The habits of the rainbow snake in Virginia. *Copeia.* 1945;1945(1):28–30.
 39. Günther ACLG. The Reptiles of British India. Ray Societ. Hardwicke R, editor. London; 1864. 540 p.
 40. Gow G. Graeme Gow’s Complete Guide to Australian Snakes. Harpercollins; 1991. 181 p.
 41. Karns DR, Voris HK, Goodwin TG. Ecology of oriental-australian rear-fanged water snakes (Colubridae: Homalopsinae) in the Paris Ris Park Mangrove Forest, Singapore. *Raffles Bull Zool.* 2002;50(2):487–98.
 42. Jayne BC, Voris HK, Ng PKL. Snake circumvents constraints on prey size. *Nature.* 2002;418(6894):143.
 43. Pauwels OSG, Lenglet G, Trape J-F, Dubois A. *Grayia smithii* (Leach, 1818). Smith’s African Water Snake. *Diet. African Herp News.* 2000;31 October:7–9.
 44. Marques OA V., Sazima I. Historia natural dos repteis da Estacao Ecologica Jureia-Itatins. In: Estacao Ecologica Jureia-Itatins: ambiente fisico, flora e fauna. Holos, Edi. 2004. p. 257–77.
 45. Berry PY, Lim GS. The breeding pattern of the puff-faced water snake, *Homalopsis buccata* (Boulenger). *Copeia.* 1967;1967:307–13.
 46. van Hoesel JKP. *Ophidia Javanica*. Bogor, Indonesia: Museum Zoologicum Bogoriense; 1959.
 47. Tweedie MWF. The snakes of Malaya. Singapore: Government Printing Office; 1953. 139 p.
 48. Ehmann H. Reptiles. In: *Encyclopedia of Australian animals*. Angus & Ro. Pymble, N. S. W.; 1992.
 49. Guinea ML, McGrath P, Love B. Observations of the Port Darwin Sea Snake *Hydrelaps darwiniensis*. *Northen Territ Nat.* 1993;14:28–30.
 50. Murphy JB, Schlager N. *Grzimek’s Animal Life Encyclopedia.* 2003.
 51. Kropach CN. The yellow-bellied sea snake, *Pelamis*, in the eastern Pacific. In: Dunson WA, editor. *The biology of sea snakes*. Baltimore: University Park Press; 1975. p. 185–213.
 52. Karthikeyan R, Balasubramanian T. Species diversity of sea snakes (Hydrophiidae) distributed in the Coramantal Coast (East coast of India). *Int J Zool Res.* 2007;3(3):107–31.

53. Gorman GP, Licht P, McCollum F. Annual Reproductive Patterns in Three Species of Marine Snakes from the Central Philippines. *J Herpetol.* 1981;15(3):335–54.
54. Shine R, Reed RN, Shetty S, Cogger HG. Relationships between sexual dimorphism and niche partitioning within a clade of sea-snakes (Laticaudinae). *Oecologia.* 2002;133(2002):45–53.
55. Ineich I, Bonnet X, Brischoux F, Kulbicki M, Seret B, Shine R. Anguilliform fishes and sea kraits: neglected predators in coral-reef ecosystems. *Mar Biol.* 2007;51(2):793–802.
56. Haagner G V., Branch WR. A taxonomic revision of the dusky-bellied water snake, *Lycodonomorphus laevisissimus* Serpentes: Colubridae. *J African Zool.* 1994;237–50.
57. Taylor P. An observation on the feeding habits of *Lycodonomorphus rufulus*. *J Herpetol Assoc Africa.* 1970;6(1).
58. Razzetti E, Msuya CA. Field Guide to the amphibians and reptiles of Arusha National Park (Tanzania). Varese, Italy: Edizioni Negri and Istituto OIKOS; 2002. 84 p.
59. Rödel M-O, Spawls S. *Natriciteres olivacea*. IUCN Red List Threat Species Version 20142. 2010;
60. Filippi E, Capula M, Luiselli L, Agrimi U. The prey spectrum of *Natrix natrix* (LINNAEUS , 1758) and *Natrix tessellata* (LAURENTI , 1768) in sympatric populations. *Herpetozoa.* 1996;8(3/4):155–64.
61. Luiselli L, Capizzi D, Filippi E, Anibaldi C, Rugiero L, Capula M. Comparative Diets of Three Populations of an Aquatic Snake (*Natrix tessellata*, Colubridae) from Mediterranean Streams with Different Hydric Regimes. *Copeia.* 2007;2007(2):426–35.
62. Gibbons JW, Dorcas ME. North American Watersnakes, A Natural History. Animal Nat. University of Oklahoma Press; 2004. 496 p.
63. Kofron CP. Foods and Habitats of Aquatic Snakes (Reptilia, Serpentes) in a Louisiana Swamp. *J Herpetol.* 1978;12(4):543–54.
64. Rose F. Aspects of the biology of the Concho watersnake (*Nerodia harteri paucimaculata*). *Texas J Sci.* 1989;41:115–30.
65. Dorcas ME, Mendelson JR. Distributional notes on *Nerodia harteri harteri* in Parker and Palo Pinto counties, Texas. *Herpetol Rev.* 1991;22:117–8.
66. Green BD, Dixon JR, Mueller JM, Whiting MJ, Thornton OWJ. Feeding ecology of the Concho water snake, *Nerodia harteri paucimaculata*. *J Herpetol.* 1994;28:165–72.
67. Ernst CH, Ernst, Evelyn M. Snakes of the United States and Canada. Smithsonian Books; 2003. 680 p.
68. Wang Y, Lau M. *Opisthotropis lateralis*. IUCN Red List Threat Species 2012 eT192152A2047730. 2012;
69. Carvalho MA, Nogueira F. Serpentes da área urbana de Cuiabá, Mato Grosso: aspectos ecológicos e acidentes ofídicos associados. *Cad Saude Publica.* 1998;14(4):753–63.
70. Shine R. Strangers in a strange land: ecology of the Australian colubrid snakes. *Copeia.* 1991;1991:120–31.
71. Hall RJ. Ecological observations on Graham's water snake, *Regina grahami* (Baird and Girard). *Am Midl Nat.* 1969;81(1):156–63.
72. Godley JS, McDiarmid RW, Rojas NN. Estimating prey size and number in crayfish-eating snakes, Genus *Regina*. *Herpetologica.* 1984;40(1):82–8.
73. Branson BA, Baker EC. An ecological study of the Queen Snake, *Regina septemvittata* (Say), in Kentucky. *Tulane Stud Zool Bot.* 1974;18:153–71.

74. Wood JT. Observations on *Natrix Septemvittata* (say) in Southwestern Ohio. *Am Midl Nat.* 1949;42(3):744–50.
75. Dwyer C, Kaiser H. Relationship between skull form and prey selection in the thamnophiine snake genera *Nerodia* and *Regina*. *J Herpetol.* 1997;31:463–75.
76. Franz R. Observations on the food, feeding behavior, and parasites of the striped swamp snake, *Regina alleni*. *Herpetologica.* 1977;33:91–4.
77. Godley JS. Foraging ecology of the striped swamp snake, *Regina alleni*, in southern Florida. *Ecol Monogr.* 1980;50(4):411–36.
78. Durso AM, Willson JD, Winne CT. Habitat influences diet overlap in aquatic snake assemblages. *J Zool.* 2013;291(3):185–93.
79. Palmer WM, Paul JR. The Black Swamp Snake, *Seminatrix pygaea paludis* Dowling, in North Carolina. *Herpetologica.* 1963;19(3):219–21.
80. Mao J-J. Population ecology of the genus *Sinonatrix* in Taiwan. Trier; 2003.
81. Rossman DA, Ford NB, Seigel RA. *The Garter Snakes: Evolution and Ecology.* Animal Nat. University of Oklahoma Press; 1996. 336 p.
82. Fitch HS. A biogeographical study of the ordinoideis artenkreis of garter snakes (genus *Thamnophis*). Berkley an. University of California publications in zoology; 1940. 149 p.
83. Fitch HS. The feeding habits of California garter snakes. *Calif Fish Game.* 1941;27:2–32.
84. Fox WR. *Relationships Among the Garter Snakes of the Thamnophis Elegans Rassenkreis.* University of California Press; 1951. 485-529 p.
85. Lind AJ, Welsh HHJ. Ontogenetic changes in foraging behaviour and habitat use by the Oregon garter snake, *Thamnophis atratus hydrophilus*. *Anim Behav.* 1994;48:1261–73.
86. Fitch HS. Study of Snake Populations in Central California. *Am Midl Nat.* 1949;41(4):513–79.
87. Fleharty L. Comparative ecology of *Thamnophis elegans*, *T. cyrtopsis* and *T. rufipunctatus* in New Mexico. *Southwest Nat.* 1967;12:207–30.
88. Rosen PC, Schwalbe CR. Status of the Mexican and narrow-headed gartersnakes (*Thamnophis eques megalops* and *Thamnophis rufipunctatus rufipunctatus*) in Arizona. Albuquerque, New Mexico; 1988.
89. Stebbins RC. *A Field Guide to Western Reptiles and Amphibians.* Peterson F. Boston, Massachusetts: Houghton Mifflin Harcourt; 2003. 560 p.
90. Das I. *A Photographic Guide to Snakes and Other Reptiles of India.* London, United Kingdom: New Holland Publishers Ltd; 2002. 144 p.
91. De Silva A, Das I. *A Photographic Guide To Snakes & Other Reptiles Of Sri Lanka.* Photograph. New Holland Publishers Ltd; 2004. 144 p.
92. Zhao E. *Snakes of China.* Anhui Science and Technology Press; 2006.
93. McKnight DT, Harmon JR, McKnight JL, Ligon DB. Notes on the diets of seven sympatric snakes in the genera *Agkistrodon*, *Nerodia*, *Sistrurus*, and *Thamnophis*. *Herpetol Notes.* 2014;7(September 2015):171–7.
94. Luiselli L, Akani GC. An investigation into the composition, complexity and functioning of snake communities in the mangroves of. 2002;40:220–7.
95. Wall F. *Ophidia taprobanica; or, The snakes of Ceylon.* Colombo, Sri Lanka: H.R. Cottle; 1921. 638 p.
96. Mendelson JR, Adams A. *Diadophis punctatus* (Ring-necked Snake). Diet. *Herpetol Rev.*

- 2014;45(4):709–10.
97. Shine R. Ecology of the Australian Elapid Snake *Echiopsis curta*. *J Herpetol.* 1982;16(4):388–93.
 98. Donato CR, Dantas MAT, Da Rocha PA. *Epicrates cenchria* (Rainbow Boa). Diet and foraging behavior. *Herpetol Rev.* 2012;43(2):1–2.
 99. Silva D, Vallim de Gouveia R, Trindade I, Novelli I. *Erythrolamprus aesculapii* (false coral). Diet. *Herpetol Rev.* 2013;44(1):154.
 100. Marques OA V., Sazima I. Diet and feeding behavior of the Coral snake, *Micrurus corallinus*, from the Atlantic forest of Brazil. *Herpetol Nat Hist.* 1997;5(1):88–93.
 101. Masood MF. Ecological distribution of snakes' fauna of Jazan region of Saudi Arabia. *Egypt Acad J Biol Sci.* 2012;4(1):183–97.
 102. El-Deib S. Lipid changes in blood serum and tissues of the Egyptian Cobra “*Naja haje haje*” during the hibernation cycle. *J Therm Biol.* 2005;30:51–9.
 103. Cesar P, Dourado M, Borges-nojosa DM, Passos DC, Bezerra CH. Ecology of *Philodryas nattereri* in the Brazilian semi-arid region. *Herpetol J.* 2011;21:193–8.
 104. Broadley DG. Predation on reptile eggs by African snakes of the genus *Prosymna*. *Herpetologica.* 1979;35(4):338–41.
 105. Akani GC, Eniang EA, Ekpo IJ, Angelici FM, Luiselli L. Food Habits of the Snake *Psammophis phillipsi* from the Continuous Rain-Forest Region of Southern Nigeria (West Africa). *J Herpetol.* 2003;37(1):208–11.
 106. Junker K, Lane EP, Dlamini B, Kotze A, Boomker J. Post mortem identification of *Kalicephalus colubri colubri* (Nematoda: Diaphanocephalidae) in a captive mole snake (*Pseudaspis cana*) in South Africa. *J S Afr Vet Assoc.* 2009;80(1):54–6.
 107. Fitzsimons V, Brain CK. A short account of the reptiles of the Kalahari Gemsbok National Park. *Koedoe.* 1958;1(1):99–104.
 108. Shine R. The Evolution of Viviparity: Ecological Correlates of Reproductive Mode within a Genus of Australian Snakes (*Pseudechis*: Elapidae). *Copeia.* 1987;1987(3):551–63.
 109. Shine R. Constraints , Allometry , and Adaptation : Food Habits and Reproductive Biology of Australian Brownsnakes (*Pseudonaja* : Elapidae). *Herpetologica.* 1989;45(2):195–207.
 110. Leviton AE. Contributions to a review of Philippine snakes, II: The snakes of the Genera *Liopeltis* and *Sibynophis*. *Philipp J Sci.* 1963;92(3):367–81.
 111. Savitzky AH. Coadapted Character Complexes among Snakes : Fossoriality , Piscivory , and Durophagy. *Am Zool.* 1983;23(2):397–409.
 112. Judd WW. Observations on the food of the little brownsnakes, *Storeria dekayi*, at London, Ontario. *Copeia.* 1954;1954(1):62–4.
 113. Greene HW, Jaksic FM. The feeding behavior and natural history of two Chilean snakes, *Philodryas chamissonis* and *Tachymenis chilensis* (Colubridae). *Rev Chil Hist Nat.* 1992;65:485–93.
 114. Reguera S, Santos X, Feriche M, Mocino-Deloya E, Setser K, Pleguezuelos JM. Diet and energetic constraints of an earthworm specialist, the Mesa Central Blotched Garter Snake (*Thamnophis scaliger*). *Can J Zool* [Internet]. 2011;89:1178–87. Available from: <http://www.nrcresearchpress.com/doi/abs/10.1139/z11-096>
 115. Ganesh SR, Chandramouli SR. Endangered and Enigmatic Reptiles of Western Ghats – An Overview. In: Singaravelan N, editor. *Rare Animals of India*. Bentham Science Publishers; 2013. p. 35–61.

Appendix 2: Phylogeny of the selected species based on Pyron et al. 2013 (blue tear drop = ‘aquatic’ species).



Appendix 3: List of anatomical landmarks and curves used for the template.

Anatomical landmarks:

1. Middle of the left nostril
2. Middle of the right nostril
3. Extreme point of the rostrum
4. Extreme point of the left part of the jaw
5. Extreme point of the right part of the jaw
6. Left commissure
7. Right commissure
8. Extremity of the mental scale
9. Most dorsal point of the left eye
10. Most dorsal point of the right eye

Curves:

Curve 1: left eye

Curve 2: right eye

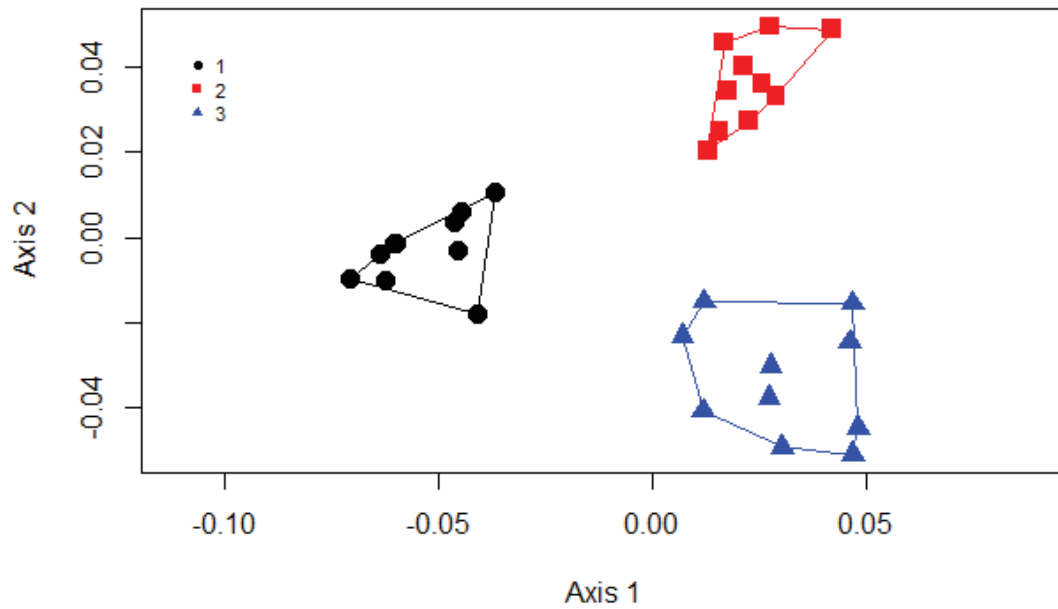
Curve 3: from landmark 6 to landmark 8 along mouth

Curve 4: from landmark 7 to landmark 8 along mouth

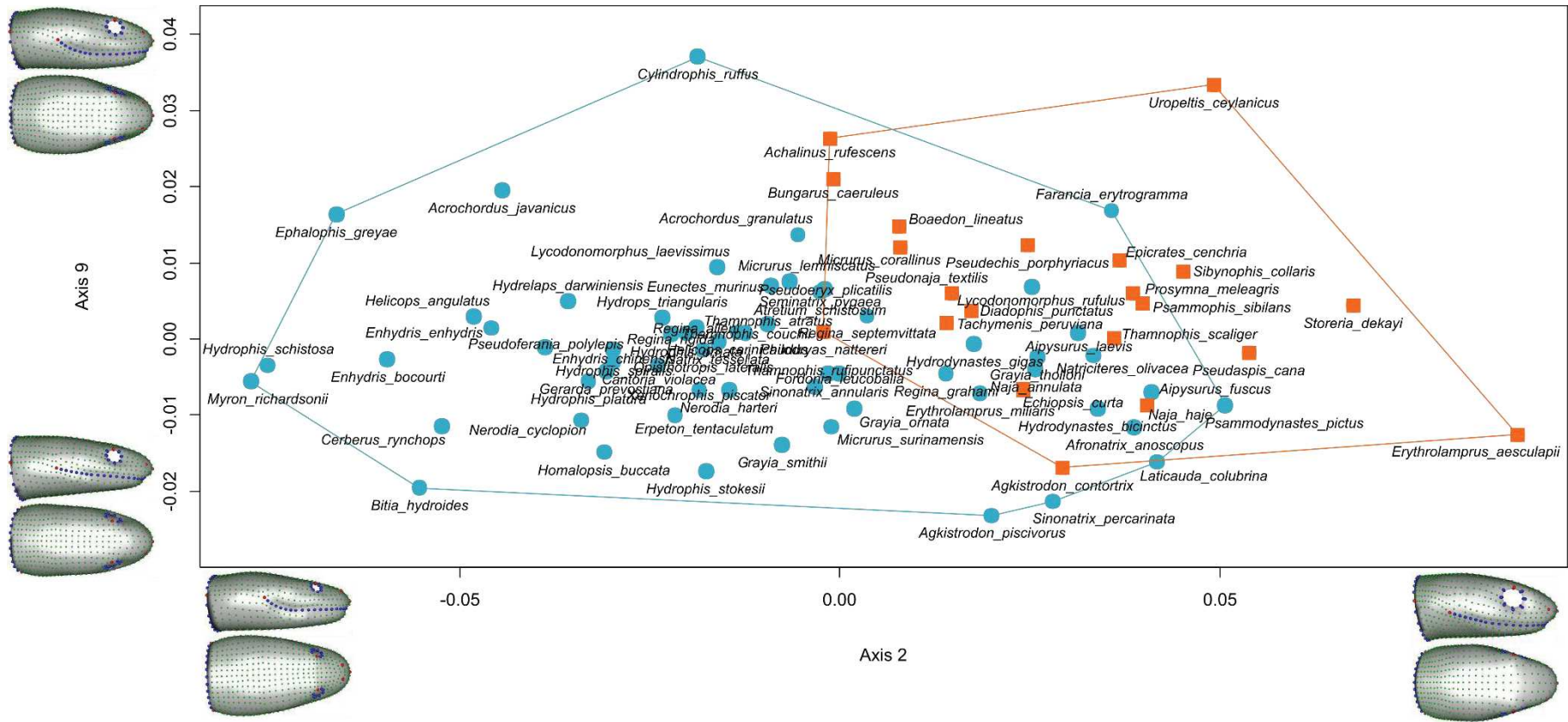
Curve 5: from landmark 4 to landmark 5 along dorsal part of the head

Curve 6: from landmark 4 to landmark 5 along ventral part of the head

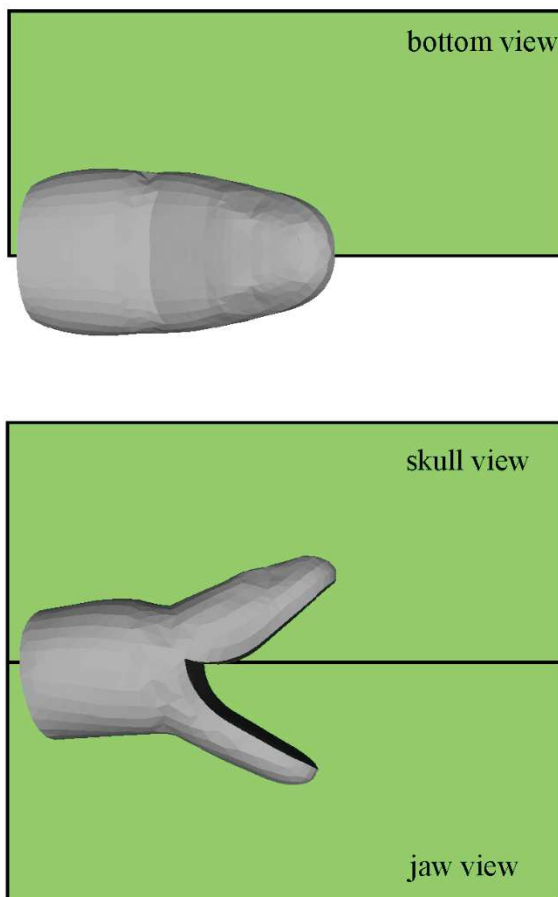
Appendix 4: Assessment of the error in landmark positioning using a principal component analysis. Landmarks were placed ten times on three different specimens of the same species. The principal component plot shows that variation due to the placement of the landmarks is lower than variation among individuals.



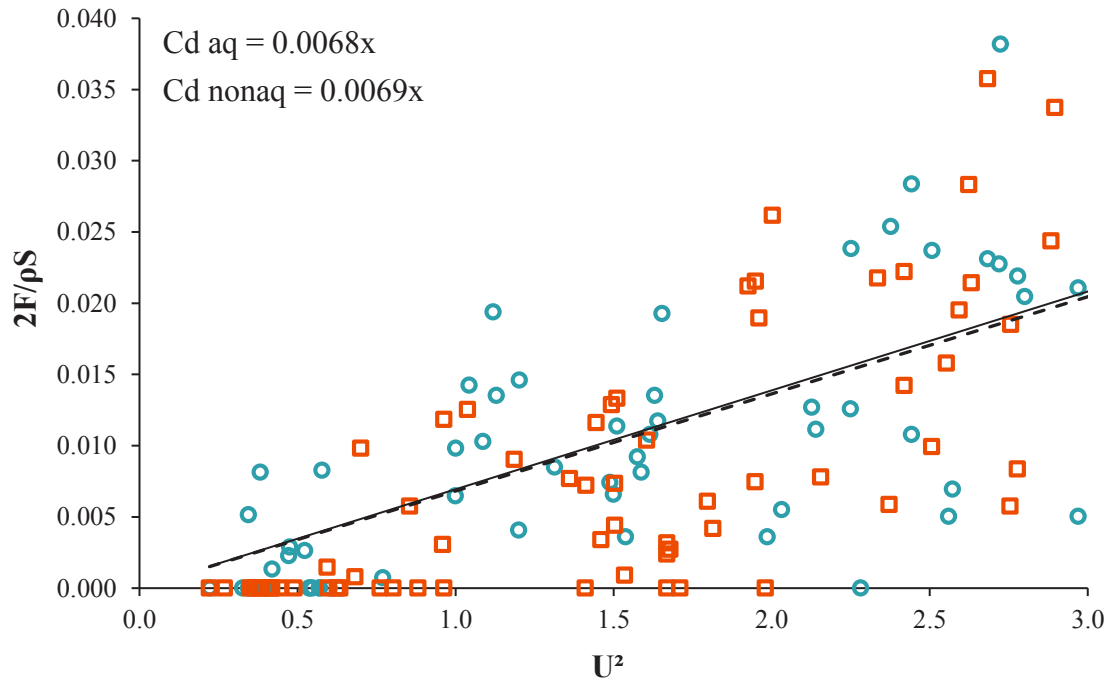
Appendix 5: Scatter plot of the principal components two and nine showing that species that capture elusive aquatic prey (blue circles) differ from those that do not (orange squares). Axes two and nine respectively account for 13.7 and 1.5% of the head shape variance.



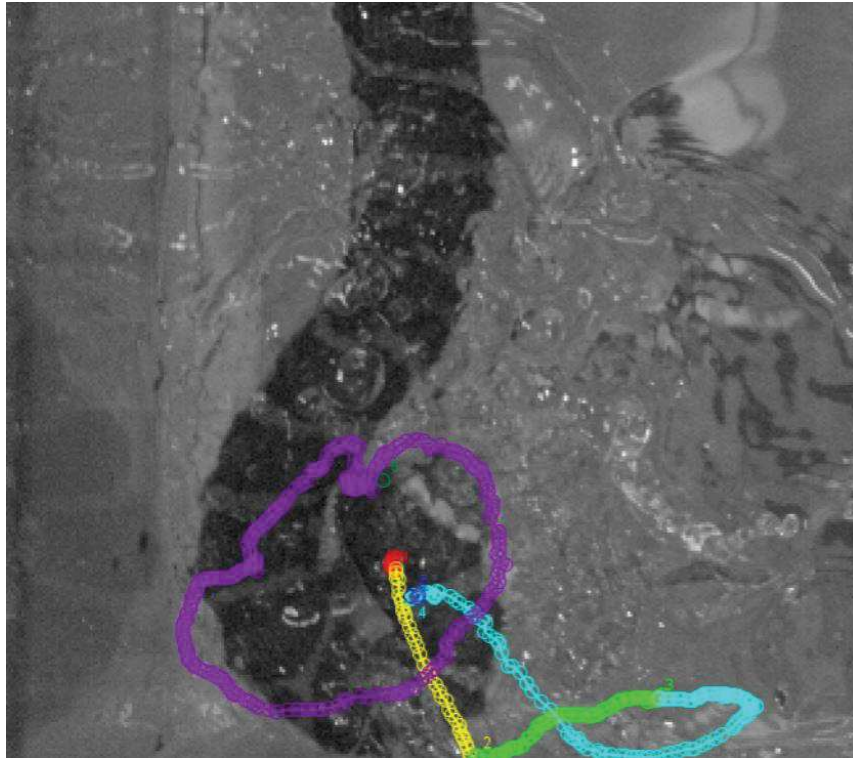
Appendix 6: Particle Image Velocimetry planes used to characterize the fluid flow around the head of the two models.



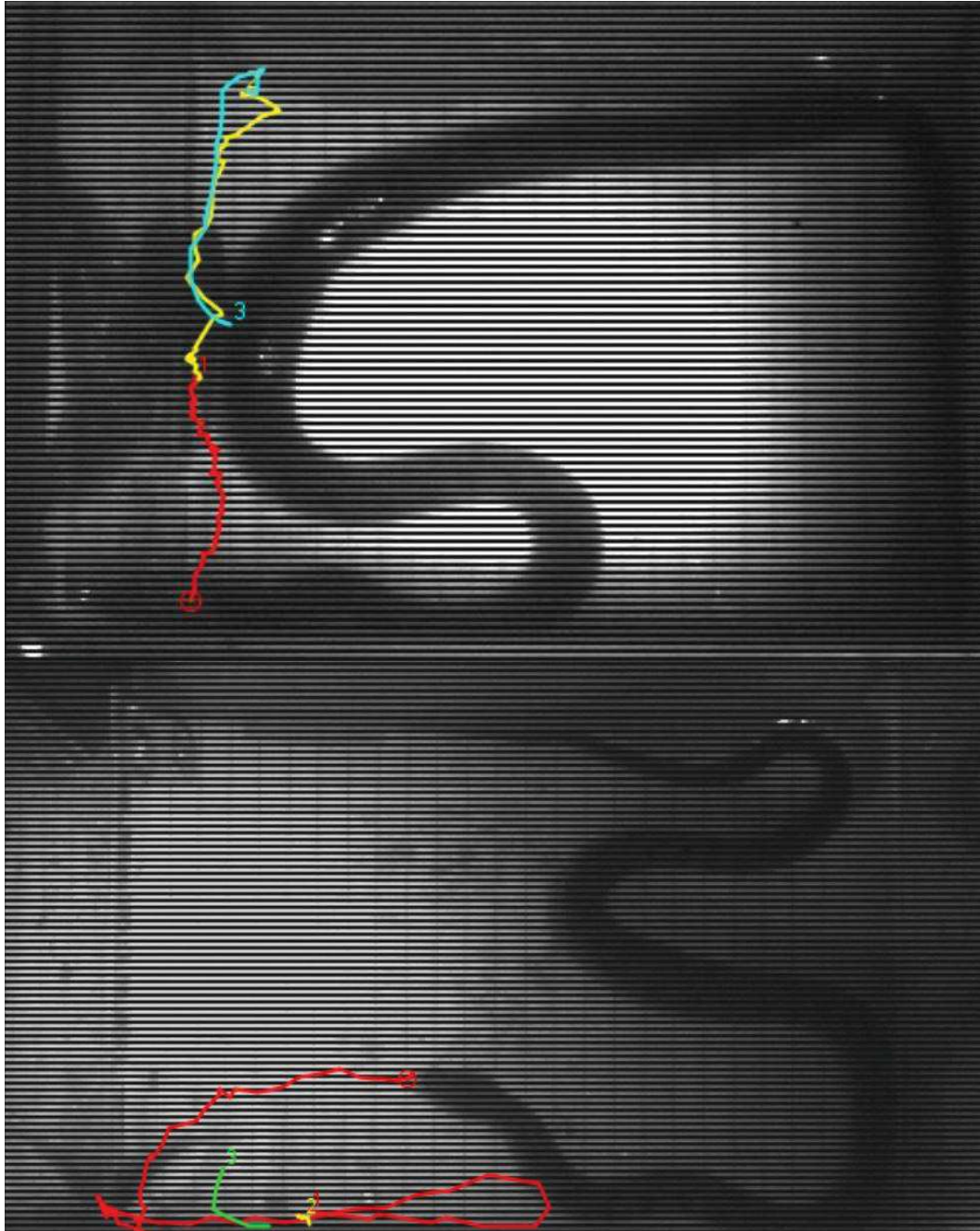
Appendix 7: Drag term $2F_d/\rho S$ depending on the velocity term of the strike (U^2) for the two snake head models with a closed mouth. Squares: non-aquatic model, circles: aquatic model. Linear regression lines are drawn. The y coefficient corresponds to the drag coefficient of each shape.



Appendix 8: Example of tracking on an individual *E. bocourti*. This strike was composed of two phases, it began at the red point. Next, the individual attempted a frontal strike (yellow path), struck the glass of the tank, re-orientated toward the prey (green, blue paths) and finally performed a successful lateral strike (purple path). The whole strike lasted less than 6 seconds. The picture is taken once the snake has caught the fish.



Appendix 9: Example of tracking for two individual *C. schneiderii*. The tracks were quite long. However, these captures lasted 0.6 sec and 0.24sec.



Appendix 10: Master thesis of Martyna Goral on the hydrodynamics of frontal versus lateral strike depending on the head shape of aquatically foraging snakes.



Master of Science in Fluid Mechanics, Pierre and Marie Curie University and
École Polytechnique

INTERNSHIP REPORT

Hydrodynamics of the lateral strike in aquatic snakes

Auteur :
Martyna GORAL

Supervisors :
Ramiro GODOY-DIANA, CNRS researcher at the PMMH, ESPCI in Paris
ramiro@pmmh.espci.fr

Marion SEGALL, PhD student at MNHN and PMMH, ESPCI in Paris
marion.segall@espci.fr

Internship done in the PMMH laboratory, Physique et Mécanique des Milieux Hétérogènes, UMR 7636
CNRS - ESPCI Paris Tech - 10 rue Vauquelin 75005 Paris

Abstract :

Aquatic snakes have to circumvent strong hydrodynamic constraints during prey capture underwater. However, unlike most of other aquatic predators, they did not develop a specific adaptation to predation in this media. But surprisingly, more than two hundred species of snakes eat aquatic preys as fish, crustaceans or some amphibians. Prey capture can be performed under two different strategies involving only the snake head: the frontal strike and the lateral strike. In addition it has been demonstrated in recent work that the head shape of aquatic snakes has converged meaning that they have a similar head shape even if there is a diversity of shapes only less pronounced than for terrestrial snakes. In a previous study done in the team a frontal strike experiment has been performed and linked to the drag coefficient of five head shapes 3D printed models selected from a morphological analysis. The present work presents a new experiment that allows to perform a lateral strike as well as a frontal strike in a water tank in order to understand how shape is related with strategy used. To design the experiment main parameters have been extracted from a video analysis of *Hydrophis platurus* snakes. During a lateral strike the angular velocity reaches in average 45 rad/s and the angular acceleration 1000 rad/s². The strike lasts in average 68 ms with a total rotation angle of 75° and a rigid body rotation length of 3 cm. The head models used in the experiment were 3D printed with a housing for the force sensor which measured the force applied on the models during the motion imposed by the mechanical system. From the measurements it has been found that generally aquatic snakes are more efficient with the lateral strike since the drag coefficient is lower. However the results vary with the method used and are not always consistent with the previous experiment in frontal strike.

Résumé :

Les serpents aquatiques sont soumis à de fortes contraintes hydrodynamiques durant leur manoeuvre d'attaque dans l'eau et pourtant plus de deux cents espèces se nourrissent de proies aquatiques telles que des poissons, des crustacés ou bien des amphibiens. Cependant ils n'ont pas développé une adaptation spécifique à la prédation dans ce milieu contrairement à d'autres espèces animales aquatiques. La manoeuvre d'attaque de ces serpents peut se manifester avec deux stratégies différentes n'impliquant que la tête: l'attaque frontale et l'attaque latérale. Il a récemment été démontré que la forme de la tête des serpents aquatiques a convergé, c'est-à-dire que les têtes sont semblables de part leur forme et que la variabilité de ces formes est moins prononcée que pour les espèces terrestres, même si la diversité est toujours présente. Récemment une expérience concernant l'attaque frontale a été menée au sein de l'équipe comparant cinq modèles de formes de têtes imprimées en 3D et sélectionnées à partir d'une analyse morphologique. La présente étude concerne une nouvelle expérience qui mime l'attaque latérale, ainsi que l'attaque frontale dans l'eau afin de mieux comprendre le lien entre la forme de la tête et la stratégie d'attaque utilisée. Des paramètres caractéristiques ont été déterminés à partir d'analyses de vidéos de *Hydrophis platurus* afin de concevoir l'expérience. La vitesse angulaire moyenne atteinte par le serpent durant l'attaque latérale est de 45 rad/s de même que l'accélération angulaire moyenne atteint 1000 rad/s². Une attaque dure environ 68 ms avec un angle totale de rotation de 75° et une longueur de rotation de corps rigide de 3 cm. Les modèles de têtes étaient imprimés en 3D avec un logement pour le capteur de force qui mesurait la force appliquée sur la tête lors du mouvement imposé par la mécanique du système. À partir de ces mesures il en résulte que les formes testées sont en général plus efficaces en attaque latérale, donc avec un coefficient de traînée plus faible. Cependant les résultats varient avec la méthode utilisée pour l'analyse des données et parfois ne sont pas en accord avec l'expérience précédente en attaque frontale.

Key words : Snakes, lateral strike, snake kinematics, head shape, force measurements, drag coefficient

Contents

I	Introduction	1
II	Video analysis	2
1	Protocol	3
2	Trajectory, velocity and acceleration	3
3	Kinematics	6
4	Model average strike	6
III	Experimental setup	8
5	Snake head design	8
6	Sensor calibration and Labview script	9
7	Frontal strike and surface estimation	11
IV	Results	13
8	Data analysis	13
9	Validation of the experiment with the frontal strike	15
10	Reynolds number, real vs. experimental	17
11	Results for the lateral strike	20
V	Discussion	22

Part I

Introduction

Living beings are fascinating objects of study due to their sometimes surprising adaptation capacities. Some of them manage to survive in extreme conditions or with functional disadvantages in the middle more advantaged livings. It is the case for aquatic snakes who were terrestrial once and had to adapt to the aquatic life despite strong hydrodynamic constraints [9]. In addition they did not develop a suction feeding system as fishes did and still managed to survive.

This evolution can find its explanation in the study of hydrodynamic constraints experienced by the snakes. It is natural to think that the environment has a great influence on species survival. With the process of natural selection some individuals could reproduce and perpetuate the species whereas other could not feed themselves and died.

In addition of their morphological inheritance from terrestrial snakes, aquatic snakes have to deal with the hydrodynamic constraints of the medium which had two major consequences: the overall head shape convergence among aquatic species and a potential capture behavior adaptation. Prey capture can be performed using two different strategies: the frontal strike and the lateral strike, as shown in Figure 1 [4]. Even if the whole body moves, only the head is involved in the strike. The capture behavior adaptation consists in choosing either one the other strategy, knowing that species are specialized in one strategy and have one associated head shape [1]. The aim of the present study is to explore this relationship between the snake head shape and the hydrodynamics linked to the strategy used.

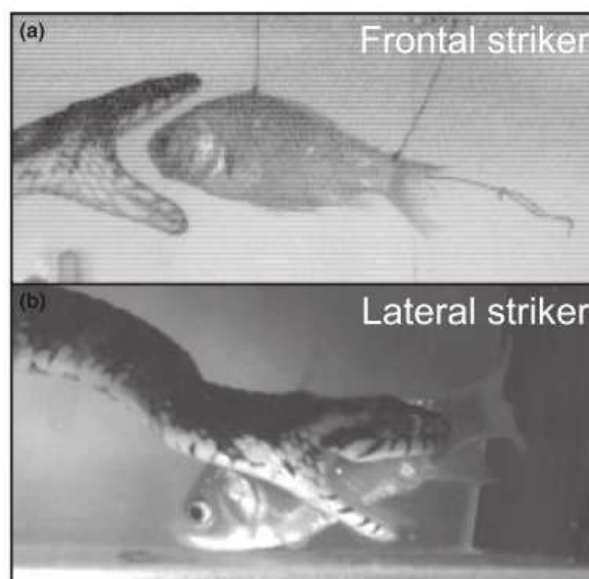


Figure 1: Images from movies recorded with high-speed cameras illustrating a frontal strike in *Natrix tessellata* (a) and a lateral strike in *Nerodia fasciata* (b) [4]

The head shape is crucial for the survival of a snake and over time this shape converged. In 1991 Young [10] has predicted that aquatic snakes should have a specific shape, more streamlined with longer and thinner heads however recent work [6] has shown from a comparative analysis including a broad range of species that in fact the typical aquatic snake head is shorter and bulkier than the terrestrial one. The head shape convergence has also been demonstrated [4]. The passage to an aquatic medium impacted the snake head shape in a sense that the shape variability among aquatic species is lower than for terrestrial species. Thus, they have a similar head shape even if there is a diversity of shapes only less pronounced than for terrestrial snakes. This convergence occurred because the individuals having this head shape were more efficient to capture prey and

feed themselves. The strike efficiency can be characterized by the efficiency to move in water that is to say, the capacity to circumvent the resistance imposed by water. The drag coefficient quantifies this resistance: lower the drag coefficient easier the strike. Segall *et al.* [6] showed that the drag coefficient of aquatic snakes is indeed lower than the one of terrestrial snakes.

For snakes, the Reynolds number characterizing the flow regime is high meaning that the viscous effects are negligible compared to the inertial effects. From a physical point of view the forces at play during a strike are the drag and an inertial contribution including the acceleration of the body and the acceleration of the surrounding fluid mass, called the added mass. Both the drag coefficient and the added mass depend on the head shape, and more precisely on the surface exposed to the flow over the strike [3]. The relationship between drag and added mass is not well known, it has been studied only for simple object like spheres [5]. Since the surfaces exposed are different for the frontal and the lateral strike, it is natural to think that the hydrodynamic forces will depend on the strategy used. However, the strategy selection can also be influenced by the escape behavior [2] of the prey triggered by the bow wave which is generated by the snake motion [8] [4].

In the Biomimetics and Fluid Structure interactions group of the PMMH (Physique et Mécanique des Milieux Hétérogènes) laboratory experiments were performed on the characterization of the frontal strike hydrodynamic forces. Five fictive head shapes were tested in a water tank, each representing an extrema of variability among all the aquatic snake species. The drag coefficients were derived using the force measurements and the frontal surface estimations for each head shape, as shown in Figure 2. The goal of the present study is to perform an experiment characterizing the lateral strike hydrodynamics and comparing it to the previous results obtained for the frontal strike. Finally, it should be possible to understand how the shape is related to the strategy used and maybe we would be able to predict the best prey capture strategy only by looking at the head shape of different species.

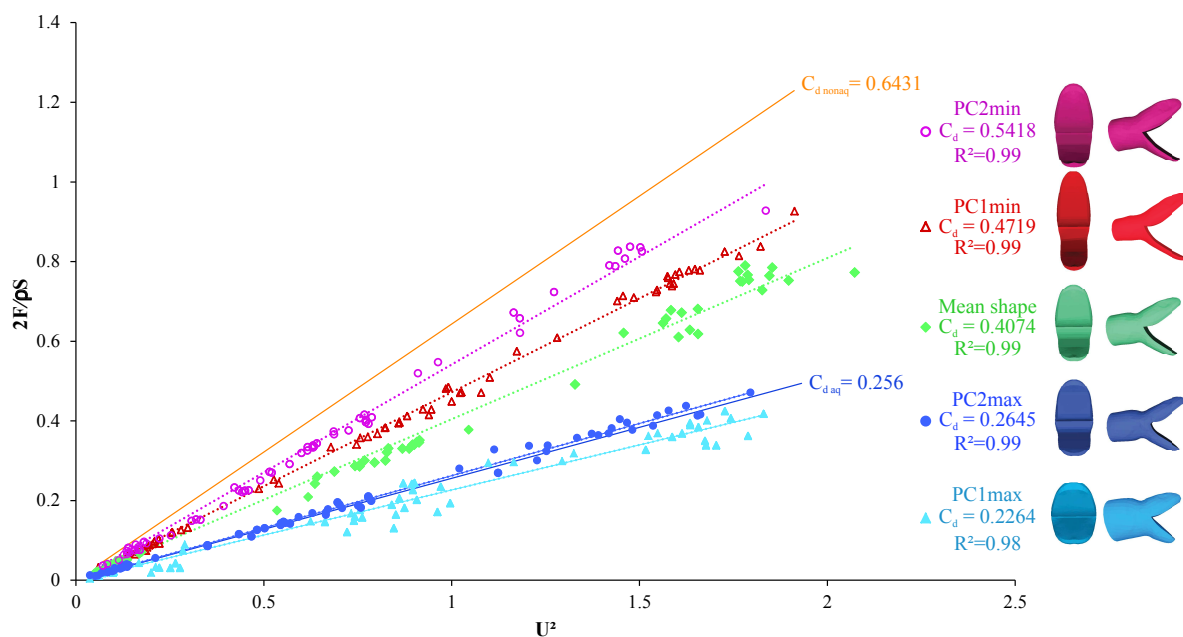


Figure 2: Drag contribution to the force as a function of the squared velocity of the frontal strike for the five head models tested

Firstly, the results of a kinematic study from video analysis will be presented. Characteristic parameters were determined to help in the experiment design which will be described in the second part, followed by the results and a conclusion.

Part II

Video analysis

In order to parametrize the experimental setup I did some video analysis of *Hydrophis platurus* snake lateral strikes. A montage is shown in Figure 4. They were taken by Marion Segall in Costa Rica. The main parameters extracted from the videos are: the rigid body rotation length, the average velocity and acceleration, the mean strike total rotation angle and the total strike period. The models used in the experiments have greater dimensions than the real snake in order to satisfy some conditions explained later, thus the most important parameters are the first ones in order to obtain similar Reynolds numbers from the videos and the experiments.

1 Protocol

The protocol consisted in manually tracking the rotation center, which is taken as the origin and the very tip of the head. The coordinates of the head are obtained for the two extremities I and P , as shown in Figure 3. The angular evolution over time of the snake head is derived to obtain the velocity and then the acceleration. Finally the average is taken over the 7 videos. The maneuver is unsteady and the velocity is expected to have a peak, as well as the acceleration. On the videos the snake first translates, then dives into the water while opening its jaw, rotates and catches the fish. Only the pure rotation is considered in this study, thus the translation is suppressed by subtracting the rotation center on each frame. The strike starts when the snake starts to open the jaw and ends when the jaw closed on the fish.

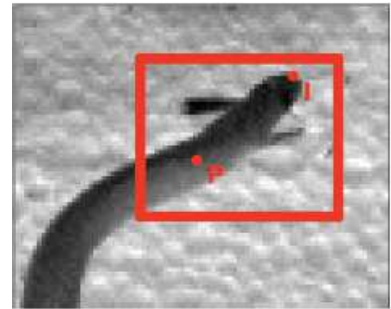


Figure 3: tracking



Figure 4: Video montage, $f = 250$ Hz, time between two frames 4.10^{-3} s

2 Trajectory, velocity and acceleration

On Figure 5 we can see the head trajectory during a lateral strike, where each color represents a video. The videos were taken in 2D whereas the strike is performed in 3D. For this reason the trajectory may be interpreted as an ellipsoid with a variant rigid body rotation length but in reality,

and it is also visible on the videos, this length is preserved. The acquisition frequency is $f = 500$ Hz so the time dt between two frames is 2 ms. The Eq. (1) is used to obtain the angle θ from the coordinates. Over time the angle θ increases as expected, it is shown in Figure 6.

$$\begin{cases} \text{if } x > 0 & \theta = \tan^{-1} \frac{y}{x} \\ \text{if } x < 0 & \theta = \pi - \tan^{-1} \frac{y}{x} \end{cases} \quad (1)$$

The angular velocity $\dot{\theta}(t) = \Omega(t)$ is obtained by numerical derivation of $\theta(t)$. The velocity direction is not very important and in terms of modulus we obtain the Figure 7.

From almost all the videos the curves obtained present two peaks: one main et one secondary. It seems to appear at the same time over the strike. The fastest strike is also the longest, the velocity reaches 100 rad/s and the strike lasts over 70 ms.

The accelerations in rad/s^2 was derived numerically using Matlab functions. It is shown in Figure 8. The strike begins with an acceleration followed by a deceleration phase.

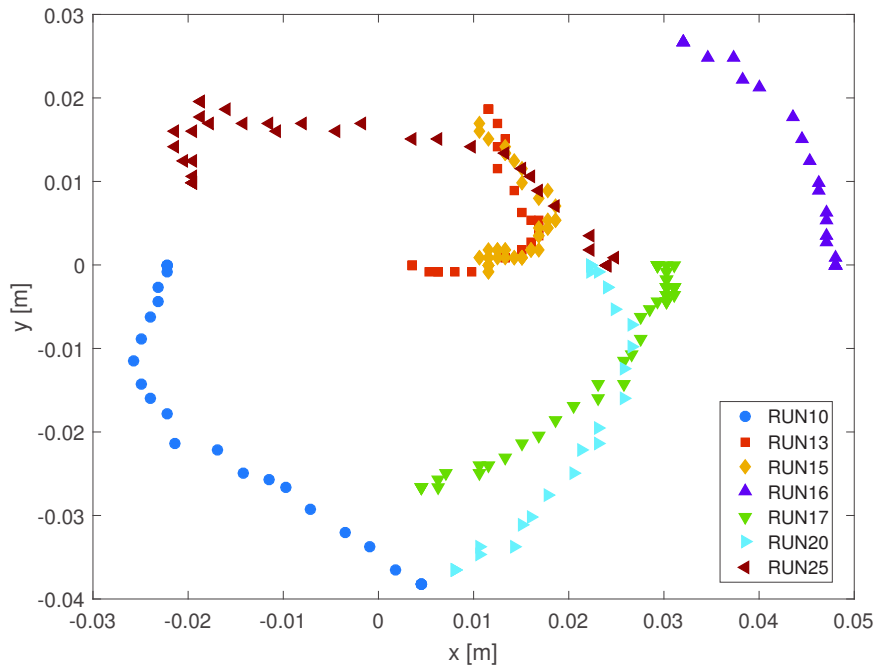


Figure 5: Trajectory of the tip of the head (point I) in space axis x and y where each color is a different video

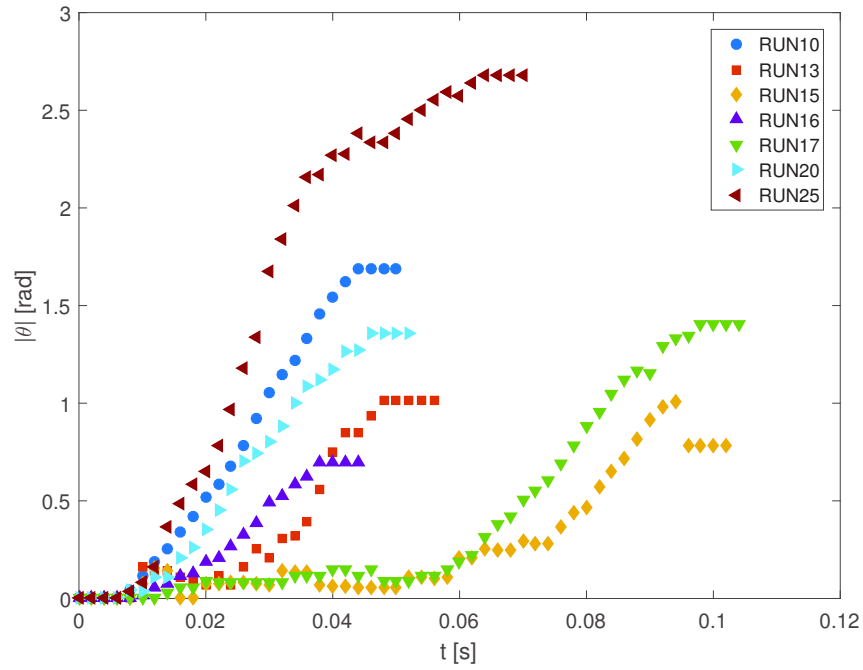


Figure 6: Angular trajectory of the tip of the head (point I) θ as a function of time, where each color is a different video

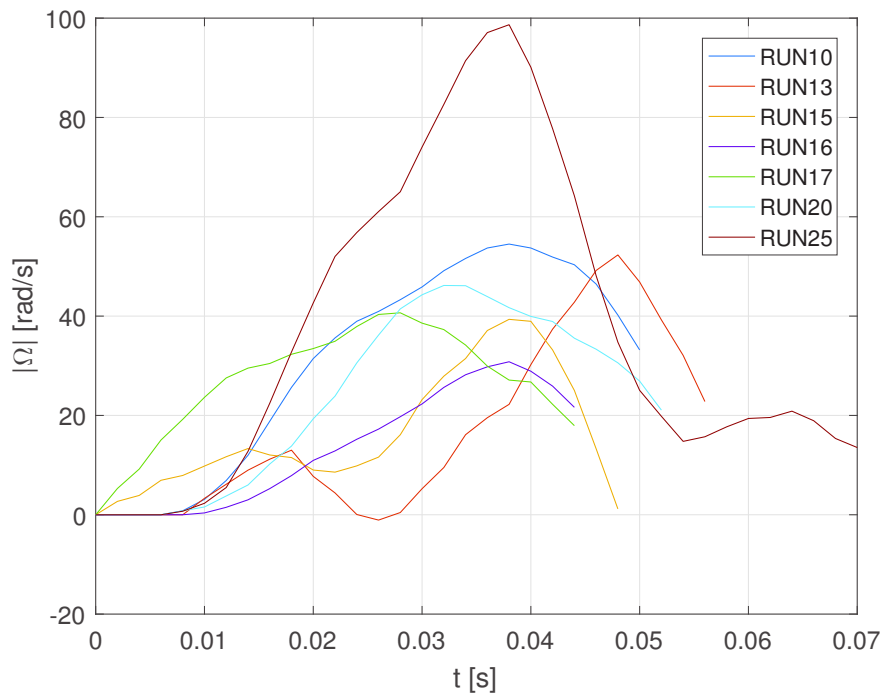


Figure 7: Angular velocity in function of time, where each color is a different video

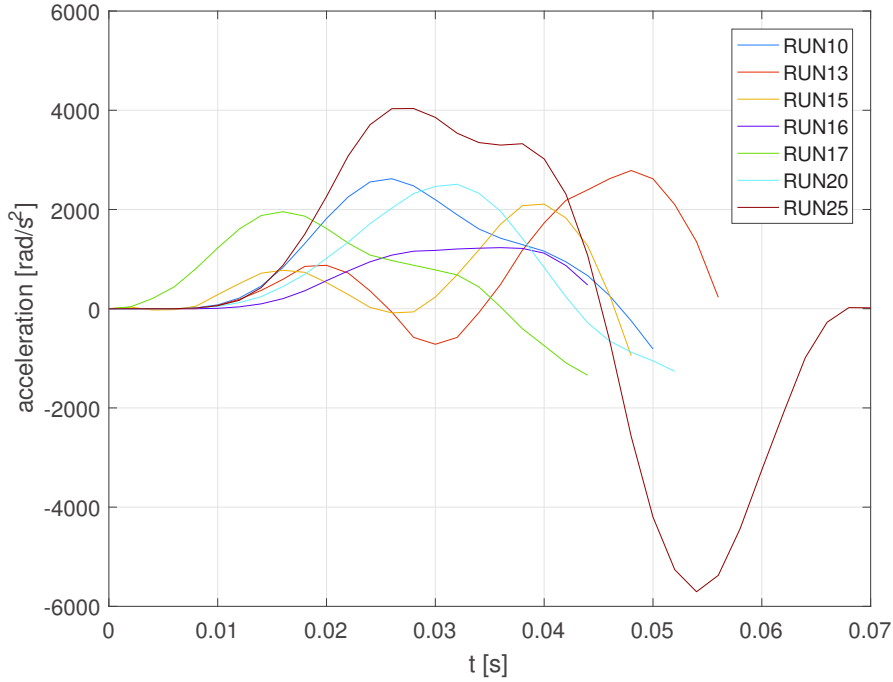


Figure 8: Angular acceleration in function of time, where each color is a different video

3 Kinematics

Figure 9 shows the snake head mid-line evolution over time. It is basically a simplification of the video which allows us to visualize the rotation center more precisely. This Figure is an example for one video, where the time between two curves is 6 ms. The circle symbolizes the tip of the snake head. The rigid body rotation center is taken as the first intersection of the curves, which is closest to the head. The second intersection point is responsible for the "S" shape of the snake body and will not be discussed here, it depends more on a locomotion study and we limit ourselves only to the strike kinematics. The rigid body rotation length L is taken as the length from the intersection to the tip of the head. On the figure it is not obvious since the intersection is not clear and L seems to vary which is the consequence of a three dimensional rotation. Simply by reasoning, a length would be smaller over the plane than in the plane, so L can be taken as the longest length from the intersection to the tip of the head, it is the most faithful length that can be obtained with the videos. The rigid body rotation length values are listed in Table 1.

Video	RUN10	RUN13	RUN15	RUN16	RUN17	RUN20	RUN25
L [cm]	2,98	2,58	3,56	5,38	3,39	3,21	2,73

Table 1: Rigid body rotation length L per video

4 Model average strike

All the parameters were averages over the seven videos. The averaged velocity and acceleration can be seen in Figures 10 and 11. Thus, the model strike reaches an angular velocity of 45 rad/s, an angular acceleration of 1000 rad/s² and lasts 68 ms. The mean rigid body rotation length values is saved with the value of 3 cm. The head diameter is also considered, namely for the Reynolds number estimations, and fixed at 1,2 cm. The mean strike lasts 68 ms and its total rotation angle is 75 °.

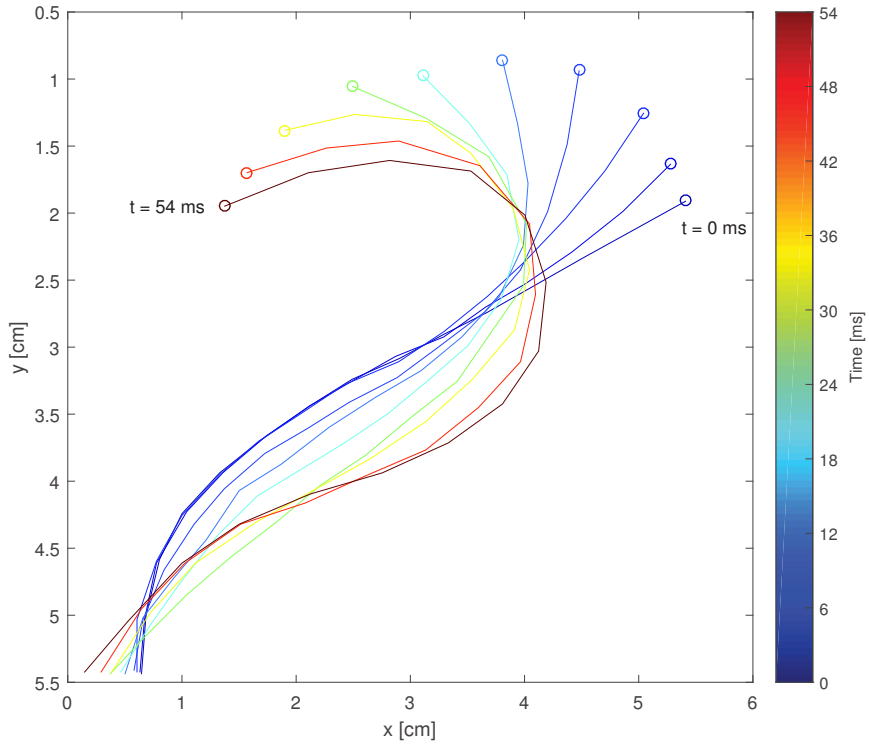


Figure 9: Snake body mid-line plots over time for one video

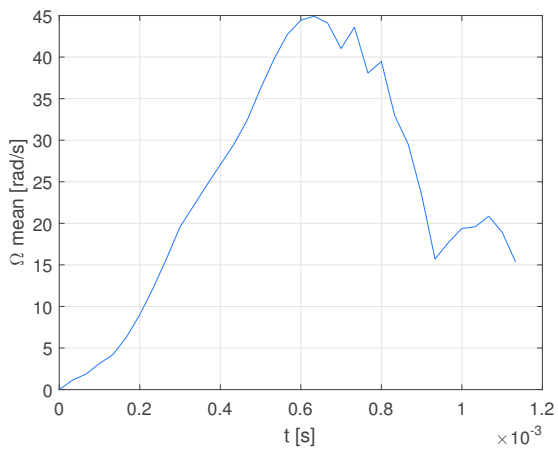


Figure 10: Mean angular velocity

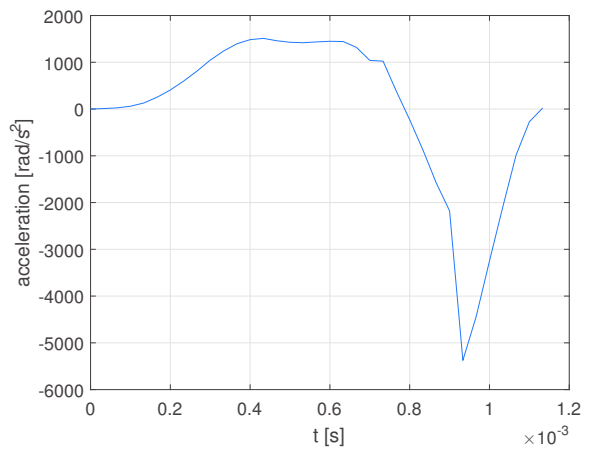


Figure 11: Mean angular acceleration

Part III

Experimental setup

The experimental setup mimics a lateral strike by means of a 3D printed snake head which serves as a model and a spring which drives the motion. Two sensors are used: an encoder to track the model's angular position and a force sensor placed in the head. As shown in Figure 12, the model is placed under water in a tank, it is attached an arm itself related to a pivot. The pivot binding permits to lower the friction efforts applied on the system. The encoder is placed in extension of the vertical axis, at the rotation center. This setup allows us a good optical access with a traction system similar to the snake strike. At first the spring is extended to a fixed angular position that we call θ_0 , then the sensors and the camera are turned on and the pivot arm is released. The spring is then pulling all the way to the initial non-extended position, just like snake muscles would push the head against the flow until it reaches the prey. In order to have a broad range of velocities the spring is extended with various θ_0 angles, from 20° to 90° . A foam square is placed at the end of the trajectory to minimize the impact and avoid damaging the force sensor. This experiment was entirely built from scratch, we tested different leads, namely one with a track which was supposed to guide the head mounted on the axis, nevertheless in all our attempts the friction was too high to permit a clean motion or the pieces were not aligned which resulted in a non-horizontal rotation.

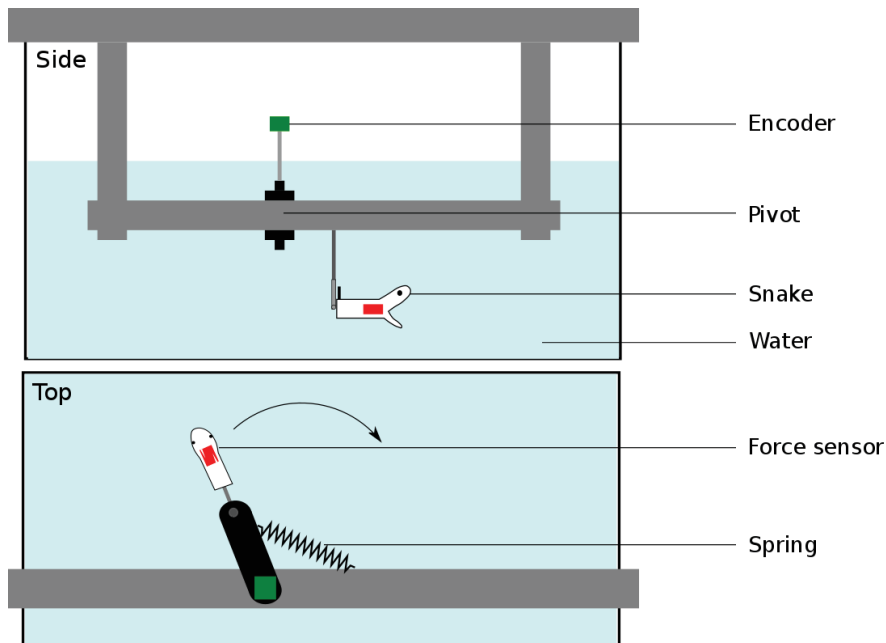


Figure 12: Experimental setup in lateral strike

5 Snake head design

The main goal of the internship is to study the influence of head shape on the hydrodynamic forces experienced by aquatic snakes during a lateral strike. Thus five different head shapes were 3D-printed and tested in an experiment which will be detailed in the next part. The shapes are the same as the ones shown in the introduction Figure 2. They correspond to different snake species more or less remote in terms of shape variations. As mentioned above, the force sensor was placed in the snake head in order to measure the applied on the head while minimizing side effects and flow perturbations. Like for the general setup, the model design had few versions. The one finally used is shown in Figure 13. The force sensor is screwed on the head side which is in the flow wake. The screw is drowned, always to minimize flow perturbations. Since the fixations are the same on every head, we shall still see differences between the shapes. The model dimensions were adapted

to allow the insertion of the sensor. It has been decided to magnify the original heads with a factor of 1,5 and print it in 3D with the maximal fine resolution. On the other side, the sensor is screwed to an aluminum fork, itself screwed to the axis joining the pivot piece. Thus, the model is only in contact with the sensor at a precise location and the sensor is united to the pivot system. Both the head and the driving system are independent to some degree, their common point is the sensor fixation on the model. The force sensor measures a displacement imposed by pressure between the two screwed parts, thus only in the horizontal direction. To minimize forces that can appear in the vertical direction because of the model's weight, special care was taken when designing the sensor housing and to make the head as neutrally buoyant as possible.

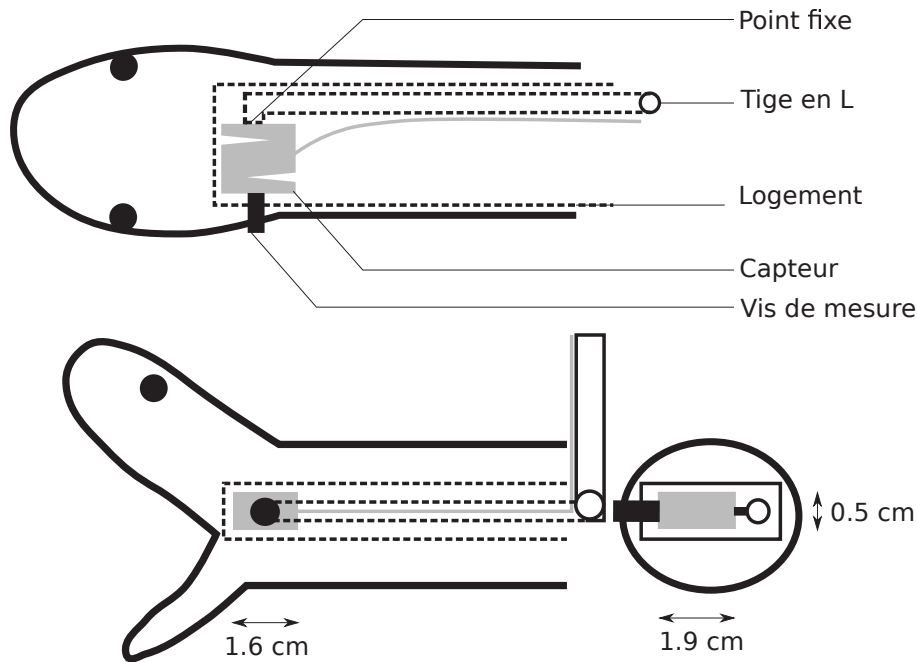


Figure 13: Snake head design scheme for lateral strike

6 Sensor calibration and Labview script

The sensors outputs are coded on Labview, a programming software using a graphic language. Since the strike is very fast it was important to synchronize the encoder with the force sensor. It has been done by means of a data acquisition card DAQ-mx from National Instruments which has an internal clock. Each path is independent thus can be treated simultaneously. A view of the script is shown in Figure 14 and the front window in Figure 15. The encoder is powered with a $5\text{ V} \pm 10\%$ and 10 mA signal delivered by the generator. Its voltage ratio extends from 5 to 95 % of V_{CC} the power supply input. Thus referring to the standard output graph giving the output voltage in function of the angle in degrees a factor has been calculated to convert the electrical signal to an angle in radians. With our encoder model the effective electrical angle available varies from 10° to 360° , so between 0 and 10° the signal gives 0 V, at 10° it gives 5 % of V_{CC} that is to say 0,25 V and at 360° it gives 95 % of V_{CC} that is to say 4,75 V. The factor is given by the slope in [rad/V] and is equal to 1,3575. In the experiment the spring is extended from the right to the left so when it is released the motion is carried out in the counter clockwise direction from the bottom view, whereas the encoder increasing voltage is in the clockwise direction. To get an increasing angle in radians in the motion direction an additional conversion was added to the script and consists in subtracting 2π from the result and multiplying by -1.

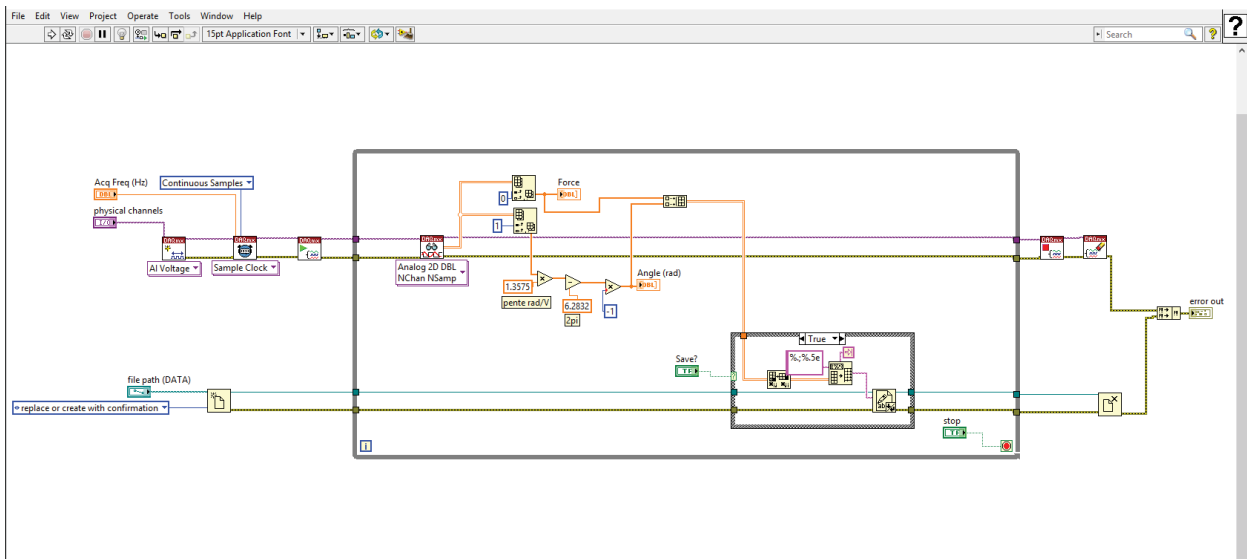


Figure 14: Labview script written for the experiment

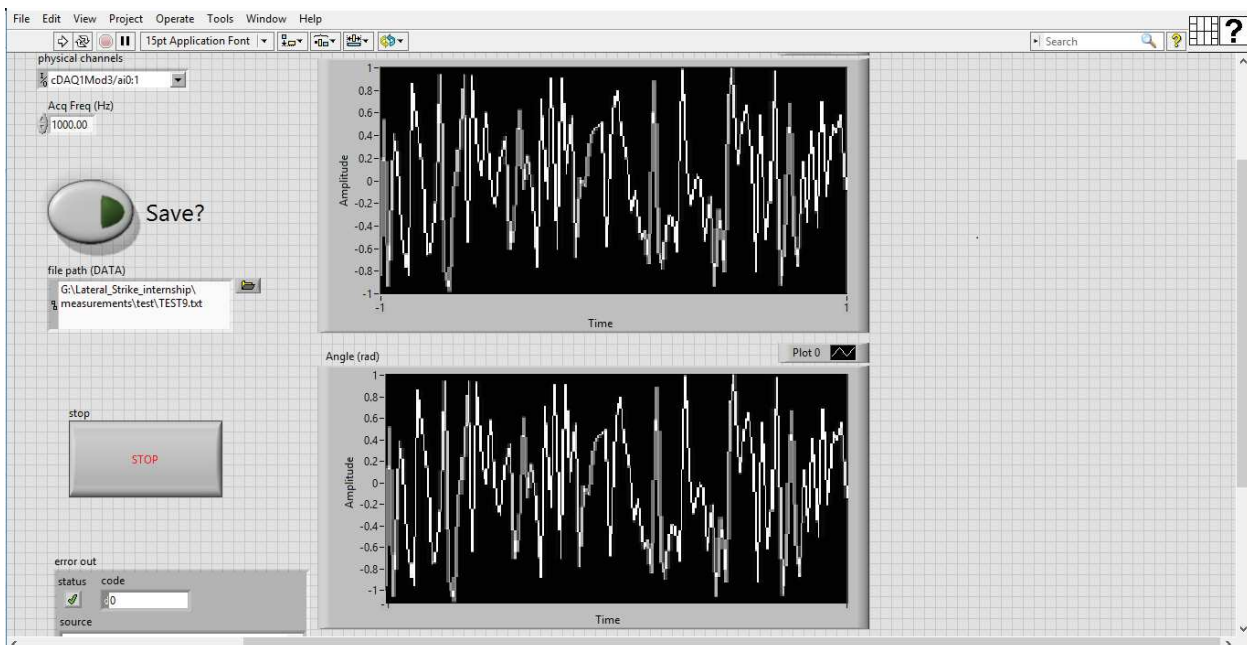


Figure 15: Front window of the Labview interface

Finally the raw data contain the force sensor signal in Volts and the angular position of the head in radians, all performed at 1000 Hz. The conversion from volts to newtons was done after the sensor calibration. The sensor does not have exactly the same response for a bias depending on whether it is not attached or attached to a model. On Figure 16 one can find the calibration lines corresponding to both cases. The difference observed can be explained by a higher confinement of the sensor while attached. The conversion factor is slightly different and the one obtained with the sphere is kept because it is more faithful to the experiment where the force sensor is always attached to a model. This factor is equal to 0,6281 N/V.

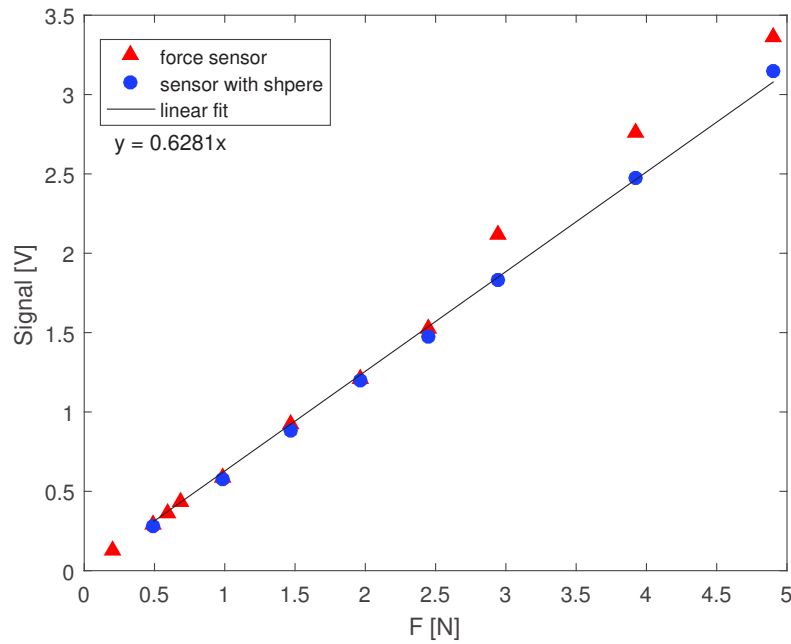


Figure 16: Calibration for the force sensor, alone and with the sphere as model

7 Frontal strike and surface estimation

A frontal strike experiment has been done previously in the team and it resulted in the determination of drag coefficients for the 5 snake head models that I used. These results are considered as a relative reference for the lateral strike experiment validation. Since both experiments in frontal strike are based on the same strategy with the same head shapes tested the results concerning the hydrodynamic force should be similar. However is a major difference in the setup may influence the absolute values of the measured variables. In order to perform a frontal strike with the present setup, an adaptation of head model design was needed in order to adapt the sensor's orientation, so the measured force is related to the frontal surface of the head exposed to the flow. The experimental setup is shown in Figure 17 and the new head design in Figure 18. The electrical circuit for the sensors remained the same as for the lateral strike. New models were 3D-printed, with the same dimensions and resolution than the previous ones. The acquisition parameters also remained unchanged.

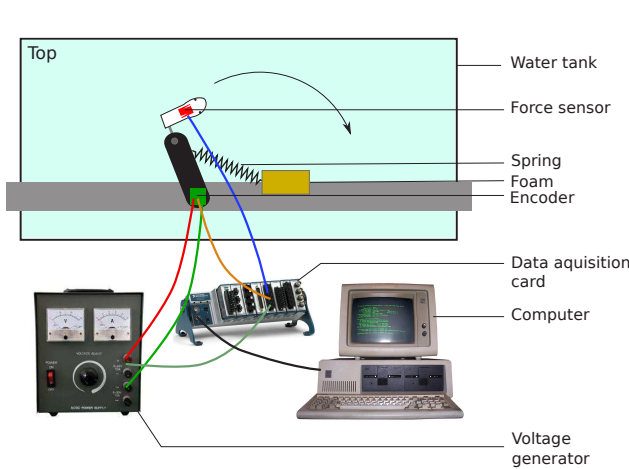


Figure 17: Setup for frontal strike

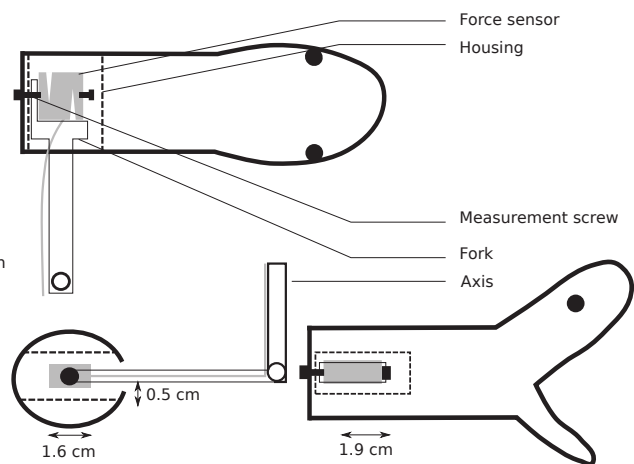


Figure 18: Snake head design

Over a motion, the form drag defined in Eq. (4) is related to the surface exposed to the flow, which is different for each model. The aim of this study is precisely to quantify the forces induced by the shape differences and related it to real snake strike behavior. Some models are really alike and the shape difference is hard to notice, thus real surface estimations have been done. Their determination was done from photographs transformed into binary images as shown on Figure 19 and Figure 20 and the area extracted with the measurement tool of ImageJ. The photographs were taken as perpendicular as possible to the model. The surfaces values are visible on Table 2 for the 5 snake head models for both strikes and the sphere which is used as reference.



Figure 19: Surfaces exposed to the flow in lateral strike for five models: $pc1_{max}$, $pc1_{min}$, $mean$, $pc2_{max}$ and $pc2_{min}$ (from left to right)



Figure 20: Surfaces exposed to the flow in frontal strike for five models: $pc1_{max}$, $pc1_{min}$, $mean$, $pc2_{max}$ and $pc2_{min}$ (from left to right)

model	$pc1_{max}$	$pc1_{min}$	$mean$	$pc2_{max}$	$pc2_{min}$	sphere
S (lateral) [mm ²]	4,669	3,006	3,760	3,978	3,39	1,931
S (frontal) [mm ²]	4,534	3,984	4,160	4,4518	4,409	

Table 2: Surface area exposed to the flow for the snake head models and the sphere, in lateral and frontal strike

Part IV

Results

8 Data analysis

The experimental campaign was performed as follows: one set of data per strike (lateral and frontal) corresponding to five repeated measurements for eight initial angles θ_0 varying from 20° to 90° per model. Five snake head models from the Figure 2 were tested in lateral and frontal strike. In addition a model sphere was tested in order to have a physical reference with a shape that has been well studied in the past. The total amount of data stands at 440 measurements. The raw data containing the force and position signals are not readable without some numerical processing, as shown in Figure 21

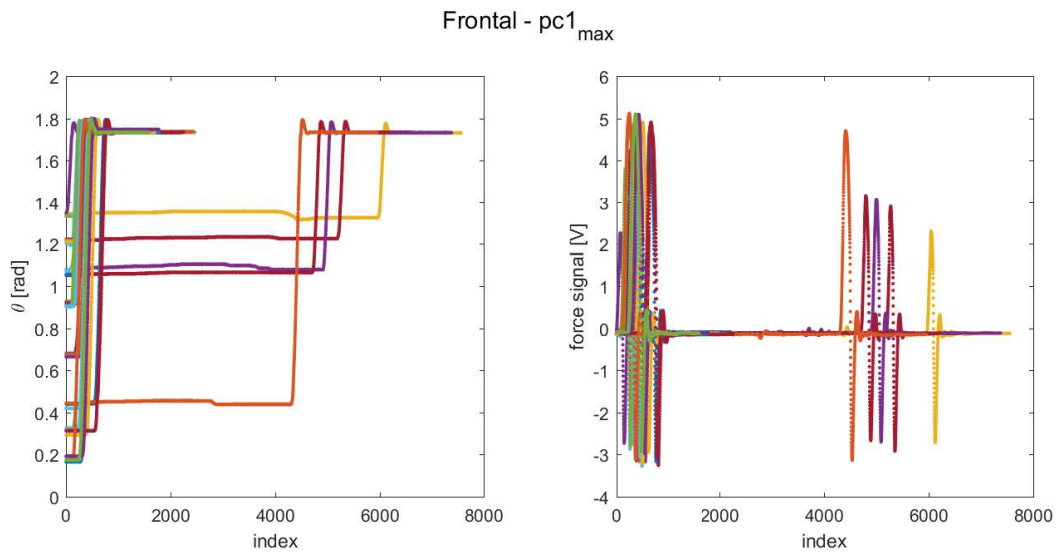


Figure 21: Raw position (left) and force (right) signals for $pc1_{max}$ in frontal strike

After trimming, shifting and converting the obtained data are shown in Figure 22. All the measurements were cropped before the foam stop.

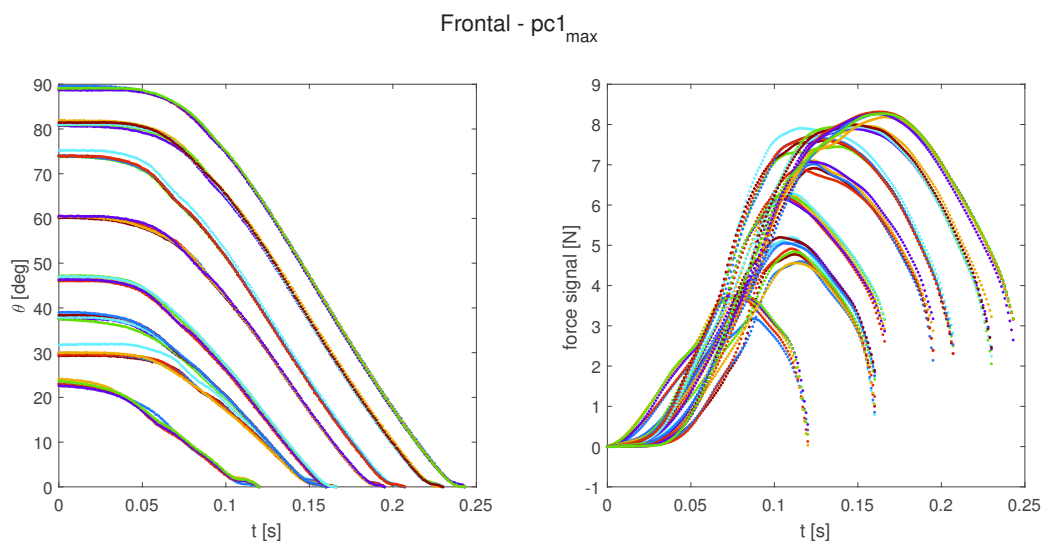


Figure 22: Rearranged position (left) and force (right) signals for $pc1_{max}$ in frontal strike

Finally, thanks to the analogical synchronization of the sensors it is possible to represent different variables with the same temporal abscissa (Figure 23 and 24). The angular velocity $\Omega(t) = \dot{\theta}(t)$ has been derived from the angular position by means of a Matlab function, as well as the angular acceleration $\dot{\Omega} = \ddot{\theta}(t)$.

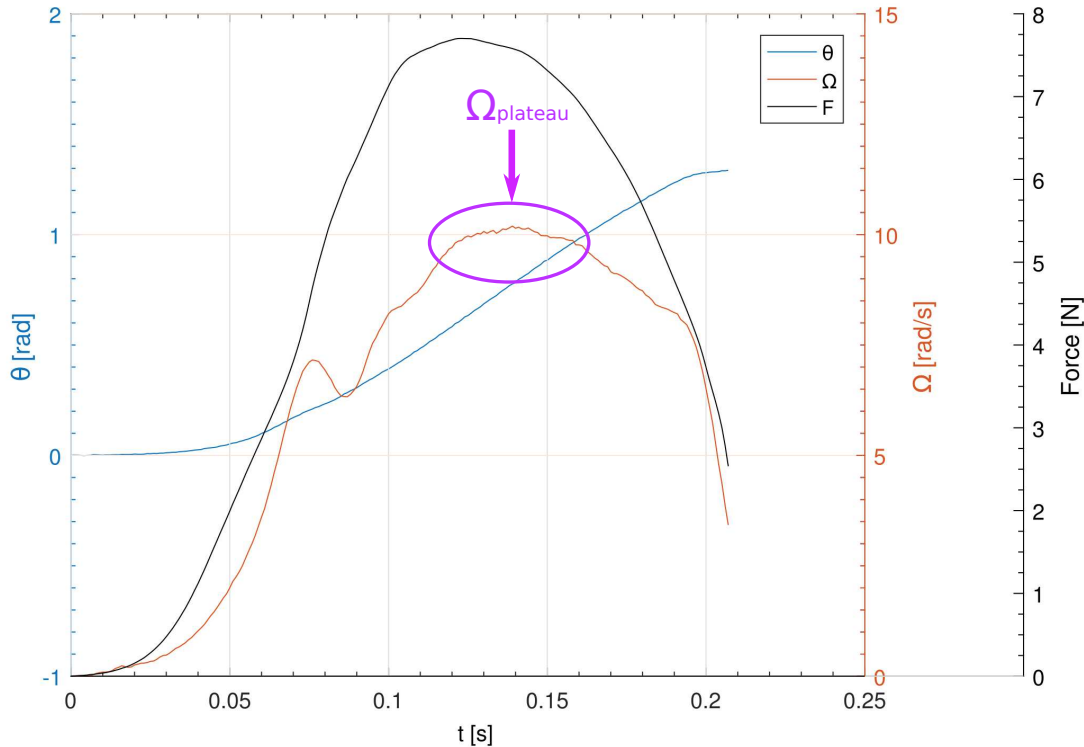


Figure 23: Temporal evolution of the angular position θ , the angular velocity Ω and the force for $pc1_{max}$ in frontal strike, $\theta_0 = 70^\circ$

At first when the spring is released, the axis on which the sensor is fixed drives the model. the physical connection between the axis and the model is carried by the sensor's screw. At the beginning the measured force increases (the sensor is extended, in traction) which means that the model is lagging behind the axis actuated by the spring. The force reaches a maximum at the middle of the motion and decreases, meaning that the sensor is less and less pulled so the model joins the axis. On almost all the experiments the angular velocity presents a plateau, in Figure 23 it is considered between 0.12 s and 0.16 s. The plateau determination was done manually for all the measurements. The force maximum and the velocity maximum are shifted in time, first appears the force peak and then the velocity plateau. On Figure 24 one can see the initial acceleration peak corresponding to the velocity bump then after few fluctuations the acceleration decreases. It is nil at the plateau of constant velocity. The first half of the strike is governed by inertia because of the presence of the acceleration peak. However it is not straight forward to discern the role of the inertia and the drag during the strike. Nevertheless it is probably not linked to the strike strategy since the shape of the plots is more or less the same in lateral strike and frontal strike.

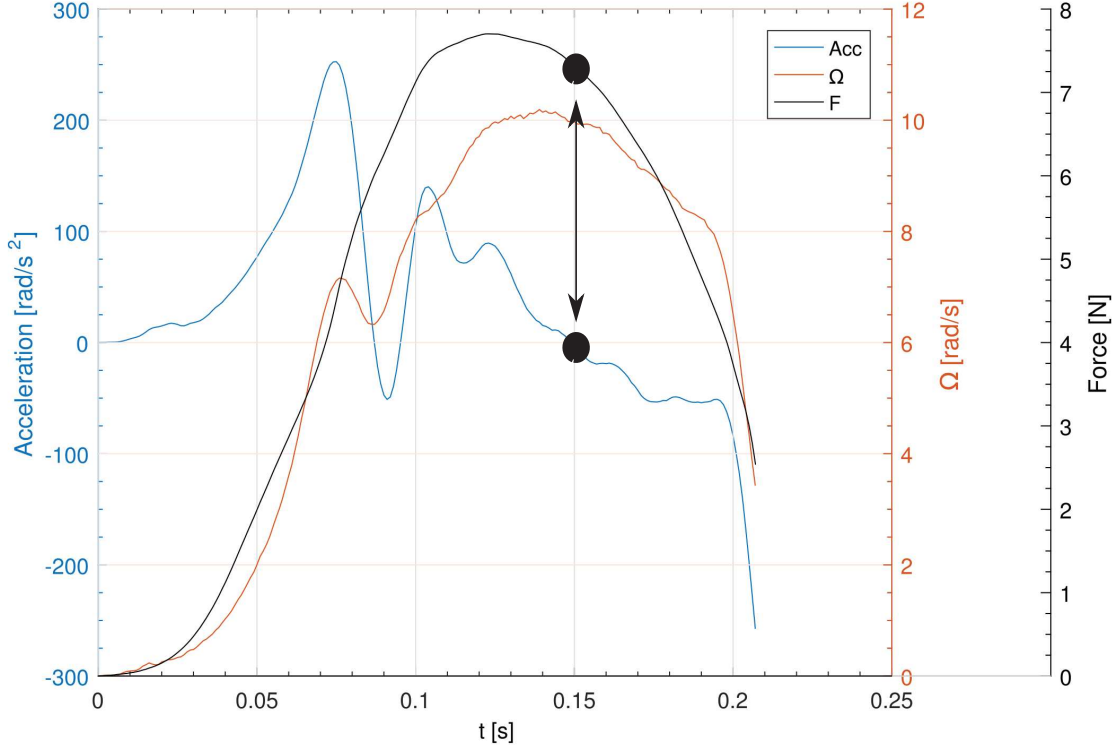


Figure 24: Temporal evolution of the angular acceleration $\dot{\Omega}$, the angular velocity Ω and the force for $pc1_{max}$ in frontal strike, $\theta_0 = 70^\circ$

9 Validation of the experiment with the frontal strike

The main difference between the previous experiment and the present one is the spring configuration. Indeed, in the first setup the spring was compressed and the model released. The whole was attached to a track with compressed air to minimize the friction. Thus, after an acceleration imposed by the spring extension the system reached a state where the acceleration was nil and only the drag remained. In the present experiment the spring is first extended and pulls the axis all along the motion, the system is never free and there is no plateau of constant force. However it is closer to a real snake strike animated by muscles.

One idea to extract the drag from the measurements is to consider the regime where we suppose the drag is dominant. The force is considered in Eq. (2).

$$F = \underbrace{\frac{1}{2}\rho S c_D \dot{x}^2}_{\text{Drag force}} + \underbrace{(m + M)\ddot{x}}_{\text{Inertial force}} \quad (2)$$

Where $\dot{x} = \Omega_{plateau} \times L$ is the velocity, with L the distance between the center of rotation and the sensor, $L = 25$ cm and $\Omega_{plateau}$ the angular velocity averaged on the plateau of constant velocity. S is the surface exposed to the flow, c_D is the drag coefficient, the water density is $\rho = 1000$ kg/m³, m is the mass of the model, M is the added mass and finally $\ddot{x} = \dot{\Omega}_{plateau} \times L$ is the acceleration.

When the velocity is constant, the acceleration is nil and the force only equals to Eq. (3) from which we extract the drag coefficient Eq. (4).

$$F = \frac{1}{2}\rho S c_D \dot{x}^2 \quad (3)$$

$$c_D = \frac{2F}{\rho S \dot{x}^2} \quad (4)$$

There are different possibilities for the choice of F , however when taking the average of F , F_{max} or $F = F(x_{plateau})$ where $x_{plateau}$ is the abscissa of $\Omega_{plateau}$, the results are not the one expected from the previous experiment in frontal strike. It did not work for the sphere either.

After few different attempt the selected protocol consisted in taking the velocity $\dot{x} = U = \Omega_{plateau} \times L$ and the force value predicted by the previous frontal strike experiment. Indeed, using Eq. (2) and replacing c_D by the ones found previously, for each model in frontal strike, one obtains the associated force. The results derived previously by the team are shown in Figure 2.

In practice the associated force appears at the very end of the strike. The protocol was based on only one " c_D forcing" corresponding to the model $pc1_{max}$ for which the drag coefficient equals to 0,2264. By taking this value, for the experiments at $\theta_0 = 70^\circ$, the associated force appears at the end of the strike, more precisely at $\theta \sim 99,5\% \theta_{max}$. The inverse protocol was tested to derive the expected c_D from the force taken at $\theta \sim 99,5\% \theta_{max}$. For each of the five models in frontal strike, a drag coefficient close to the previous results was found. This method consisted in "forcing" the good result, so it is not objective itself but it should be sufficient to compare frontal and lateral strikes for different shapes of snake heads, which is the aim of the internship.

The Figure 25 and the Figure 26 represents respectively the drag contribution to the force as a function of the squared velocity of the frontal strike for the five head models tested and the same for the sphere. The drag coefficient is given by the slope of the curves, different for each model. This slope changes when the velocity increases, which will be explained in the next section. The drag coefficient per head is obtained by taking the average of the drag coefficients per measurement, the values can be found in Table 3.

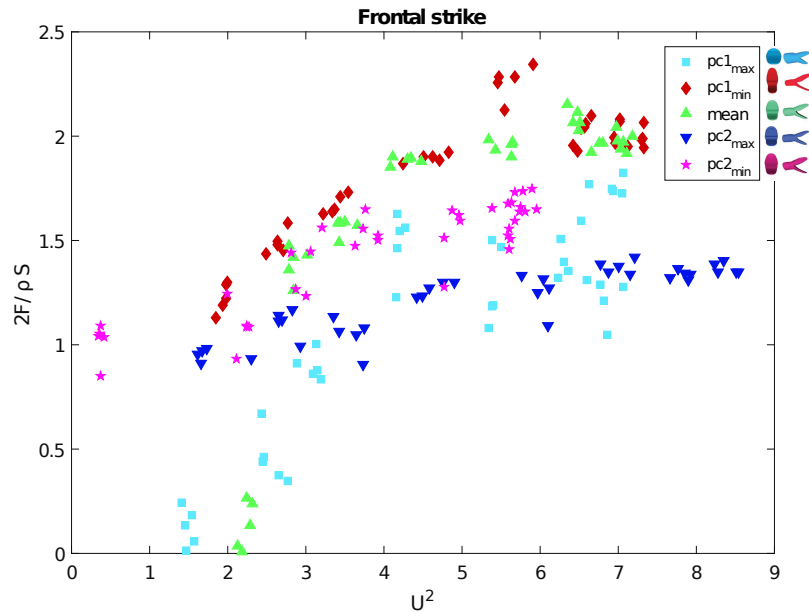


Figure 25: Drag term $2F/\rho S$ depending on the squared velocity of the frontal strike for the five head models tested

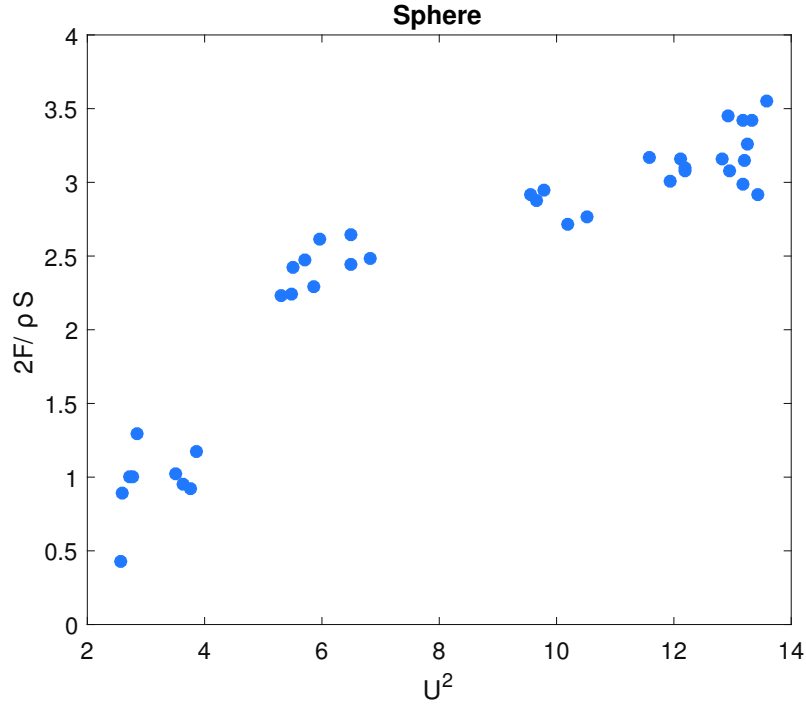


Figure 26: Drag term $2F/\rho S$ depending on the squared velocity of the frontal strike for the sphere

model	$pc1_{max}$	$pc1_{min}$	$mean$	$pc2_{max}$	$pc2_{min}$	sphere
c_D (previous experiment)	0,2264	0,4719	0,4074	0,2645	0,5418	0,5 (in theory [7])
c_D	0,2266	0,4325	0,3347	0,2813	0,6605	0,3217

Table 3: Drag coefficients for the five head models tested in frontal strike compared to the reference results of the previous experiment and the drag coefficient of a sphere compared to a reference value

10 Reynolds number, real vs. experimental

All the work concerning the video analysis and extracting the main parameters involved in a lateral strike was needed for the Reynolds number estimation. To have a faithful experiment both Reynolds numbers have to be similar. It is the insurance that the experiment is performed in the same flow regime than the real snake strike.

The Reynolds number is defined as follows:

$$Re = \frac{D\Omega_{mean}L}{\nu} \quad (5)$$

Where D is the snake body diameter, L is the rigid body rotation length, Ω_{mean} is the angular velocity averaged over the 5 head models and ν the kinematic viscosity equal to 1.10^{-6} m²/s for water at ambient temperature.

From the videos, the extracted parameters were: $L \sim 3$ cm, $D \sim 1,2$ cm and $\Omega_{mean} \sim 45$ rad/s (it is the maximum value of Ω averaged over the seven videos), thus $Re = 1,62.10^4$.

For the experiments $L \sim 25$ cm is the distance between the center of rotation and the force sensor, $D \sim 5$ cm and Ω_{mean} was estimated from a data analysis over all the measurements. Then an average was done over measurements of the same θ_0 initial angle, it is represented on the Figure 27. This Ω_{mean} angular velocity is used to calculate the Reynolds number which depends on the initial

position of the model. For the reference, the same scheme was done to the sphere measurements, they are shown in Figure 28, where on the left graph each point represents one experiment. As expected the velocity increases with θ_0 and is generally higher for the sphere than for the models. The non linearity of the velocity distribution may be caused by the non linearity of the spring. When totally extended, the spring stiffness decreases which results in a lower velocity variation between two θ_0 positions.

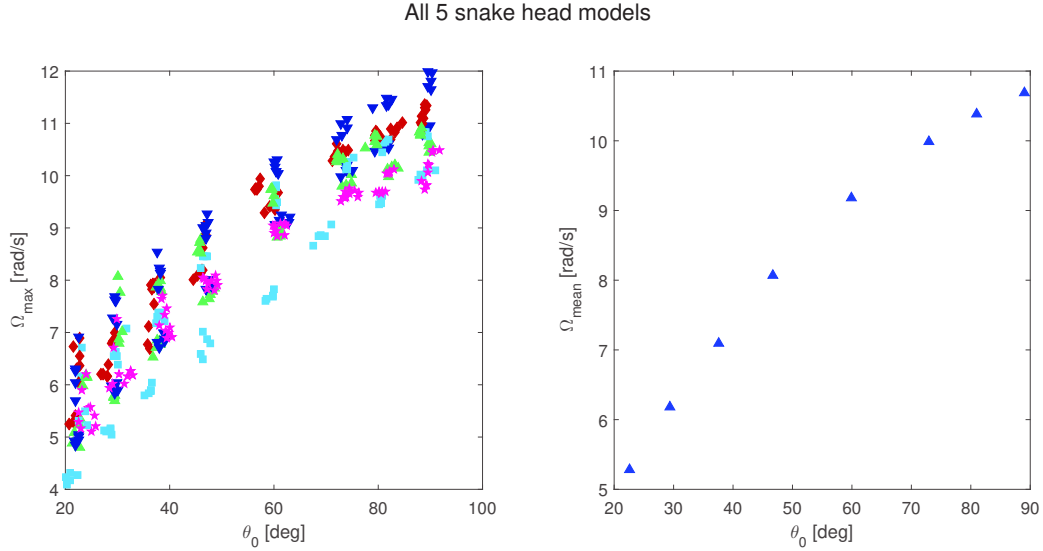


Figure 27: Angular velocity as a function of the initial θ_0 angle for each model for frontal and lateral strikes combined (left) and the same velocity averaged over the models (right)

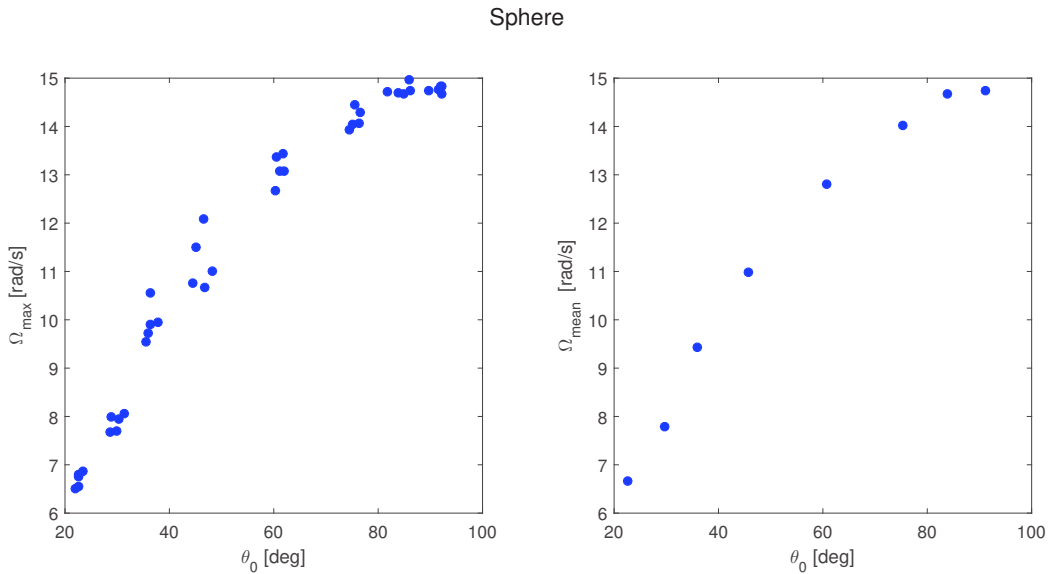


Figure 28: Angular velocity as a function of the initial θ_0 angle for the sphere (left) and the same velocity averaged the experiments (right)

For the snake heads the Reynolds number shown in Figure 29 reaches $1,4 \cdot 10^4$ and $2 \cdot 10^5$ for the sphere which is in the transition to the turbulence [7]. It is in addition one order of magnitude higher than for real snakes, as calculated previously. This can explain the low drag coefficient for the sphere seen in Table 3. To verify this hypothesis the Figure 30 represents the drag coefficient for the sphere, as a function of the Reynolds number. There is indeed a decrease of drag coefficient from almost 0,5 to 0,2 for high Re.

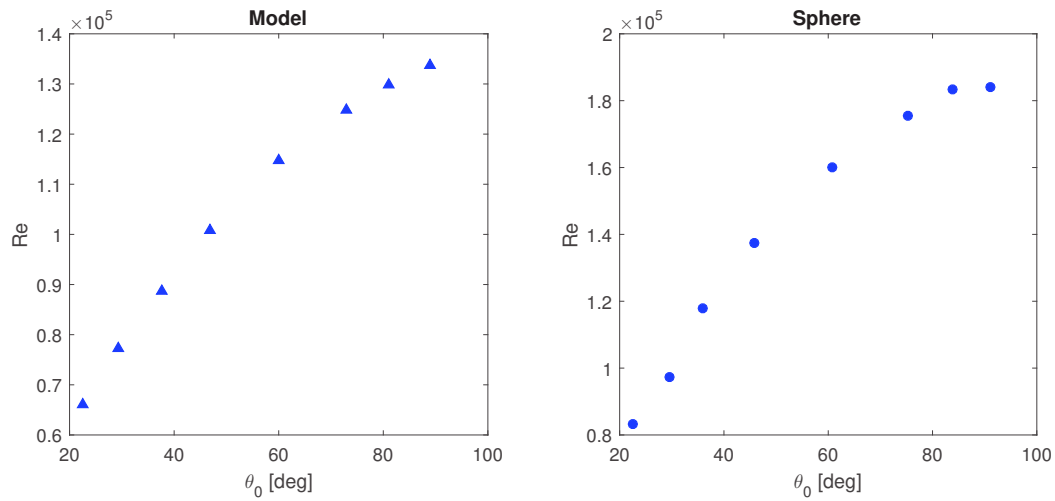


Figure 29: Reynolds number as a function of the initial θ_0 angle for the snake head (left) and the sphere (right)

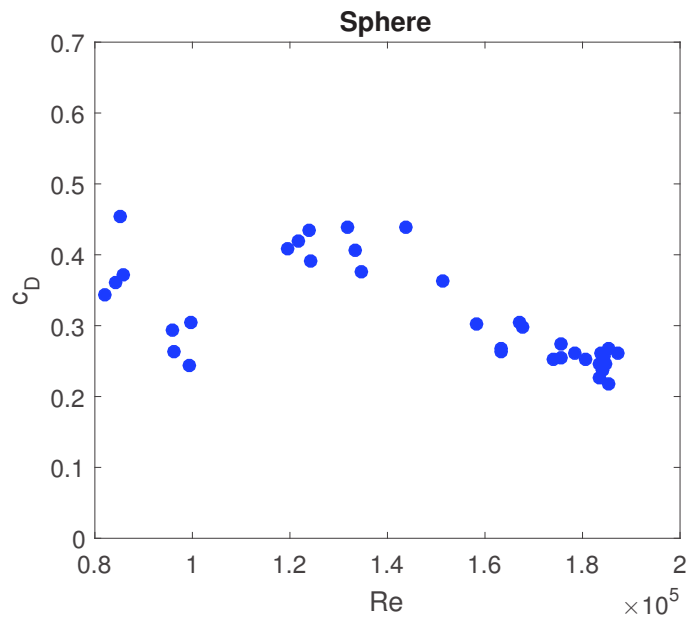


Figure 30: Drag coefficient as a function of the Reynolds number for the sphere in water

Finally it is hard to confirm the validity of the results since the reference sphere case is not a constant on which to refer. That is why it has been preferred to consider the results derived from the previous experiment in frontal strike as a reference.

11 Results for the lateral strike

The results for the lateral strike as shown in Figure 31 are more dispersed than for the frontal strike (Figure 25). The summary in terms of values is shown in Table 4.

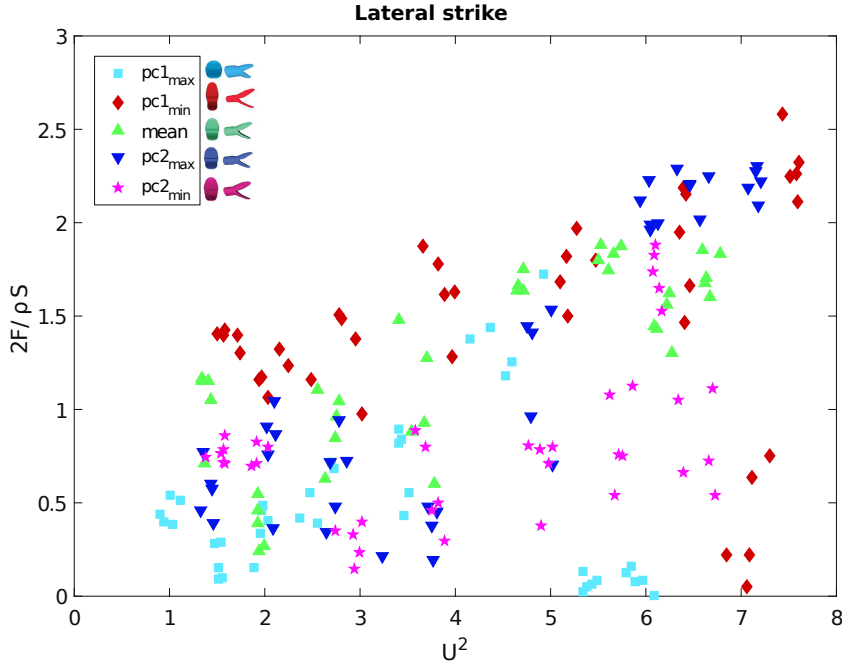


Figure 31: Drag term $2F/\rho S$ depending on the squared velocity of the lateral strike for the five head models tested

model	$pc1_{max}$	$pc1_{min}$	$mean$	$pc2_{max}$	$pc2_{min}$	sphere
c_D frontal (previous experiment)	0,2264	0,4719	0,4074	0,2645	0,5418	0,5 (in theory [7])
c_D frontal	0,2266	0,4325	0,3347	0,2813	0,6605	/
c_D lateral	0,1903	0,4142	0,3460	0,2934	0,2333	0,3217

Table 4: Drag coefficients for the five head models tested in lateral strike compared to the drag coefficients obtained in frontal strike and the reference results of the previous experiment

The data dispersion does not facilitate the drag interpretation however the averaged values seem to make sense. Indeed, the values are not very different and it is possible to deduce which shape is more efficient in water than the other. The model with the lower c_D is still the $pc1_{max}$ and in general the drag seem to be lower in lateral strike than in frontal strike. Nevertheless one can see a real change for the model $pc2_{min}$ which had the larger c_D in frontal strike and found itself at the second place in lateral strike which is curious since it is the closest shape to terrestrial species and in her PhD Marion Segall demonstrated that terrestrial snakes produce more drag in water in comparison to aquatic snakes in frontal strike. According to the present results the drag is slightly increased for $pc2_{max}$ and $mean$. For these shapes the strategy used does not seem to have an impact on the drag coefficient at play during the strike.

These results are very dependent on the data noise and some points are clearly not physical at high velocity. It may also be linked to the Reynolds number. There is probably something in the measurements which is not taken in account. In addition the protocol of force extrapolation used based is on the hypothesis that the measured force is only due to the drag although there can be an inertial contribution.

If instead of the extrapolated force and the angular velocity at the plateau, the maximum of force

and velocity are plotted, the results obtained look more accurate (Figure 32). However in frontal strike the slopes which give the drag coefficient indicate a different order for the models than in the previous experiment. To unformalized the results it has been decided to take the models weigh in account since their masses vary with the model and the strategy. This results from a honeycomb 3D printing for the frontal strike whereas for the lateral strike the models were filled. In order to take in account the mass the drag term $2F / \rho S$ was divided by m the mass of each head model and multiplied by ρV where ρ is the water density and V is the volume of each model. The Figure 33 shows the same data but weighted with an adimensional mass. The drag coefficients are given by the slope of the curves and shown in Table 5. Some of them are not realistic, especially in comparison with the previous experiment in frontal strike. It is also too large for the sphere. Nevertheless all models present less drag in lateral strike than in frontal.

$$M_{adim} = \frac{\rho V}{m} \tag{6}$$

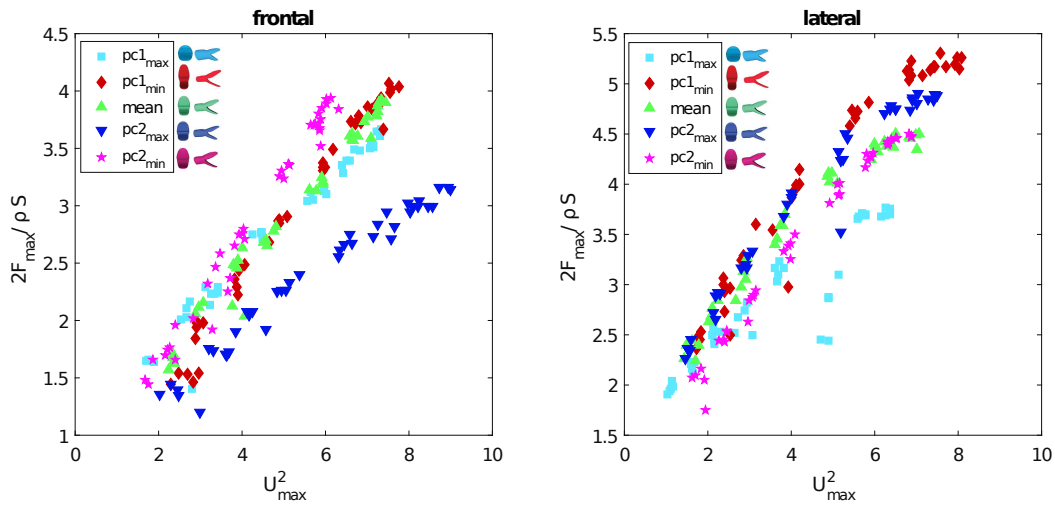


Figure 32: Drag term $2F/\rho S$ depending on the squared velocity of the frontal strike for the five head models tested of the frontal and lateral strike for the five head models tested

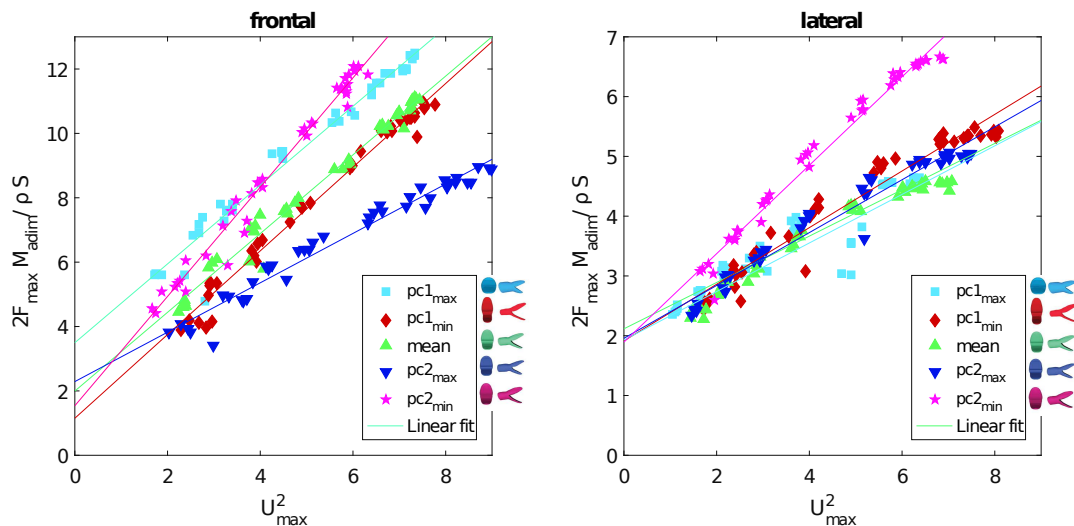


Figure 33: Drag term $2F/\rho S$ weighted with an adimensional mass depending on the squared velocity of the frontal strike for the five head models tested as a function of the squared velocity max of the frontal and lateral strike for the five head models tested. The straight lines are linear regressions

model	$pc1_{max}$	$pc1_{min}$	$mean$	$pc2_{max}$	$pc2_{min}$	sphere
c_D frontal (previous)	0,2264	0,4719	0,4074	0,2645	0,5418	0,5 (in theory [7])
c_D frontal	1,224	1,300	1,223	0,7673	1,698	/
c_D lateral	0,3876	0,4736	0,4062	0,442	0,7397	0,9762

Table 5: Drag coefficients for the five head models derived from the maximum force and velocity and weighted with an adimensional mass

Part V

Discussion

Finally, from observations of real aquatic snakes general parameters characterizing the lateral strike kinematics have been determined.

To measure the hydrodynamic forces applied on the snake head an experiment that mimics the lateral strike has been designed. This experiment was also performed in frontal strike, in order to compare with the results obtained with the previous experiment done within the team and involving the same strategy. The originality of the present experiment is the possibility to perform it in both lateral and frontal strike, and we believe that the pulling spring kinematics is closest to what happens during a real strike.

From the Reynolds number and drag coefficient estimations of the sphere it appears that the experiments were performed in the transition to turbulence regime so that the slope of the plots representing the drag term $2F/\rho S$ varies in function of the squared velocity U^2 . Since the drag coefficient in function of the Reynolds number is not known for a snake head shape, the results obtained in the previous frontal strike experiment served as a relative reference. The data analysis based on the hypothesis that only the drag remains when the velocity is constant are not conclusive because of the points dispersion. Furthermore the force values were selected in order to match the previous experiment's results. The results obtained using F_{max} and U_{max} look more accurate but follows a non realistic drag coefficient very different from the previous experiment in frontal strike. However by looking at the Figure 34 one can say that both experiments in frontal strike (the previous and the present) could be compared thanks to the linearity of the force in function of the Reynolds number. Plots for each head shape are joining for both experiments. If the experiment is relevant it is probably not the case of the interpretations which do not take in account the inertial contribution to the measured force.

Since the present experiment itself was accurate and reproducible it is possible to compare frontal and lateral strike hydrodynamics. The drag coefficient ratios weighted with the mass in order to take in account the mass differences between the models are shown in Table 6. Generally all the shapes tested which represent extrema of shape variability among aquatic snakes have more interests in performing a lateral strike. When the difference in hydrodynamics between both strategies is not pronounced other factors can take over the strategy choice which can explain why some species are choosing the frontal strike.

$$ratio = \frac{c_{D\text{frontal}}}{c_{D\text{lateral}}} \quad (7)$$

model	$pc1_{max}$	$pc1_{min}$	mean	$pc2_{max}$	$pc2_{min}$
c_D ratio (F_{max} U_{max} method)	3,158	2,745	3,011	1,736	2,296

Table 6: Drag coefficients for the five head models derived from the maximum force and velocity and weighted with an adimensional mass

Over all a CFD analysis could help in answering the question of how the shape is related to the strategy used and how it impacts the the hydrodynamic forces. From the experiment in lateral strike, which seems to be the most advantageous strategy for all aquatic snakes, it is hard if not impossible with force measurements on the head to extract the drag coefficient. The complex relation between drag and added mass needs to be deepen, as well as the knowledge about real snakes behavior in order to confront the experimental results.

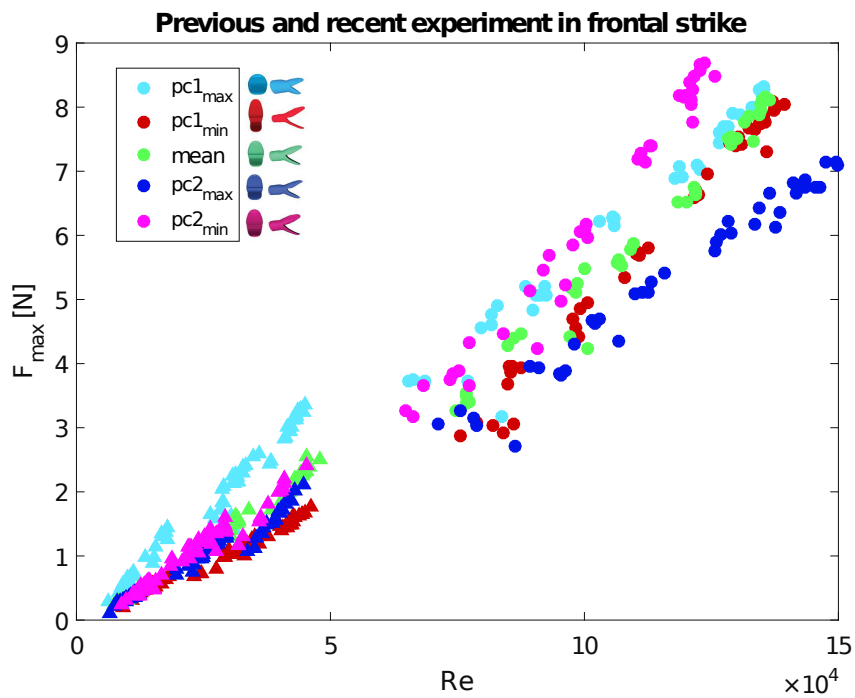


Figure 34: F_{max} as a function of the Reynolds number for the previous experiment in frontal strike done within the team (represented by the triangles) and the present experiment (represented by the circles)

Acknowledgement

I would like first to thank the PMMH laboratory and Ramiro Godoy-Diana for having given me the opportunity to do this internship. Naturally I thank Marion Segall for supervising and advising me, and without whom I would never discover the fascinating subject of snakes. I sincerely thank Ramiro Godoy-Diana for his expertise, availability and supervising. During six months I got help from technicians and engineers from the laboratory whom I would also like to thank, namely Tahar Amorri, Amaury Fourgeaud, Justine Laurent and Thierry Darnige.

References

- [1] M. E. Alfaro. Forward attack modes of aquatic feeding garter snakes. *Functional Ecology*, 16:204–215, 2002.
- [2] K. C. Catania. Tentacled snakes turn C-starts to their advantage and predict future prey behavior.
- [3] T. L. Daniel. Unsteady aspects of aquatic locomotion. *Integrative and Comparative Biology*, 1984.
- [4] A. Herrel, S. E. Vincent, M. E. Alfaro, S. Van Wassenbergh, B. Vanhooydonck, and D. J. Irschick. Morphological convergence as a consequence of extreme functional demands: Examples from the feeding system of natricine snakes. *Journal of Evolutionary Biology*, 2008.
- [5] J. Pantaleone and J. Messer. The added mass of a spherical projectile. *American Journal of Physics*, 79(12):1202–1210, 2011.
- [6] M. Segall, R. Cornette, A.-C. Fabre, R. Godoy-Diana, and A. Herrel. Does aquatic foraging impact head shape evolution in snakes?
- [7] S. Vogel. *Life in Moving Fluids*. 1981.
- [8] S. V. Wassenbergh, J. Brecko, P. Aerts, I. Stouten, G. Vanheusden, A. Camps, R. V. Damme, and A. Herrel. Hydrodynamic constraints on prey-capture performance in forward-striking snakes. *Journal of the Royal Society*, 7(773-785), 2009.
- [9] P. W. Webb. Simple physical principles and vertebrate aquatic locomotion. *American Zoologist*, 28:709–725, 1988.
- [10] B. A. Young and B. A. Youngt. The influences of the aquatic medium on the prey capture system of snakes. *JOURNAL OF NATURAL HISTORY*, 25:519–531, 1991.

Appendix A: List of abstracts of conference talks.

ICVM 2016, 11th International Congress of Vertebrate Morphology, International Society of Vertebrate Morphology, Washington DC, USA. **Segall, M.**, Godoy-Diana, R. and Herrel, A.

Aquatic prey capture in snakes: the link between morphology, behavior and hydrodynamics.

Aquatic animals have to face the physical constraints imposed by the mechanical properties of the fluid through which they move. Movement under water is resisted by drag and acceleration reaction forces, which can impair the displacement of the animal. The forward strike during prey capture will generate a pressure wave that can trigger the escape response of a mobile prey and thus decrease the capture success. Most animals have circumvented these constraints by developing a suction feeding system, but some animals cannot because of anatomical limits. As the physical constraints are highly dependent on the shape of the object, we hypothesize that the animals that cannot perform suction will have morphologically converged to be more streamlined. Moreover, we hypothesize that the behavior of species that do not present a streamlined head will aim to reduce the hydrodynamic forces associated with a strike under water. We chose snakes as biological model to test our hypotheses, as these animals cannot use suction and have evolved aquatic life-styles convergently. We predict that the head shape of aquatic snake species is more streamlined in comparison with that of non-aquatic species. The variability in the head shape of aquatic snakes is large and some species have a large, massive head. We suggest that these species have adapted their behavioral strategies to efficiently capture prey. To test our predictions, we compared 3D scans of the head shape of 83 species. We also developed a 3D printed model to mimic a snake attack under water in a laboratory experiment, characterizing the fluid flow associated with different head shapes and different behaviors using flow field velocimetry and force measurements.

SMEF 2016, 9th National Symposium of « Morphometry and Evolution of Forms ». Paris, France. **Segall, M.**, Cornette, R., Fabre, A-C., Godoy-Diana, R. and Herrel, A.

Does underwater prey capture impact head shape evolution in snakes?

Evolutionary trajectories are often biased by development and historical factors. However, environmental factors can also impose constraints on the evolutionary trajectories of organisms leading to convergence of morphology in similar ecological contexts. The physical properties of the medium an animal moves through imposes strong constraints such that aquatic animals are principally faced with drag-related forces impeding movement. These hydrodynamic constraints are strong and have resulted in the independent evolution of suction feeding in most groups of secondarily aquatic tetrapods. Despite the fact that snakes cannot use suction they have invaded the aquatic milieu many times independently. Here we test whether the aquatic environment has constrained head shape evolution in snakes and whether shape converges on that predicted by biomechanical models. Our results show that aquatic snakes partially conform to our predictions and have a narrower anterior part of the head and dorsally positioned eyes and nostrils. This morphology is observed irrespective of the phylogenetic relationships among species suggesting that the aquatic environment does indeed drive the evolution of head shape in snakes thus biasing the evolutionary trajectory of this group of animals.

ZOOLOGY 2014, 21st Benelux Congress of Zoology, Royal Belgian Zoological Society, Liège, Belgium. **Segall, M.**, Polidori, G., Arfaoui, A. and Herrel, A.

Hydrodynamic constraints associated with prey capture strategies in snakes.

Water is a dense and viscous medium. Although these properties constrain movement, numerous snake species capture prey under water. Consequently, these snakes have to circumvent the hydrodynamic constraints while being unable to rely on suction feeding mechanisms because of the extreme reduction of their hyoid apparatus. A way to cope with the hydrodynamic constraints is to adapt behavior. There are two main foraging strategies used by snakes that capture prey under water including sit-and-wait and pursuit foraging. We here test the hypothesis that these different prey capture strategies result in different hydrodynamic profiles. Moreover, we attempt to understand the effect of the acceleration of the head of the snake on the hydrodynamic profile and prey capture success. To do so we use Computational Fluid Dynamics to simulate the unsteady flow associated with prey capture behavior in *Natrix tessellata*. Our results show that both magnitude and duration of the acceleration play a crucial role in driving the hydrodynamic constraints. A short and high acceleration appears to be the less constrained prey capture strategy, consistent with the most widespread strategy used in snakes.

Appendix B: List of abstracts of conference posters.

ICVM 2016, 11th International Congress of Vertebrate Morphology, International Society of Vertebrate Morphology, Washington DC, USA. **Segall, M.**, Cornette, R., Godoy-Diana, R. and Herrel, A.

Water as a driver of evolution: the example of aquatic snakes.

Natural selection favors animals that are the most successful in their fitness-related behaviors, such as foraging. Secondary adaptations pose the problem of re-adapting an already 'hypothetically optimized' phenotype to new constraints. When animals forage underwater, they face strong physical constraints, particularly when capturing a prey. The capture requires the predator to be fast and to generate a high acceleration to catch the prey. This involves two main constraints due to the surrounding fluid: drag and added mass. Both of these constraints are related to the shape of the animal. We experimentally explore the relationship between shape and performance in the context of an aquatic strike. As a model, we use 3D-printed snake heads of different shapes and frontal strike kinematics based on in vivo observations. By using direct force measurements, we compare the drag and added mass generated by aquatic and non-aquatic snake models during a strike. Our results show that drag is optimized in aquatic snakes. Added mass appears less important than drag for snakes during an aquatic strike. The flow features associated to the hydrodynamic forces measured allows us to suggest a mechanism rendering the shape of the head of aquatic snakes well adapted to catch prey underwater.



ESPCI PARIS
FUNEVOL
UNIVERSITÉ PARIS DESCARTES

What shapes the head of aquatic snakes?

Marion Segall^{1,2}, Anthony Herrel^{1,3}, Ramiro Godoy-Diana², Raphaël Cornette⁴

1. Laboratoire FUNEVOL, UMR CNRS/MNH 7179, "Mécanismes adaptatifs : des organismes aux communautés", 55 Rue Buffon, 75005, Paris, France.
2. Laboratoire Physique et Mécanique des Milieux Hétérogènes, UMR CNRS 7636 / PSL - ESPCI, 10 rue Vauquelin, 75005, Paris, France.
3. Evolutionary Morphology of Vertebrates, Ghent University, K.L. Ledeganckstraat 35, B-9000 Ghent, Belgium.
4. ISYEB UMR7205 CNRS, MNHN, UPMC, EPHE, 45 rue Buffon, 75005, Paris.



FONDATION BETTENDORFF SCHUELLER
UNIVERSITÉ PARIS DESCARTES
ile de France

contact: marion.segall@live.fr

Introduction

The main asset of a limbless animal is its head. It is under a strong selective pressure resulting from many extrinsic and intrinsic factors. Aquatically foraging snakes are limbless animals that manage to capture elusive prey underwater with their heads despite of the hydrodynamic constraints. Previous studies have demonstrated that aquatic foraging snakes have morphologically converged (1) toward a head shape that is supposed to reduce the hydrodynamic constraints related to both locomotion and feeding underwater (2). However, a large morphological variability has been observed among these aquatic foragers (3). This could suggest that other extrinsic factors can shape the head of snakes. In the present work, we assess what other factors may have impacted the head shape of aquatically foraging snakes.

Hypotheses & Predictions

- **Ecology:** among aquatically foraging snake species, some have more terrestrial, semi-aquatic or only aquatic habits. Morphological requirements could be different depending on the preferred media in which the snake lives.
- **Presence of a gland:** the presence of venom or Duvernoy's glands could influence the head shape of snakes. Moreover, venom facilitates prey handling by tranquilizing them. Thus, non-venomous snakes could have a more bulky head to maintain their prey.
- **Prey shape:** snakes swallow their prey whole. If the prey is large, they may show a wider head, whereas if they eat elongate prey, they may have evolved longer heads to facilitate the swallowing.

Statistical analyses & Results

- A PCA was done and further statistical tests were ran on 90% of the overall variability.
- Phylogenetic MANOVAs:
 - **Prey shape:** $F_{1,60} = 3.34$, $P_{phy} = 0.03$
 - **Ecology:** $F_{2,59} = 4.30$, $P_{phy} = 0.32$
 - **Presence of gland:** $F_{1,60} = 4.99$, $P_{phy} = 0.69$

	Variance	Univariate K statistic		Phylogenetic ANOVA	
	Proportion (%)	K	P-value	$F_{1,60}$	P-value
PC1	53.4	0.40	0.002	2.26	0.25
PC2	11.1	0.36	0.0009	4.33	0.10
PC3	7.9	0.42	0.0009	0.01	0.94
PC4	7.1	0.24	0.03	3.71	0.11
PC5	5.1	0.17	0.32	0.20	0.72
PC6	3.4	0.31	0.12	8.74	0.02
PC7	2.6	0.48	0.02	0.58	0.55

Table 1: Results of the statistical analyses performed on the first eleven principal components. The ANOVA compares bulky vs. long prey eaters. Statistical significance highlighted in bold.

Specimens & Template

- 3D scans of the head of 316 specimens
- 62 species, =5 specimen per species
- Average shape per species used for analyses
- Template:

- 10 anatomical landmarks
- 6 curves
- 837 sliding landmarks



Fig. 1: Template manually positioned on the 3D scan of a specimen of *Xenochrophis piscator*.

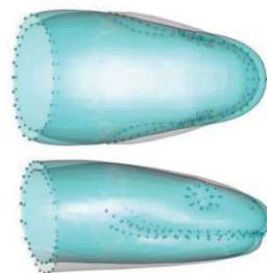


Fig. 2: Comparison of the shapes associated with PC6. The blue shape represents snakes that prefer long prey and in grey is the shape representing snakes that prefer bulky prey. Anatomical landmarks and curves were positioned on each shape to facilitate the comparison.

Discussion

- **Ecology** does not seem to impact head shape. It would mean that the hydrodynamic requirements associated with feeding are more important than locomotion in aquatic snakes.
- **The presence of glands** appears not to constrain head shape in aquatic snakes. We expected that the head would be larger because of the venom gland and/or that the venom would facilitate prey handling and so impose less constraints on the shape. Plus, we expected non-venomous snakes to have bulky heads as they require more power muscles to maintain the prey but it is possible that both presence of gland and high power muscles results in a similar "bulky" shape.
- **Prey shape** represents around 3% of the overall variability. As predicted, the shape associated with the swallowing of larger prey involves a more bulky head and snakes that prefer long preys have a more elongated head shape. However, as shown in fig. 2, the difference is subtle.
- The head is the most important asset of snakes so it is under a large selective pressure. A probable scenario is that many different aspects of snakes' lifestyle act in synergy and/or antagonistically to shape their head.

Acknowledgments

We thank the herpetological collections of the MNHN, FMNH, AMNH, MCZ and CAS and their respective curators Alan Ruester (FMNH), David A. Kluitman (AMNH), Jens Vindum (CAS) and Jose P. Rosado (MCZ). We especially wanted to thank the staff of the Laboratoire Reptiles et Amphibiens of the MNHN, The 'plate-forme de morphométrie' of the UMS 2700 (CNRS, MNHN) is acknowledged for allowing us to use the surface scanner. We thank the organizers of the symposium to invite us to present this work.

References

1. Segall M, Cornette R, Fabre A-C, Godoy-Diana R, & Herrel A. Does underwater prey capture impact head shape evolution in snakes? (under review) *Proc R Soc Lond B*.
2. Young BA. The influence of the aquatic medium on the prey capture system of snakes. *J Nat Hist*. 1991; Apr;25(2):519-31.
3. Fabre A, Bickford D, Segall M, Herrel A. The impact of diet, habitat use, and behavior on head shape evolution in homalopsid snakes. *Biol J Linn Soc*. 2016;118:634-47.



SICB 2017, Annual Meeting, the Society for Integrative and Comparative Biology, New Orleans, LA, USA. **Segall, M.**, Herrel, A., Godoy-Diana, R.

Does morphological convergence of the head enhance prey capture performance in aquatically foraging snakes?

Underwater prey capture is a challenge for aquatic animals because of the high density and viscosity of water that impairs the movement of the predator and that can trigger the prey startle response. To circumvent these constraints, aquatic predators can adapt their morphology to be more streamlined. Snakes are an excellent model to assess whether these physical constraints have driven the evolution of their phenotypes as they have invaded both freshwater and marine environments. To circumvent the hydrodynamic constraints of prey capture underwater, previous studies suggested that the “ideal” head shape for an aquatic snake would be long and thin. In a recent publication, we demonstrated morphological convergence of head shape of aquatic snakes, but with a different pattern: aquatic species have more bulky and short head than the non-aquatic foragers. These results, although quite surprising, can make sense from a fluid mechanics point of view. Indeed, the physical constraints are directly related to the surface area that is facing the flow during the movement in addition to its shape. The aim of this new study is to assess whether this bulky and short head is more efficient to capture prey underwater. To do so, we use 3D-printed models of snake heads to measure the forces imposed on the different shapes during an impulsive motion that mimics an underwater strike. In addition, a force sensor was placed at the end of the strike arena to detect the magnitude of the pressure wave generated by the different shapes. Our results show that the force imparted upon the aquatic shape is indeed lower than the one recorded for the non-aquatic shape, meaning that having a thin and long head might not be as efficient as previously thought.



ESPCI PARIS

Does morphological convergence of the head enhance prey capture performance in aquatically foraging snakes?

Marion Segall^{1,2}, Anthony Herrel^{1,3}, Ramiro Godoy-Diana²



1. Laboratoire FUNEVOL, UMR CNRS/MNHN 7179, "Mécanismes adaptatifs : des organismes aux communautés, 55 Rue Buffon, 75005, Paris, France.
 2. Laboratoire Physique et Mécanique des Milieux Hétérogènes, UMR CNRS 7636 : PSL - ESPCI, 10 rue Vauquelin, 75005, Paris, France.
 3. Evolutionary Morphology of Vertebrates, Ghent University, K.L. Ledeganckstraat 35, B-9000 Ghent, Belgium.

contact: marion.segall@live.fr

Introduction

Aquatic motion, and especially prey capture, is highly constrained because of the physical properties of water¹. The main constraints related with aquatic prey capture are **drag** in case of a steady speed motion and **added mass** during acceleration. Shape plays an important role in these physical constraints so aquatic predators should have adapted their morphology. As the solutions are limited by both hydrodynamics and the anatomy of the animals, **morphological convergence** often occurs. We studied convergence in the **head shape** of aquatic snakes by comparing 62 species that are **aquatic foragers** with 21 **non-aquatically foraging species**². We found a morphological convergence of the head shape of snake that forage on active preys underwater. However, the relation between this convergence and its significance in term of hydrodynamics is not straightforward. Here, we aim to illustrate the complex relationship between what seems to be a **morphological adaptation and its adaptive significance**. To do so, we 3D printed the two shapes resulting from our previous work, the shape of a typical "aquatic forager" and a "non-aquatic forager", and we simulated strikes underwater to compare the forces that are associated with the different morphologies.

Hypotheses & Predictions

Aquatic snakes should have evolved to optimize the underwater prey capture efficiency by **minimizing the drag and added mass** associated with a strike. Another important factor in prey capture success is the **detection by the prey**, as most aquatic preys have anti-predatory systems based on pressure detection, we measured the distance with the prediction that aquatic snakes should be detected latter than non-aquatic snakes.

Shapes

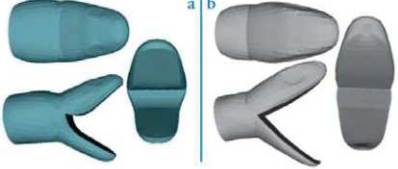
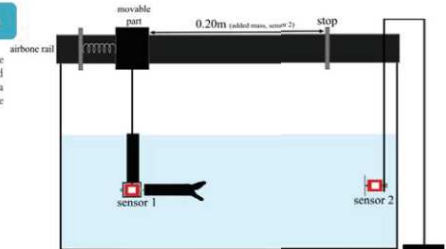


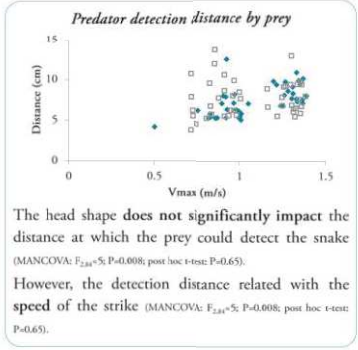
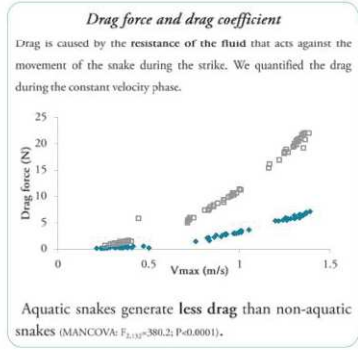
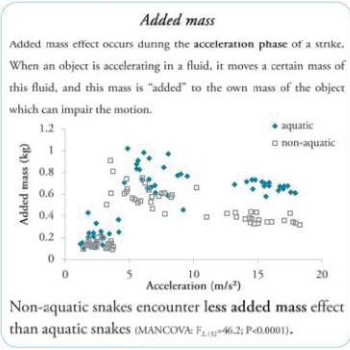
Fig. 1: 3D models of head shape of snakes used during the experiments viewed from above, right side and frontal view. a. aquatic head, b. non-aquatic.

Experimental setup

Fig. 2: Experimental design used to simulate snake prey capture strike. Sensor 1 was used to record the forces on the head during a strike and sensor 2 was used to record the force felt by a prey.



Results



Discussion

- The **drag** results fit our predictions, aquatic snakes generate less drag meaning that they move more efficiently at **constant speed** in comparison with non-aquatic snakes. Although, drag is more possibly more related to **locomotor efficiency** and not prey capture which is a rapid acceleration towards the prey.
- The **acceleration phase** does not seem as optimized as predicted *a priori* because the **added mass** is greater in aquatic snakes. However, we do not know the effect of the added mass on the animal. It might be possible that drag plays a major role in different vital behavior for snake and that drag and added mass could not be optimized simultaneously, but this remains to be tested.
- As expected, the link between morphology and function is not straightforward but our results are promising and require further exploration of this complex functional problem.

Acknowledgments

We thank Olivier Brouard, Amary Fourgeaud and Tahar Amorri for their precious help in the experimental design as well as Xavier Benoit-Gonin for his help with the 3D printer. Justine Laurent are acknowledged for their help with the sensors and computer coding.

References

1. Fish FE. Influence of hydrodynamic design and propulsive mode on mammalian swimming energetics. *Ann Zool.* 1993;42:79-101.
2. Segall M, Cornette R, Fabre A-C, Godoy-Diana R, & Herrel A. Does underwater prey capture impact head shape evolution in snakes? *Proc R Soc Lond B.* 2016;283(1645)



Appendix C: Abstract of the book chapter that is to be published.

Feeding in snakes: form, function, and evolution of the feeding system

Brad R. Moon, David A. Penning, **Marion Segall** and Anthony Herrel.

Snakes are a diverse group of squamate reptiles characterized by a unique feeding system and other traits associated with elongation and limblessness. Despite the description of transitional fossil forms, the evolution of the snake feeding system remains poorly understood, partly because so few snakes have been studied thus far. The idea that the feeding system in most snakes is adapted for consuming relatively large prey is supported by studies on anatomy and functional morphology. Moreover, because snakes are considered to be gape-limited predators, studies of head size and shape have shed light on feeding adaptations. Studies using traditional metrics have shown differences in head size and shape between males and females in many species that are linked to differences in diet. Research that has coupled robust phylogenies with detailed morphology and morphometrics has further demonstrated the adaptive nature of head shape in snakes and revealed striking evolutionary convergences in some clades. Recent studies of snake strikes have begun to reveal surprising capacities that warrant further research. Venoms, venom glands, and venom-delivery systems are proving to be more widespread and complex than previously recognized. Some venomous and many non-venomous snakes constrict prey. Recent studies of constriction have shown previously unexpected responsiveness, strength, and effects on prey. Mechanisms of drinking have proven difficult to resolve, although a new mechanism was proposed recently. Finally, although considerable research has focused on the energetics of digestion, much less is known about the energetics of striking and prey handling. A wide range of research on these and other topics has shown that snakes are a rich group for studying form, function, behavior, ecology, and evolution.

Remerciements

Attention ! Ces remerciements ne sont pas organisés en fonction de l'affection ou de l'importance que vous avez dans ma vie !

Merci à MECADEV (UMR7179) et au PMMH (UMR7636) de m'avoir accueillie pendant ces trois belles années. Un merci tout particulier à Fabienne Aujard et Philippe Petitjeans, directrice et directeur respectifs des deux UMR. Je tiens à remercier les gestionnaires des deux UMR dont le travail est parfois bien sous-estimé mais sans qui rien ne serait possible : Nadine, Yamso et Manuela (MECADEV) et Claudette et Fred (PMMH). Merci de m'avoir aidée avec ma phobie administrative et merci pour toutes ces parties de rigolade !

A Patricia Ern et Catherine Quilliet. Merci à vous deux. Il était non seulement important pour moi d'avoir des retours de physiciens sur mon travail de thèse, mais aussi d'avoir un jury le plus paritaire possible. Alors des femmes physiciennes, quel plaisir ! Je dois dire que j'appréhendais beaucoup vos questions et votre avis sur ce travail, n'ayant pas moi-même de recul sur ce que je faisais d'un point de vue de la mécanique des fluides. Mais je n'ai pas été déçue. Vous m'avez fourni de quoi réfléchir sur mes expériences, mes données et les nouvelles interrogations qu'elles pouvaient soulever tout en gardant une bienveillance et une compréhension de la difficulté de réaliser un travail interdisciplinaire. J'ai beaucoup aimé nos échanges lors de la soutenance et je vous remercie de votre de temps, de votre patience et de vos retours qui enrichissent la version finale de ce manuscrit.

To Harvey Lillywhite, thank you for accepting to be part of my PhD board. Despite your very busy agenda, you accepted and this means a lot to me. Thank you for the time you spent carefully reviewing my work. I hope that we will meet in the future to discuss about aquatic snakes and mainly about *Acrochordus*.

To Sam Van Wassenbergh, I always have been very impressed by your work and by you, as a person. So, I was very happy when you accepted to be part of my board even if, I

have to say, I was a bit anxious about your questions. In the end, it was a great discussion during the defense and I enjoyed it. Thank you for these interesting feedbacks. I wish you all the best for the future.

Je tiens à remercier Anthony Herrel, sans qui rien n'aurait été possible. Tu m'as montré qu'on pouvait vivre de sa passion et pour ça, je ne te remercierai jamais assez. Tu m'as supportée (dans tous les sens du terme) pendant 5 ans (ne t'en fais pas, tu vas bientôt pouvoir souffler !). Je sais à quel point je peux être casse-pied et têtue, tu mériterais une médaille rien que pour ça. Merci de m'avoir aidée à faire du terrain, à trouver un financement de thèse, un financement de post doctorat. Merci d'avoir relu et corrigé tout ce que j'ai écrit. Merci pour ta patience. J'espère que nous aurons l'occasion de nous recroiser dans le futur !

A Ramiro Godoy-Diana, un énorme merci pour avoir accepté de faire partie de ce projet. Quand je cherchais un physicien qui s'y connaît en mécanique des fluides, et qu'Olivia m'a mis en contact avec toi, je n'aurais pas pu mieux tomber ! Je n'y connaissais pas grand-chose en mécanique des fluides et, il faut dire ce qui est, je n'avais pas vraiment envie de m'y mettre. Mais finalement, grâce à toi, j'ai compris tout l'intérêt de cette partie du projet. Merci pour ta patience et ta bonne humeur. C'est vraiment agréable de travailler avec toi. On a encore du boulot mais je trouve qu'on ne s'en est pas mal sorti avec ce projet. Encore merci. Et j'espère qu'on se reverra dans le futur (qui sait, je n'en ai peut-être pas terminé avec la mécaflu !)

A Raphaël Cornette, que dire ? Je ne sais pas vraiment par où commencer, ni sur quel plan tu m'as le plus apporté. Commençons par le moins important : merci de m'avoir appris la morphométrie, de m'avoir poussé à explorer ce vaste domaine qui s'est finalement trouvé être le cœur de ma thèse ! Travailler avec toi a été et sera toujours un plaisir. Ca va être difficile de te quitter, pas seulement d'un point de vue scientifique mais aussi d'un point de vue personnel. Des personnes comme toi, c'est rare, d'autant plus dans notre beau milieu de la recherche. Je regrette que tu n'aies pas ta place en 1^{ère} de couverture de ma thèse en tant que directeur, parce que c'est ta vraie place ! Tu m'as tellement apporté et je ne te rends pas justice dans ce manuscrit. Tu es une belle personne et un très bon scientifique. J'espère que nos chemins se recroiseront. Encore merci Raf.

A Thierry Decamps, ingénieur de recherche de FUNEVOL. Tu m'as beaucoup aidée, que ce soit pour faire sauter des grenouilles ou pour synchroniser les caméras Phantom (bon, on ne reviendra pas sur mon échec du Costa Rica !). Tu m'as supportée au plateau technique pendant un moment. Tu ne m'as pas jetée dehors quand on a légèrement décoré ton bureau ! Merci pour tout !

A Olivier Brouard, Amaury Fourgeaud et Tahar Amaury, « les gars de l'atelier », un énorme merci pour m'avoir aidé à monter la manip. C'était super de travailler avec vous (et en plus, on a bien rigolé !). Un gros bisou et bon courage à vous trois !

Merci à Thierry Darnige et Xavier Benoit-Gonin, ingénieurs au PMMH pour leur aide avec la conception de la manip.

Un énorme merci à Justine Laurent ! Tu as été tellement patiente et tellement gentille avec moi. Grâce à toi on a réussi à monter une belle manip avec des résultats vraiment sympa. Et puis, surtout, merci pour toutes ces discussions à propos de la vie et de plein d'autres choses. Je te souhaite plein de bonnes choses pour la suite et, si tu passes à NY, viens nous voir !

A Stéphane Douady, merci d'avoir accepté de faire partie de mon comité de thèse, malgré tes réticences à propos de ce projet (ce qui nous a valu des échanges très intéressants). Il y a des personnes qui marquent une vie, et tu es l'une des personnes qui ont marqué la mienne. Merci.

A François Brischoux, merci également d'avoir fait partie de mon comité de thèse. Merci de m'avoir fait abandonner l'idée du terrain en Nouvelle Calédonie pour partir au Costa Rica ! Merci de m'avoir fait « goûter » au *Pelamis*, ce sont des bêtes fascinantes et je n'arrive pas à m'en décrocher ! J'espère qu'on aura l'occasion de se revoir !

Mahmood Sasa, Fabian Bonilla, Alejandro Solorzano y Carlos Bravo Vega, gracias a todos! My stay in Costa Rica was not only scientifically good but also personally amazing ! I hope I will be able to come soon to drink more chili guaros with you ! Pura vida !

A David Taresté, directeur des études de FdV, merci de m'avoir aidée et soutenue pour obtenir mon financement. Merci de t'être démené pour que je puisse commencer plus tôt ma thèse. Merci d'avoir toujours été à l'écoute de mes soucis. Merci pour ces moments partagés au CRI. J'espère te revoir un jour. (PS : si on ne trouve pas de poste dans le futur, Ameline et moi on est toujours partantes pour ouvrir un bar à chat au CRI. On compte sur toi pour nous soutenir !)

A Léo et Julien, comment pourrait mal se dérouler une thèse avec des co-bureaux comme ça ! Vous êtes tous les deux de très belles rencontres, autant sur le plan scientifique que personnel. J'ai du mal à me dire que nos pauses thé/café sur la terrasse, à discuter de tout et n'importe quoi sont terminées. Merci pour tout ce que vous m'avez apporté. Merci d'avoir été là, d'avoir amené des gâteaux, d'être venus boire des bières quand ça allait et quand ça n'allait pas ! Merci pour votre joie de vivre. On reste en contact, quoi qu'il arrive !

Liz and Ali, thank you for these times we shared the same office. It was great to meet nice persons like you. I wish you all the best for the future.

A Emmanuelle Pouydebat et Alexandra Houssaye, vous avez apporté de la joie et des rires dans ce labo et dans ma vie. Vous avez toujours été là quand j'en avais besoin et j'espère pouvoir un jour vous rendre la pareille. Vous êtes plus que des collègues pour moi. J'aimerais pouvoir vous ressembler, autant scientifiquement, parce que pour moi vous êtes toutes les deux très fortes dans ce que vous faites, que personnellement. Vous ne méritez que du bonheur. Vous êtes belles ! Et je vous kiffe grave ! Ne m'oubliez pas ! (De toute façon, je vous enverrai toujours des gif mignons régulièrement !)

Mon petit Mathieu, je survole le Canada alors que je commence ta petite dédicace, peut-être un signe ? On a eu des hauts et des bas mais tu feras toujours partie de ma vie. On a discuté de science et de la vie, autour de beaucoup (trop ?) de gin tonic. Tu es quelqu'un de bien et tu mérites d'être heureux.

A Marc Herbin, merci pour ton soutien, pour ton aide et pour ta jovialité indéfectible !

Merci à Helder, Anne-Claire, Maïtena, vous allez me manquer. Et merci au reste de l'équipe FUNEVOL, les anciens comme les nouveaux.

Aux copains de FdV, Adrien, Lise, Paul, Quentin, Francès, Carlos et j'en oublie sûrement, merci d'avoir enjolivé les soirées au CRI. Vous êtes tous des amours !

A Charles, je dois dire que j'ai beaucoup appris à tes côtés, peut-être même beaucoup trop ! Merci de t'être occupé de moi et de m'avoir nourrie sur la fin de ma thèse ;) On se sera bien marré ! Et, j'espère que tu trouveras l'occasion de réutiliser le triangle, malgré mon départ. Mais, il y a du potentiel dans le labo !

A Martyna, merci d'avoir été « la meilleure stagiaire » ! ;)

Au reste du PMMH, autant étudiants que chercheurs, merci de m'avoir accueillie et d'avoir contribué à la réussite de cette thèse.

A Dimitri, encore une belle rencontre ! Merci de m'avoir tant appris sur les reptiles. Je pense que tu sais tout ce que j'ai à te dire. Tu as toujours été là pour moi, et je serai toujours là si tu en as besoin. Merci de faire partie de ma vie...

A Anne Laure, des années à me supporter. Tu as bien essayé de t'éloigner à 600km mais je suis tenace ! Merci d'être ce que tu es et de m'avoir toujours soutenue. C'est à mon tour de partir, plus loin certes mais je ne doute pas que tu seras toujours là pour moi de la même façon que je serai là pour toi.

A Ameline, mon chaton, je ne te remercierai jamais assez pour ce que tu es, pour ce que tu m'as apporté, pour ce que tu représentes... Tu es l'une de mes meilleures amies et ça n'est pas rien ! On a passé tellement de moments toutes les deux, des bons comme des mauvais. Tu es l'une des plus belles personnes que je connaisse. Tu as illuminé le labo de ta joie de vivre et de ta bonne humeur. On ne peut pas rêver mieux comme co-bureau, comme collègue ni comme amie ! Je n'ai pas envie de trop m'épancher, j'ai peur que ça sonne comme un au-revoir alors que ça n'en est pas un puisqu'on va monter notre labo ensemble !!!

A Bérengère, on est toutes les deux peu expansives mais tu mérites que je fasse un effort. Bérengère, tu es une personne que je n'oublierai jamais. Tu m'as beaucoup aidée, plus que ce que tu ne crois. Tu es une femme belle, intelligente avec une personnalité bien affirmée et évoluer à tes côtés m'a beaucoup appris. J'espère être à la hauteur de ton amitié et j'espère qu'on arrivera à garder contact malgré la distance (parce que je crois qu'on est toutes les deux mauvaises pour ça ;))

A Adrien, merci d'avoir été là, pour le meilleur et pour le pire. Tu as d'ailleurs plus été présent pour le « pire » de cette thèse que pour le meilleur, mais tu as réussi à me supporter. Ça n'est pas rien ! On s'est soutenu, on s'est aidé, et on va continuer. Merci de faire partie de ma vie.

A ma famille, mes parents, ma sœur, mon frère, mes grands-parents, ma tante. Sans vous rien n'aurait été possible. Vous avez fait de moi la personne que je suis aujourd'hui. Vous m'avez soutenue dans ma passion, dans mon choix de vie, vous avez rendu mon rêve de petite fille accessible. Ça y est, je suis herpétologue, et c'est grâce à vous. Merci d'être toujours présents, pour le meilleur et pour le pire. On a une belle famille, ça n'est pas donné à tout le monde. Je vous aime.

Pour ceux qui me connaissent, vous savez que cette section a été la plus difficile à rédiger pour la petite autiste que je suis. Je vais forcément oublier de remercier des gens, mais comme dirait une chanson « les vrais savent ». Encore une fois, ne voyez pas dans l'ordre des remerciements quelque hiérarchie dans l'importance que vous avez pour moi.

Abstract

Animal-environment interactions are determinant in driving the evolution of phenotypic variation. Most aquatic animals have developed adaptations to overcome the physical constraints inherent to an aquatic lifestyle and particularly to motion in water. These constraints are the drag and the added mass if an acceleration is involved in the motion, such as during prey capture. The aim of this project is to evaluate the role of water as a potential driver of evolution of head shape by focusing on morphological and behavioral convergences during underwater prey capture. Snakes are a good model as an aquatic life-style has originated independently in different genera. However, aquatic snakes did not develop a suction feeding system in contrast to most aquatic vertebrates. Prey-capture under water is constrained by the physical properties of the fluid and thus morphological and/or behavioral convergence is expected. By comparing the head shapes and the behavior of different species, we evaluated the impact of water on the evolution of head shape and strike behavior. By using experimental fluid mechanics approaches, we quantified the physical constraints involved in prey capture and evaluated the nature of the evolutionary response in response to these hydrodynamic constraints. This interdisciplinary approach allowed us to bring novel data to our understanding of functional constraints as drivers of phenotypic evolution.

